Studies on Migration-inhibition Activity of a 3,12-Unsubsituted Fusicoccin Derivative

Yu Haranosono

Department of Chemistry, Graduate School of Science

Osaka University

February, 2014

Table of Contents

Chapter 1: Introduction ····· 1

1–1. 14-3-3 Proteins ····· 1

1–2. Binding Motifs for 14-3-3 Proteins ····· 3

1–3. Small-Molecule Inhibitors for 14-3-3 Protein–Protein Interactions ····· 5

1–4. Small-Molecule Stabilizers for 14-3-3 Protein–Protein Interactions ····· 7

1–5. Anticancer Activities of Cotylenin A ····· 10

1–6. Anticancer Activities of Fusicoccin Derivatives ····· 12

1–7. Client Selectivity of Fusicoccin Derivatives ····· 14

1–8. Semi-synthetic Mode 3 Selective Stabilizer ····· 16

1–9. Research Objective ····· 18

Chapter 2: Characteristic Anti-tumor Activities of ISIR-005, a 3,12-Unsubstituted Fusicoccin Derivative ····· 19

2–1. Introductory Statements ····· 19

2–2. Results ····· 21

2–2–1. Cell death induced by ISIR-005 ····· 21

2–2–2. Effects of ISIR-005 on cell–cell adhesion ····· 23

2–2–3. Effects of ISIR-005 on cell–ECM adhesion ····· 23

2–2–4. Involvement of 14-3-3ζ in the effects of ISIR-005 ····· 25

2–2–5. Inhibition of cell migration by ISIR-005 ····· 26

2–3. Discussion ····· 28

2–4. Materials and Methods ····· 29

Chapter 3: Mechanism of Migration Inhibition Induced by ISIR-005 ····· 33

3–1. Introductory Statements and Preliminary Results ····· 33

3–2. Results ····· 34

3–2–1. Cancelation of ISIR-005 effects on A549 cells by a ROCK inhibitor ····· 34

3–2–2. Effect of ISIR-005 onto localization of Rnd3, an antagonist of RhoA/ROCK-1 of RhoA/ROCK-1 signaling ····· 35

3–2–3. Possibility of a binary complex of Rnd3 and 14-3-3 protein as a primary target of ISIR-005 ····· 39

3–3. Discussion ····· 45

3–4. Materials and Methods ····· 50

Chapter 4: Effect of ISIR-005 onto Stress Fibers and Cell Detachment ····· 53
4–1. Introductory Statements ····· 53
4–2. Results ····· 53
4–2–1. Effect of ISIR-005 onto β-actin and actin filaments ····· 53
4–2–2. Effect of ISIR-005 onto focal adhesion ····· 55
4–2–3. Effect of ISIR-005 onto tight-junction ····· 56
4–3. Discussion ····· 57
4–4. Materials and Methods ····· 60

Chapter 5: Mechanism of Cell Death Induction by ISIR-005 ····· 61
5–1. Introductory Statements and Preliminary Results ····· 61
5–2. Results ····· 63
5–2–1. Effect of ISIR-005 onto c-FLIP expression and localization ····· 63
5–2–2. Effects of ISIR-005 onto DAP3 and IPS-1 ····· 65
5–2–3. Effect of ISIR-005 onto activities of p53 ····· 66
5–3. Discussion ····· 69
5–4. Materials and Methods ····· 73

Chapter 6: Conclusion ····· 75

References ····· 77

Acknowledgements ····· 89

Abbreviations

All amino acids were mainly indicated as three-letter codes or one-letter codes.
The following abbreviations are also used in this thesis.

Akt/PKB	protein kinase B
ADP	adenosine diphosphate
AML	acute myeloid leukemia
ATCC	American Type Culture Collection
BCA	bicinchoninic acid
BODIPY	boron-dipyrromethene
Caspase	cysteine-aspartic-acid-protease
Cdc25	cell division cycle 25 homolog
Cdk	cyclin dependent kinase
c-FLIP	cellular-FLICE inhibitory protein
CN	cotylenin
c-Raf	Raf proto-oncogene serine/threonine-protein kinase; alternative name: Raf-1, v-Raf-1 murine leukemia viral oncogene homolog 1; v-Raf, proto-oncogene serine/threonine-protein kinase in virus-induced rapidly accelerated fibrosarcoma
DAP3	death associated protein 3
Dbs	Rho-specific guanine nucleotide exchange factor
DEAE	diethylaminoethyl
DISC	death-inducing signaling complex
DNA	deoxyribonucleic acid
D-PBS(-)	Dulbecco's Phosphate Buffered Saline without Ca^{2+} and Mg^{2+}
DR4	death receptor 4
DR5	death receptor 5
ECM	extracellular matrix
EDTA	ethylenediamine tetraacetic acid
EGFR	epidermal growth factor receptor
ER	endo-plasmic reticulum
ERα-F	estrogen receptor alpha F domain
ExoS	exoenzyme S
FADD	Fas-associated death domain protein
Fas	TNF receptor superfamily, member 6 (TNF, tumor necrosis factor)
FBS	fetal bovine serum

FC	fusicoccin
FITC	fluorescein isothiocianate
FKBP	FK506-binding protein
FLICE	FADD-like interleukin-1-beta-converting enzyme
FP	fluorescent polarization
GFP	green fluorescent protein
GST	gluthathione *S*-transferase
GTP	guanosine triphosphate
GTPase	guanosine triphosphatase
HEPES	4-(2-hydroxyethyl)-1-piperazineethanesulfonic acid
HRP	horseradish peroxidase
IFN-α	interferon-α
IgG	immunoglobulin G
IPS-1	interferon-beta promoter stimulator 1
IRTKS	insulin receptor tyrosine kinase substrate
ITC	isothermal titration calorimetry
LDH	lactate dehydrogenase
Mdm2	murine double minutes 2
MTS	3-(4,5-dimethylthiazol-2-yl)-5-(3-carboxymethoxyphenyl)- 2-(4-sulfophenyl)-2*H*-tetrazolium
NEDD8	neural precursor cell-expressed developmentary down-regulated gene 8
NUB1	NEDD8 ultimate buster 1
PARC	Parkin-like ubiquitin ligase
PAGE	poly-acrylamide gel electrophoresis
PDB	Protein Data Bank
PFA	para-formaldehyde
PI	propidium iodide
PKC	protein kinase C
PMA2	plasma membrane H^+-ATPase isoform 2
PPI	protein–protein interaction
poly-HEMA	poly 2-hydroxyethyl methacrylate
Rac1	Ras-related C3 botulinum toxin substrate 1
Ras	small molecular weight GTPase originally identified from Rat sarcoma
Rho	Ras oncogene-related small molecular weight GTP-binding protein
RhoA	Ras homolog family member A

RNA	ribonucleic acid
RPMI-1640	roswell park memorial institute-1640 medium
ROCK	Rho-associated coiled-coil-forming kinase
SAR	structure-activity-relationship
S.D.	standard derivation
SDS	sodium dodecyl sulfate
*si*RNA	small interfering ribonucleic acid
TASK	TWIK-related acid sensitive K^+ channel
TRAIL	tumor necrosis factor related apoptosis inducing ligand
TBST	Tris-buffer saline with 0.1v/v% Tween-20
THF	tetrahydrofuran
T-PBS	D-PBS(-) including 0.5v/v% TritonX-100
Tris	tris(hydroxymethyl)aminomethane
t-test	student's t
TWIK	tandem pore domain weak inward rectifying K^+ channel
wt	wild type
ZO-1	zonula occluden protein 1

Chemical structures of inhibitors and an reagent

Caspase-8 inhibitor: Z-IED-FMK

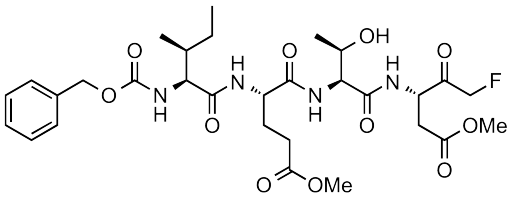

ROCK inhibitor: Y-27632

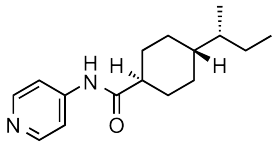

ROCK inhibitor: H1152

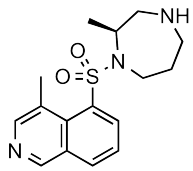

Proteasome inhibitor: MG-132

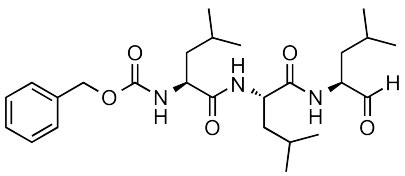

F-actin staining agent: phalloidin

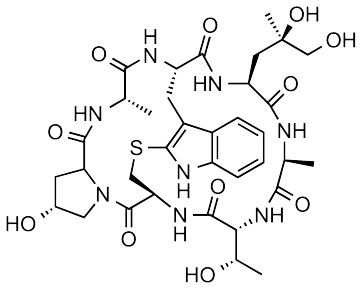

Chapter 1: Introduction

1–1. 14-3-3 Proteins

14-3-3 proteins are ubiquitously expressed and highly conserved in all eukaryotic cells.[1] In 1967, the name 14-3-3 was given to an abundant bovine brain protein due to its particular elution and migration pattern on two-dimensional DEAE-cellulose chromatography (14th fraction) and starch-gel electrophoresis (position 3.3).[2] However their functional significance had been unknown until Japanese researchers found their role in the regulation of serotonin and noradrenaline biosynthesis, *i.e.*, activation of tryptophan 5-monooxygenase and tyrosine 3-monooxygenase in 1987.[3] After this finding, functions of 14-3-3 proteins were intensively studied and it has been established that 14-3-3 protein family is one of the most important adaptor proteins in regulation of a plethora of physiological processes in eukaryotic cells. They realize their physiological effects by binding to their client proteins in phosphorylation dependent manner. The client phosphoproteins are modulated their subcellular localization or enzymatic activity through forming association complexes with 14-3-3 proteins. Furthermore, since 14-3-3 proteins physiologically exist as dimers, they can bind two different clients simultaneously letting them to communicate.[1]

Seven isoforms, β, ε, γ, η, σ, τ and ζ, are identified as human 14-3-3 proteins. These form not only homo-dimers but also hetero-dimers with other member of the family except γ and σ isoforms that prefer to form homo-dimers.[4,5] Nevertheless, structures and functions of all isoforms of human 14-3-3 proteins are quite similar to each other. Each 14-3-3 monomer consists of nine antiparallel α-helices (αA–αI) and short loops that connect between helices. Since each monomer is shaped "u" form groove for binding to phosphopeptides in the clients, dimers look like "ω" (Figure 1–1). Outside residues of αA interact with those of αC' and αD' in another monomer to form a physiologically stable dimer. The interior surface of the binding groove, which is composed of inside residues within αC, αE, αG and αI, is highly conserved in all 14-3-3 isoforms. At the center of the groove, Lys and Arg in αC (Lys49 and Arg56, respectively, in ζ isoform) and another Arg in αE (Arg127 in ζ) form a positively charged cluster for capturing negatively charged phosphate of the client. These three residues are completely conserved in 14-3-3 proteins identified from all eukaryotes. Therefore, all 14-3-3 isoforms can bind with the phosphopeptide sequences basically in a similar manner. If this electrostatic interaction between the Lys–Arg cluster of 14-3-3 proteins and the phosphate of the client is solely responsible for the complex formation, seven isoforms are branded as redundant. Although the specific client recognition of each isoform has been remained

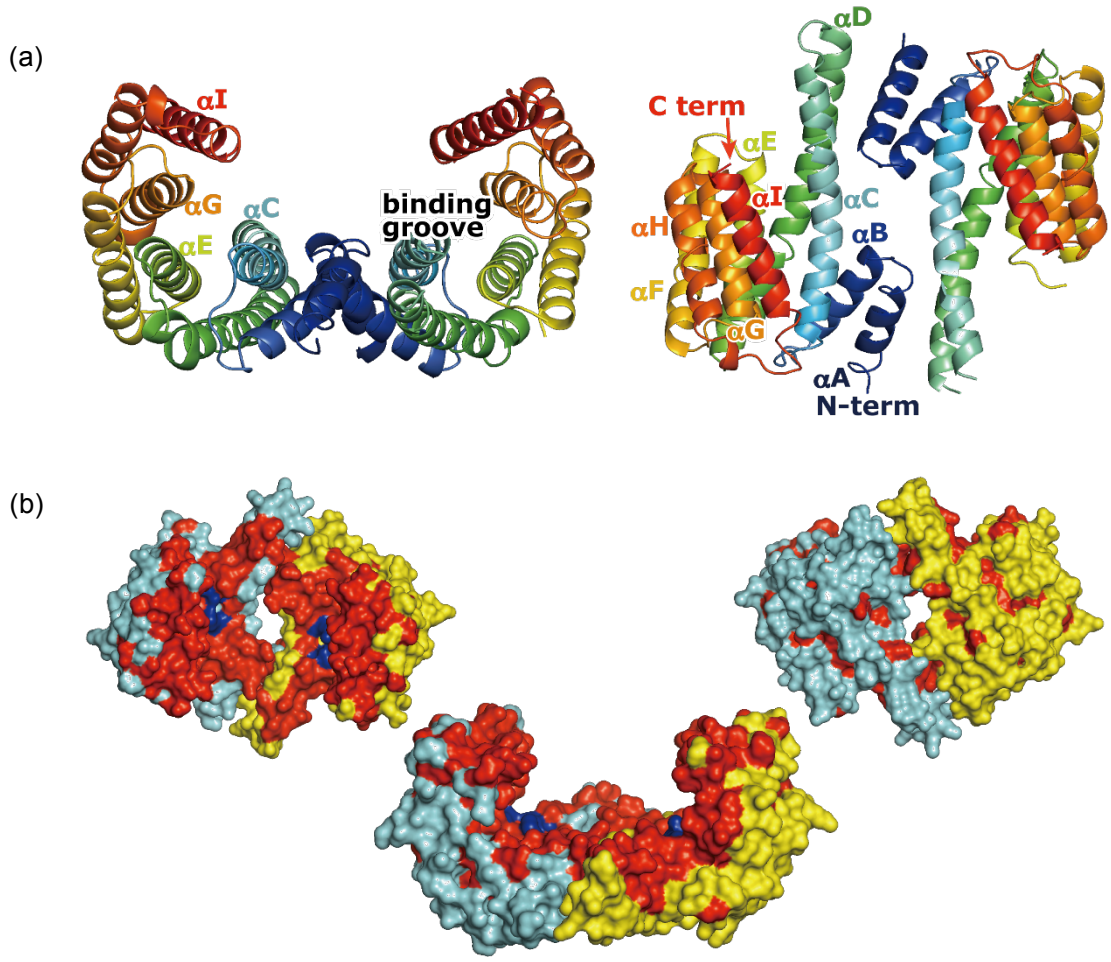

Figure 1–1. (a) The ribbon presentation of human 14-3-3ζ dimer from side (left) and top (right) views (PDB: 4IHL). (b) Surface drawing of human 14-3-3ζ dimer viewed from top (left), side (center) and bottom (right). One monomer is shown in cyan and another monomer in yellow. Blue surface is the Lys–Arg cluster and red surface is for other conserved residues that are identical among all seven human isoforms, 14-3-3e of *Xenopus laevis* and 14-3-3 isoform c of *Nicotiana tabacum*. Figures were prepared by PyMol (http://www.pymol.org).

unclear, it has been postulated that non-conserved exterior surface contributes to the secondary interaction with the specific clients. This postulation was supported by X-ray crystallographic analysis of a binary complex of serotonin *N*-acetyltransferase (AANAT) and human 14-3-3ζ.[6] As shown in Figure 1–2, each monomer of 14-3-3ζ binds with one molecule of phosphorylated AANAT$^{1\text{-}201}$ (the full length of AANAT composes of 207 amino acids). The phosphorylated extended sequence of ^{26}RQRRHpTLP^{33} contributes to the primary interaction with the groove of 14-3-3 protein. Additionally, it is obvious that α1 of AANAT interacts with the loop αH–αI of 14-3-3. Residues contribute to the secondary interaction, *i.e.*, Asp208, Lys212 and Thr215 of 14-3-3ζ, are conserved in all human 14-3-3 proteins. Therefore, in this particular case, the interactions outside of the primary binding groove do not explain the client selectivity of 14-3-3 isoforms. However, as exemplified with this case, it is plausible that client protein interact with

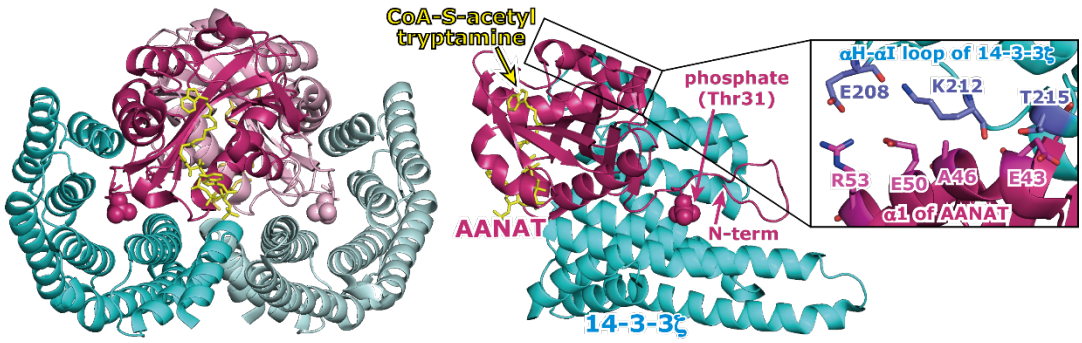

Figure 1–2. The binary complex of two molecules of serotonin *N*-acetyltransferase (AANAT) and human 14-3-3ζ dimer together with two molecules of CoA-*S*-acetyltryptamine (PDB ID: 1IB1). 14-3-3 monomer in cyan, AANAT in dark pink and CoA-*S*-acetyltryptamine in yellow for one set of the complex. Those are shown in pale cyan, pale pink and dark yellow, respectively, for another set of the complex (left). Top view of one set of the complex (right). In the rectangle, shown are the secondary interactions between the helix α1 (Arabic numeral is used for AANAT) of AANAT and the loop αH–αI of 14-3-3ζ. Figures were prepared by PyMol.

14-3-3 at the region far from the primary binding groove. If the secondary interaction is strong enough and the counter residues of 14-3-3 are non-conserved in isoforms, such client should have isoform selectivity in the complexation with 14-3-3 proteins. Since the AANAT/14-3-3ζ is the only example solved as a binary complex of full-length client and 14-3-3, argument on the isoform selectivity awaits further accumulation of experimental results.

1–2. Binding Motifs for 14-3-3 Proteins

In the majority of cases, 14-3-3 proteins recognize phosphorylated peptides as their clients. In 1996, Muslin *et al*. proved that the interaction of 14-3-3ζ against c-Raf (alternative name: Raf-1) is mediated by direct binding to phosphoserine (pS or pSer) of c-Raf. They noticed that putative biding sites in other 14-3-3 client proteins have similar sequences with those of c-Raf; ^{264}RSTpSTP^{261} and ^{618}RSApSEP^{623} in c-Raf, ^{243}RSSpSAP^{248} and ^{607}RSApSEP^{612} in B-RAF, ^{270}RSHpSYP^{275} in polyoma middle T, ^{303}RSPpSMP^{308} in Cdc25B, ^{343}RSKpSAP^{348} in PKCε and ^{686}RSHpSYP^{691} in PKCγ.[7] With these findings, they proposed RSXpSXP (X denotes any amino acid) as a binding motif for 14-3-3 proteins. Subsequently, Yaffe *et al*. tried to find out the phosphopeptide motifs for 14-3-3 proteins by use of phosphoserine-oriented peptide libraries.[8] Consequently, they found that a new consensus binding motif, RXΦXpSXP (Φ denotes aromatic amino acid such as Phe and Tyr), besides above mentioned RSXpSXP. Since phosphoserine can be replaced by phosphorthreonine, RXp(S/T)XP and RXΦXp(S/T)XP are defined as mode 1 and mode

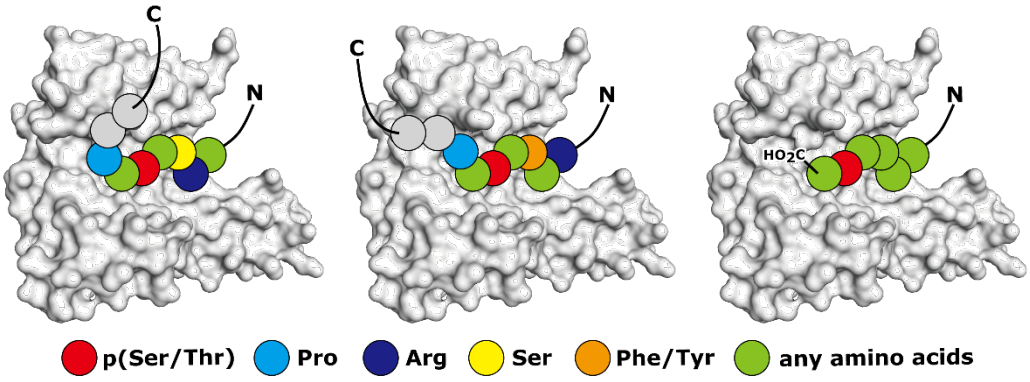

Figure 1−3. Schematic drawing of biding modes of internal motifs, mode 1 (left) and mode 2 (center), and a C-terminus motif, mode 3 (right). White surface is a perspective view of the 14-3-3ζ monomer. Coordinates are adopted from PDB ID: 1QJB. Because of +2Pro from the phosphorylation site, subsequent sequence of C-terminus side extends to outside of the binding groove either *cis*-direction in mode 1 or *trans*-direction in mode 2.

2, respectively. Subsequently, Coblitz *et al*. proposed mode 3 for p(S/T)$X_{1\text{-}2}$–COOH that can be found in several clients interacting with 14-3-3 proteins by use of their C-termini (Figure 1–3).[9] Although several phosphorylation-independent client peptides, such as R18[10] (a non-phosphorylated peptide, PHCVPRDLSWLDLEANMCLP, and an inhibitor for complexation of 14-3-3 proteins and their clients) had been known, these canonical consensus motifs were believed to be predominant in the phosphopeptides interacting with 14-3-3 proteins. However, recent bioinformatic survey of 14-3-3-binding sites by MacKintosh *et al.* revealed that many sequences other than modes 1, 2 and 3 were reported as client phoshopeptides of 14-3-3 proteins.[11] Figure 1–4 shows WEBLogo analysis of 175 binding sites in 126 proteins that are clients of 14-3-3 proteins in human cells. The +2Pro residue, defined essential in modes 1 and 2, occurs less than half. The most common residue is Arg at –3 position from the phosphorylation site. This analysis clearly points out that although the canonical motifs, modes 1 to 3, are important, attention should be paid also to non-canonical sequences in the

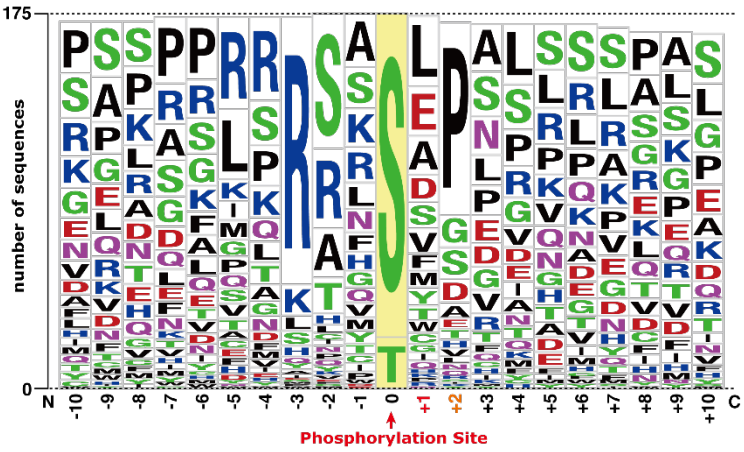

Figure 1−4. WEBLogo analysis of 14-3-3 binding sites in human clients. The table originally obtained by WEBLogo (http://weblogo.berkeley.edu) was modified manually to adjust the number of sequences at each site. For example, the number of sequences extending beyond +2 position is 168, since seven mode 3 sequences are listed in this analysis.

analysis of interactome of 14-3-3 proteins. Furthermore, it has been reported that exoenzyme S (ExoS), an ADP-ribosyltransferase toxin produced by *Pseudomonas aeruginosa*, binds with human 14-3-3 proteins in a unique fashion. The binary complex of human 14-3-3ζ and ExoS$^{353–453}$ showed that the ExoS peptide enters into the 14-3-3 binding groove from the opposite direction compared with other cases (Figure 1–5),[12] *i.e.*, when the groove is viewed from top, *N*-term to *C*-term of ExoS peptide is oriented as left to right. Thus, it is rather difficult to predict whether proteins can be clients of 14-3-3 proteins or not only by their amino acid sequences.

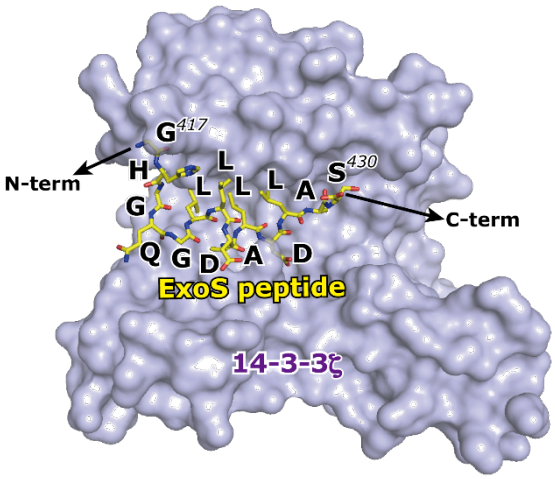

Figure 1–5. The crystal structure of human 14-3-3ζ and ExoS of *P. aeruginosa* (PDB ID: 2O02). The former is depicted as a pale purple surface and the latter is presented as sticks: C in yellow, N in blue and O in red. Only 14 residues, ^{417}GHGQGLLDALDLAS^{430}, were assignable of ExoS$^{353–453}$. Figure was prepared by PyMol.

1–3. Small-Molecule Inhibitors for 14-3-3 Protein−Protein Interactions

Through binding with diverse client proteins, 14-3-3 proteins take roles in many physiological processes, such as signal transduction, cell-cycle control, vesicular transport, DNA replication, DNA repair, apoptosis, cellular metabolism, cytoskeleton organization and malignant transformation.[13–17] Therefore, modulators of 14-3-3 protein functions potentially affect diverse physiological processes. It has been reported that expression of 14-3-3ζ isoform is elevated in the breast cancer,[18] lung cancer,[19] multiple myeloma,[20] glioma,[21] meningioma,[22] esophageal cancers,[23] squamous cell carcinoma,[24] prostate tumor,[25] oral cancer,[26] hepatoma[27] and pancreatic adenocarcinoma.[28] Overexpression of 14-3-3ζ in many cancer cell types suggested that this isoform has an important role in the tumor genesis and progression in multiple types of cancer. Owing to these findings, extensive investigation has been undergoing with 14-3-3ζ as a target in cancer therapy.[29]

The first inhibiting agent against protein–protein interactions (PPIs) between 14-3-3 proteins and their clients was the 20-amino-acid peptide, R18 (*vide supra*).[30] Subsequently, it has been shown that expression of a 62-amino-acid peptide, named difopein (Figure 1–6), composed of a dimeric form of R18 sensitized cancer cells for the anti-neoplastic drug cisplatin.[31] Difopein was also

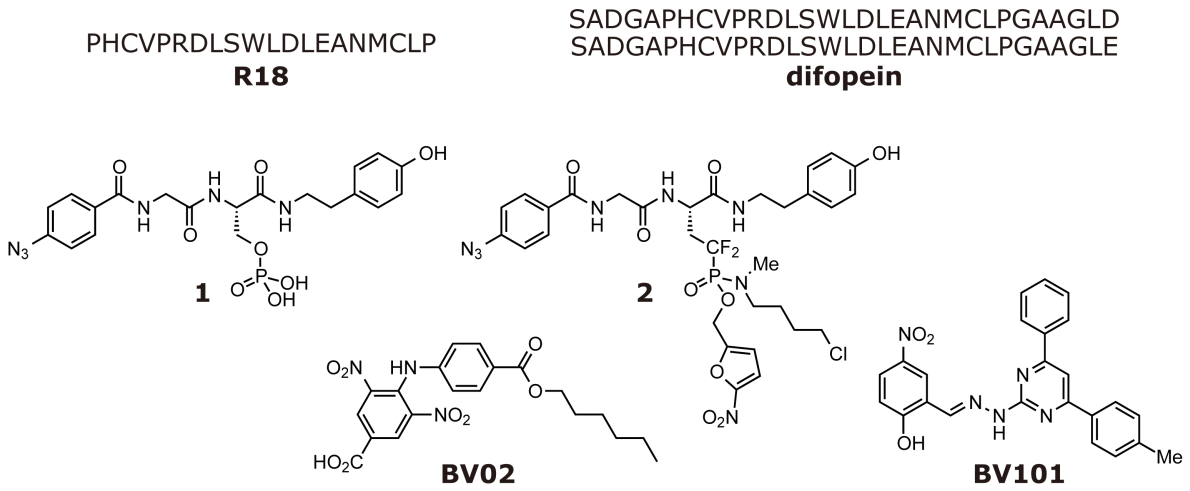

Figure 1−6. Several inhibitors for 14-3-3 PPIs.

effective *in vivo* and suppressed tumor growth in mice.[32] With these encouraging results of 14-3-3 inhibitors as anti-cancer agents, investigations turned attention to small-molecule inhibiters of 14-3-3 PPIs having cell permeability. From a small-molecule microarray composed of phosphopeptide mimetics adopting mode 2 type of sequential structures, compound **1** was obtained as an inhibitor having cell permeability.[33] Compound **2**, a prodrug derivative of **1**, was reported to show potent 14-3-3 inhibitory activity in cells (Figure 1–6).[34] Botta *et al.* reported the identification of a small-molecule inhibitor of the c-Abl/14-3-3 interaction by employing structure-based pharmacophore modeling, virtual screening and molecular docking simulations. They eventually identified BV02 and BV101 as inhibitors for 14-3-3 PPIs (Figure 1–6).[35] In 2011, the first covalent 14-3-3 inhibitor was reported.[36] Fu *et al*. screened LOPAC® library by use of fluorescent polarization (FP) evaluation and identified FOBISIN101 (Figure 1–7) as an inhibitor for the interaction between 14-3-3γ and the phosphorylated c-Raf peptide. Interestingly, the crystal structure of the binary complex of 14-3-3ζ and FOBISIN101 revealed that the N=N double bond of the inhibitor was cleaved during X-ray radiation and the fragmented molecule covalently bonded to Lys120 of 14-3-3ζ (Figure 1–7). Authors claimed that this type of compounds could be useful as

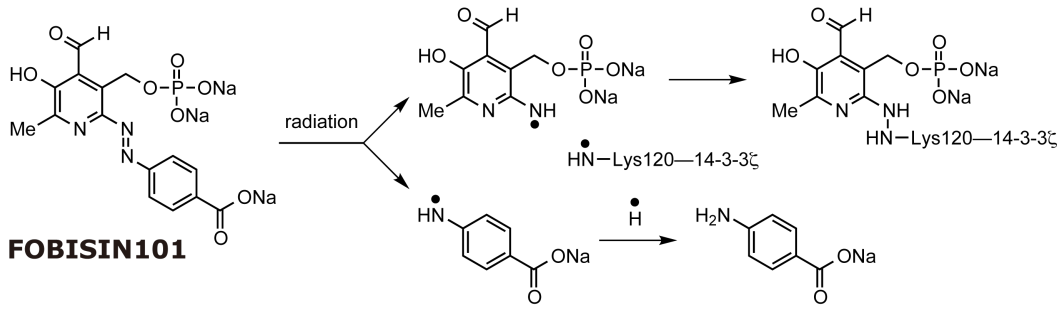

Figure 1−7. FOBISIN101 and proposed mechanism for covalent bonding with Lys120 of 14-3-3ζ.

radiation-triggered therapeutic agents for the treatment of 14-3-3 mediated diseases. However, the proposed mechanism for the covalent bonding should be validated more carefully. Actually, Ottmann *et al*. reported that compound **3**, a derivative of pyridoxal-5'-phosphate identified from virtual screening, also attached onto a Lys nearby the phosphate-accepting pocket of 14-3-3σ. They solved the crystal structure of 14-3-3σ and either **3** or FOBISIN101 and concluded that the covalent bonding is the Schiff base formation between aldehyde moiety of inhibitors and ε-amine moiety of Lys of 14-3-3σ (Figure 1–8).[37] This interpretation is quite plausible because it is well known that pyridoxal reacts with Lys to form a Schiff base. Several other inhibitors were reported in the literature.[38,39]

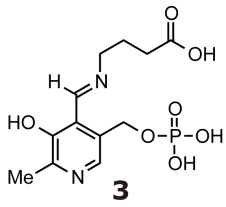

3

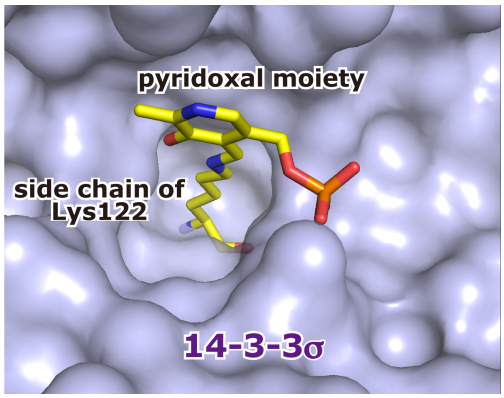

Figure 1–8. Chemical structure of compound **3** and the crystal structure of covalently bounded complex with 14-3-3σ (PDB ID: 3U9X). Lys122 in σ isoform corresponds to Lys120 in ζ. Figure was created by PyMol.

1–4. Small-Molecule Stabilizers for 14-3-3 Protein−Protein Interactions

As exemplified by paclitaxel[40] and FK506,[41] stabilizers for protein–protein interactions are also useful for modulation of cellular functions. The former stabilizes microtubules and, as a result, interferes with the cell division. Owing to this effect, paclitaxel is used clinically as an anticancer agent against lung, ovarian, breast, head and neck cancers. FK506, an immunosuppressant, binds to peptidyl-prolyl *cis-trans* isomerase FKBP1A (alternative name: 12 kDa FK506-binding protein; FKBP12). The FK506–FKBP12 binary complex formation increases affinity to an effector protein calcineurin and inhibits calcineurin/calmodulin-dependent immune signaling.[42]

Since 14-3-3 proteins are adaptor proteins in cellular processes, not only inhibitors but also stabilizers of their functions could alternate/modulate the cellular responses. However, contrary to the inhibitor case, *de novo* design of stabilizers is difficult, because there are no reliable tactics to design molecules that must interact simultaneously with two partner proteins forming PPI. Therefore, to find out stabilizers for 14-3-3 PPIs from chemical libraries, it is necessary to use binary complexes of 14-3-3 proteins and their client proteins/peptides in high-throughput screening systems. Ottmann *et al*., successfully identified two small-molecule stabilizers by screening 37,000

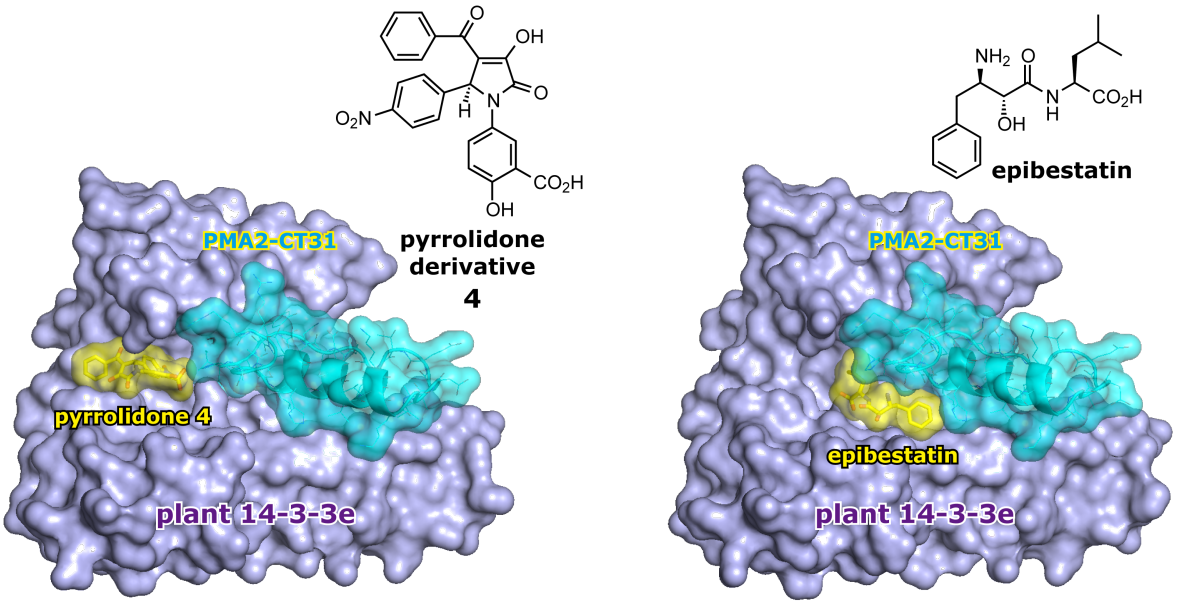

Figure 1−9. Chemical structures of compound **4** and epibestatin and crystal structures of those with the binary complex of plant 14-3-3c and PMA2-CT31 (RRELHTLKGHVEAVVKLKGLDIETIQQSYDI). PPI stabilizers are shown in sticks (C in yellow, N in blue and O in red) with yellow surface, PMA2 and 14-3-3c are shown with cyan and pale purple surfaces, respectively. Coordinates were adopted from PDB files (3M51 for **4** and 3M50 for epibestatin) and figures were created by PyMol.

compounds.[43] They immobilized PMA2-CT52 (the C-terminal 52 amino acids of PMA2, a plant P-type H^+-ATPase) fused with gluthathione *S*-transferase (GST) and monitored fluorescence caused by the binding of the tobacco 14-3-3e isoform fused with the green fluorescent protein (GFP). One of two hit compounds was pyrrolidone **4** and the other was epibestatin, a dipeptide. Their binding modes toward the binary complex of 14-3-3c and PMA2 were clarified crystallographically (Figure 1–9). Compound **4** sits deeply into the groove of 14-3-3c but does not have large interactions with PMA2-CT31. Contrary, epibestatin penetrates deeply into the PPI interface of 14-3-3c and PMA2-CT31 as shown in Figure 1–9. With these crystal structures in hand, the authors built up a small focused library around compound **4** and identified more potent stabilizer, a pyrazol derivative **5** (Figure 1–10), for the 14-3-3c/PMA2 PPI. They insisted that compound **5** is a selective 14-3-3/PMA2 stabilizer, since it did not stabilize 14-3-3/c-Raf$^{229–268}$ and 14-3-3/p53$^{319–393}$ complexes.[44]

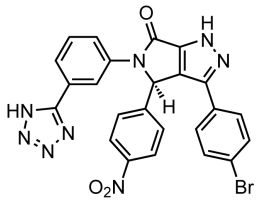

Figure 1−10. Chemical structure of pyrazol **5**.

Prior to the above-mentioned screening studies, it has been known that naturally occurring diterpene glycoside, fusicoccin A (FC-A: Figure 1–11), strongly stabilizes the 14-3-3/PMA2 complex. Historically, FC-A was isolated from a phytopathogenic fungus, *Phomopsis amygdali* (formerly known as *Fusiccocum amygdali*) as a phytotoxin responsible for the wilting disease

caused by the fungus on peach and almond trees.[45,46] Successively, Sassa *et al*. isolated cotylenin A (CN-A: Figure 1–11), a diterpene glycoside structurally closely related to FC-A, as a cytokinin-like bioactive compound from *Cladosporium* sp. 501-7W.[47] These are the representative members of a class of diterpenoids having a 5–8–5 tricyclic ring system (fusicoccane diterpene skeleton). Both of FC-A and CN-A have strong phytohormone-like activity, such as induction of stomatal opening, cell enlargement, internode elongation and seed germination.[48] At the cellular level, FC-A increases H^+-extrusion and K^+-uptake through activation of plasma membrane transport, the P-type H^+-ATPase.[49] These activities attracted much attention and led extensive investigations to identify the target protein. In 1994, three groups independently reported that a member of 14-3-3 proteins is the FC-binding protein.[50–52] Mechanism of action for

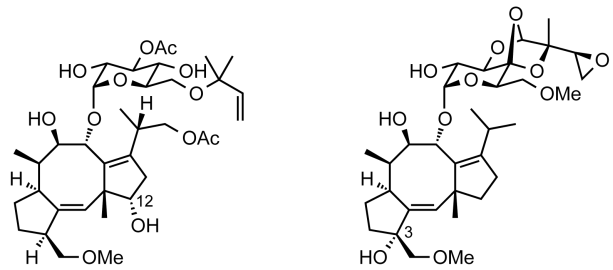

Figure 1−11. Chemical structures of fusicoccin A (FC-A) and cotylenin A (CN-A).

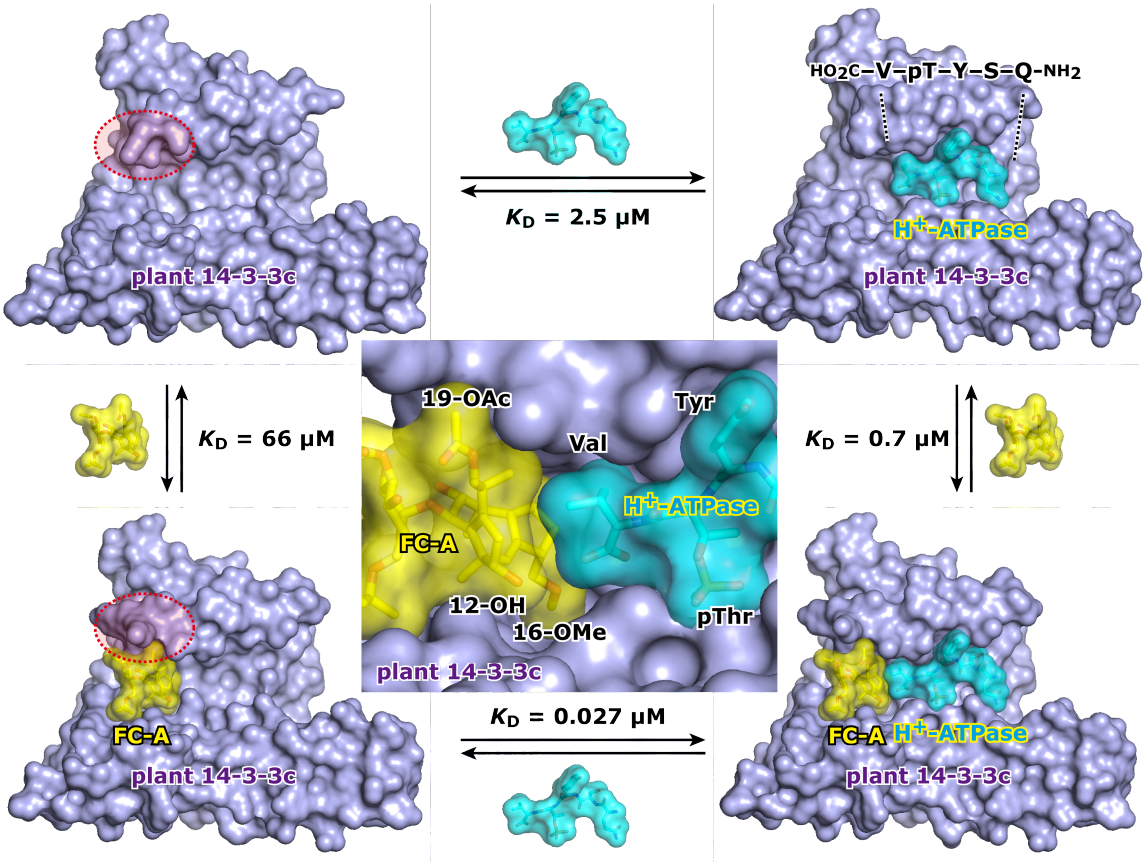

Figure 1−12. Crystal structures of plant 14-3-3c (upper-left, PDB ID: 1O9C), the binary complexes with C-terminal (QSYpTV) peptide of H^+-ATPase (upper-right, 1O9D), with FC-A (lower-left, 1O9E) and the ternary complex (lower-right, 1O9F). The close-up view of the interface between FC-A and H^+-ATPase in the ternary complex is shown at the center. Transparent red circles indicate the most deviated regions of 14-3-3c by complex formation. Figures were created by PyMol.

the activation of H^+-ATPase was clarified at the molecular level by crystallographic analysis of the ternary complex composed of FC-A, plant 14-3-3c and the C-terminal peptide of H^+-ATPase.[53] In Figure 1–12, shown are the crystal structures of apo-14-3-3c (upper-left), the binary complex of 14-3-3c and the C-terminal peptide of H^+-ATPase (NH_2–Gln–Ser–Tyr–phosphoThr–Val-COOH) found in eight isoforms among eleven isoforms of *Arabidopsis thaliana* (upper-right), the binary complex of 14-3-3c and FC-A (lower-left) together with the ternary complex of 14-3-3c, H^+-ATPase and FC-A (lower-right). These structures revealed that i) the peptide is captured by the binding groove of 14-3-3c with a usual mode as a mode 3 client, ii) FC-A sits into the peptide-unoccupied space of the binding groove, iii) van der Waals contact between FC-A and the peptide seems to contribute to the stabilization of the ternary complex and iv) structural changes of 14-3-3c by the complex formation are limited only in the side-chain conformation of the C-terminal α-helix (αI). Thermodynamic analysis of the complex formation was also carried out by isothermal titration calorimetry (ITC) [53] and the K_D values are shown together in Figure 1–12. These values suggest that FC-A targets not 14-3-3c (K_D = 66 μM) but the binary complex of 14-3-3c and the H^+-ATPase (K_D = 0.7 μM). Therefore, FC-A can be regarded as a stabilizer of PPI between 14-3-3 protein and its client. It has been also demonstrated that CN-A forms a stable ternary complex with a 14-3-3 protein and H^+-ATPase peptide.[54] Consequently, since H^+-ATPase (PMA2) is activated by association of 14-3-3 protein, it has been an accepted explanation that stabilization of the activatory complex is responsible for phyto-hormone like activities of FC-A and CN-A.

1–5. Anticancer Activities of Cotylenin A

As mentioned above, 14-3-3 proteins are ubiquitously expressed and highly conserved in all eukaryotic cells. They modulate diverse physiological processes by forming association complexes with a variety of client proteins. With these facts and the result that FC-A and CN-A stabilize 14-3-3 PPI, one can anticipate that these natural products may also affect on human cells. In 1998, Asahi *et al*. reported that CN-A induces differentiation of murine (undifferentiated M1) and human promyelocytic leukemia (HL-60) cells.[55] Such differentiation-inducing activity of CN-A was further investigated by Honma *et al*. and it has been clarified that, by treatment with CN-A, i) HL-60 cells were morphologically differentiated towards monocytes and macrophages, ii) KG-1 (human acute myeloid leukemia cells) and ML-1 (human myeloblastic leukemia cells) were also differentiated and expressed CD14 that is a marker of monocytic differentiation, iii) NB4 and HT-93 (human

acute promyelocytic leukemia) cells were also differentiated, iv) human monocytoid leukemia (U937, THP-1, P39/Fuji and JOSK-M) cells were induced to differentiate, but v) K562 (human erythromyeloblastoid leukemia) and HEL (human erythroleukemia) cells were not differentiated effectively. These results indicate that CN-A preferentially induces the monocytic differentiation of myeloid leukemia cells.[56] CN-A effectively induces differentiation not only of cultured cell lines but also of acute myeloid leukemia (AML) cells that were freshly isolated from patients in primary culture. Functional and morphological differentiation was induced in 9 out of 12 cases by treatment of CN-A and this effect was significantly enhanced by a combination use of vitamin D_3.[57] Furthermore, administration of CN-A significantly prolonged the survival of SCID mice inoculated with NB4 cells. In an *in vivo* analysis, CN-A induced the differentiation of leukemia cells in a retinoid-resistant leukemia model. Therefore, authors suggested that CN-A could be useful for differentiation therapy of retinoid-resistant leukemia.[58]

During the course of studies on combination therapies, Honma *et al*. found that CN-A suppresses the growth of several human lung cancer cells, such as A549, PC7, PC9, PC14 and ABC-1 (adenocarcinoma), EBC-1 and LK2 (squamous cell carcinoma), Lu65 and Lu99 (large cell carcinoma) and Lu135 and H69 (small cell carcinoma), synergistically with a combination of interferon-α (INF-α). With this combination therapy, death receptor 5 (DR5) and tumor necrosis factor-related apoptosis-inducing ligand (TRAIL) were significantly up-regulated and, therefore, cancer cells were led to apoptosis. Since normal cells usually express decoy receptors for TRAIL, normal human small airway epithelial (SAE) and normal human bronchial epithelial (NHBE) cells were much less sensitive against the combination treatment of CN-A and INF-α. In fact, the combination therapy inhibited the growth of human lung adenocarcinoma (PC-14) as xenografts on mice completely without any apparent adverse effects.[59] The combination of CN-A and INF-α was also effective against many other solid tumors. Among examined 39 cancer cell lines, ovarian cancer cells were highly sensitive to the combined treatment *in vitro* and *in vivo*. The differential growth-inhibition patterns of the combined treatment against a human cancer cell line panel did not correlate with those of any other drugs, suggesting that CN-A plus INF-α has a unique mode of action on cancer cells.[60]

Significant feature of CN-A is laid in the fact that it suppresses the growth of cancer cells synergistically not only with INF-α but also with rapamycin on human breast cancer cell line (MCF-7)[61] or with an anti-EGFR antibody (cetuximab) on human epithelial carcinoma cell line (A431) of which HRas was mutated to have a cetuximab resistance (A431–HRasG12V).[62] In both

cases, synergistic suppression by the combination therapy was effective against xenografts on mice.

Thus, CN-A has unique anticancer activities with favorable features. However, modes of actions of CN-A on human cells are not clarified yet.

1–6. Anticancer Activities of Fusicoccin Derivatives

Contrary to those of CN-A, biological activities of FC-A are disappointingly low towards animal cells. In 2003, Levin *et al*. reported that FC-A randomizes the asymmetry of the left-right axis during early development of *Xenopus* embryos. By gain-of-function and loss-of-function experiments, amphibian 14-3-3ε seemed to take an important role in early aspect of the left-right patterning and FC-A seemed to act as an inhibitor for the function of 14-3-3ε.[63] De Boer *et al*. examined the combination effects of FC-A with IFN-α according to the protocol reported by Honma *et al*. [59,60] (*vide supra*). Although the authors claimed that the combination therapy of FC-A and IFN-α is also effective and suppresses the tumor growth synergistically especially on ovarian cancer cell line (OVCAR3), there are several different features compared with CN-A case. While CN-A alone did not show cytotoxicity towards cancer cell lines, FC-A clearly has cytotoxicity; IC_{50} = 17.6 μM against OVCAR3 cells.[64] The cytotoxicity of FC-A was observed not only towards solid tumors but also towards non-adherent HL-60 cells.[65]

As described in the preceding section, CN-A shows desirable anticancer activities such as differentiation-induction on leukemic cells and apoptosis-induction on many solid tumors by the combination with IFN-α. However, CN-A cannot be provided from natural sources anymore because the CN-producing fungus lost its proliferative ability. Therefore, our laboratory has been deeply involved in obtaining FC derivatives that have the same biological activities with those of CN-A. The structure-activity-relationship (SAR) studies on FC derivatives revealed that the deletion of the 12- and 19-hydroxyl groups is necessary to show the differentiation-inducing activity on HL-60 cells, *i.e.*, while 16-*O*-methylfusicoccin H (16-*O*-Me-FC-H) derivative (ISIR-005), which can be semi-synthetically derived from natural FC-H,[66] showed differentiation-inducing activity, 12-deoxy-FC-A type of derivative (ISIR-020) and fusicoccin J (FC-J)[67] type of derivative (ISIR-021) did not exhibit this activity.[65] Contrary to the differentiation-inducing activity, up-regulation of DR5 in A549 cells was observed by the combination treatment with ISIR-021 and INF-α but not with ISIR-005 and INF-α, suggesting that either 3- or 12-hydroxyl is necessary for the apoptosis induction.[65] ISIR-042 having a rearranged sugar moiety showed similar activities with

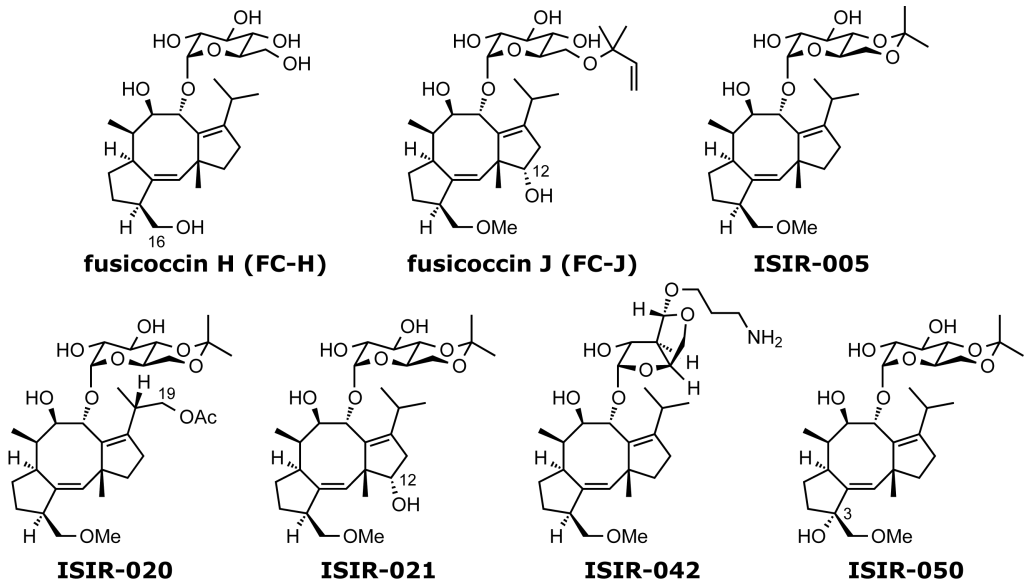

Figure 1−13. Chemical structures of natural fusicoccins (FC-H and FC-J) and several semi-synthetic fusicoccin derivatives (ISIR-005, ISIR-020, ISIR-021, ISIR-042 and ISIR-050).

ISIR-005 but it showed a unique hypoxia-selective cytotoxicity as its characteristic feature.[68]

ISIR-050, of which aglycone has the same chemical structure with that of CN-A, showed the differentiation-inducing activity towards HL-60 cells and the apoptosis-inducing activity on A549 cells in the combination therapy with the up-regulation of DR5. Therefore, ISIR-050 can be regarded as a complete mimic of CN-A. Cell-death by the apoptosis induction in the combination therapy was rescued by *si*RNA of 14-3-3ζ. This result strongly suggested that the stabilization effect of CN-A or ISIR-050 onto a certain 14-3-3 PPI is involved in the apoptosis induction. Furthermore, it has also been revealed that proto-oncogene protein c-Akt (=RAC-alpha serine/threonine-protein kinase; Akt/PKB) was deactivated by the combined treatment of CN-A or ISIR-050 with IFN-α.[65]

As mentioned above, there are several evidences suggesting that 14-3-3 PPIs are the targets of CN/FC class of compounds responsible for the anticancer activities of these diterpenoids. Recently, de Doer and Ottmann *et al*. reported that the C-terminus of estrogen receptor alpha F domain (ERα-F) is the client of 14-3-3 proteins in phosphorylation dependent manner. It has been demonstrated that the penultimate Thr^{594} is the phosphorylation site in the breast cancer cell line MCF-7 and FC-A stabilizes the binary complex composed of 14-3-3 protein and ERα-F. The authors claimed that stabilized PPI of 14-3-3 protein and ERα-F prevents the dimerization of ERα and, therefore, FC-A affects negatively on ERα–DNA interactions, the transactivation by ERα and ERα-dependent cell growth of MCF-7.[69] Since the C-terminus of ERα-F, ^{591}FPApTV^{595}-COOH, is a typical mode 3 client of 14-3-3 proteins similar to that of plant H^+-ATPase, CN-A should exhibit

the same effect on ERα-F. Actually, CN-A alone also suppresses the growth of MCF-7 to some extent. However, the growth inhibition by either FC-A or CN-A alone on MCF-7 was not strong enough to prevent tumor growth effectively. Furthermore, the synergistic growth inhibition of rapamycin was observed only with CN-A[61] but not with FC-A.[64] Therefore, although stabilization of the interaction of 14-3-3 protein and ERα-F by FC-A might contribute partly to anticancer activities of FC/CN, whole mechanism of action has not been clarified yet.

Ottmann, Kato and Schuler *et al*. also proposed that the PPI between the inhibitory phosphorylation sites of c-Raf is the target of CN-A. In fact, CN-A stabilized the binary complex of 14-3-3ζ and the peptide having two activatory sites of c-Raf, ^{229}QHRYpSTPHAFTFNTSSPSSEG SLSQRQRSTpSTPNVH^{264}, through a ternary complex formation but did not stabilize the 14-3-3 PPI with the activating interaction site, ^{618}RSApSEPSL^{625}, of c-Raf.[62] However, this inhibitory sites-selective stabilization by CN-A cannot be the main reason for the synergistic growth inhibition by cetuximab and CN-A on Ras-mutated cancer cells (*vide supra*), judged from a large discrepancy between the effective concentrations of CN-A observed in the stabilization of the binary complex *in vitro* and in the synergistic effects with cetuximab *in vivo*; EC_{50} > 60 μM and EC_{50} < 1 μM, respectively.

1–7. Client Selectivity of Fusicoccin Derivatives

As mentioned in the preceding section, several 14-3-3 PPIs are proposed to be the targets of FC/CNs. On the other hand, the multitarget-nature of this class of compounds makes the target-identification difficult. It is quite plausible that FC/CNs target several 14-3-3 PPIs simultaneously because more than 200 of 14-3-3 PPIs are working in cells to control diverse physiological processes. Therefore, to select the considerable 14-3-3 PPIs responsible for a certain phenotypic outcome, it is desirable to know the client selectivity of FC/CNs prior to further investigations of target-identification.

As shown in Figure 1–12, the i + 1 (adjacent to the phosphorylation site) residue contacts with the aglycone of FC/CNs. Therefore, it is plausible that FC/CNs have an i + 1 residue selectivity. Ohkanda *et al*. applied "Tosyl Chemistry"[70] to provide a biological tool that is capable of detecting 14-3-3 proteins in response to their binding to phosphorylated ligands.[71] The tool (042-BODIPY, Figure 1–14) has a fluorescent tag onto ISIR-042 through spacers that bring the reacting site within the spacer near to His164 of 14-3-3ζ in the ternary complex. Labeling efficiencies were evaluated

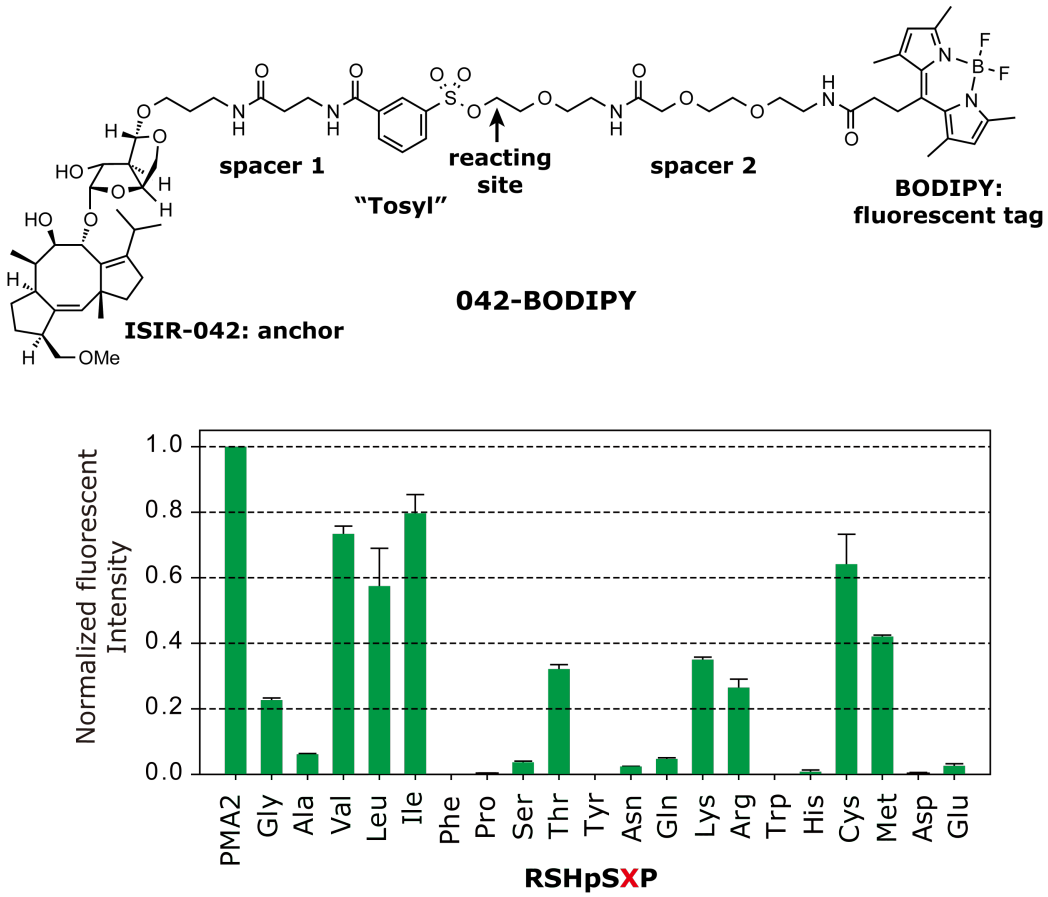

Figure 1−14. Chemical structure of 042-BODIPY (upper) and efficiencies of fluorescent transfer from 042-BODIPY to 14-3-3ζ in the presence of indicated phosphopeptides. Fluorescent intensities were read out from SDS-PAGE-gel images and normalized with that of PMA2 used as a positive control (lower).

by measuring the fluorescent intensity from labeled 14-3-3ζ on SDS-PAGE after incubating 042-BODIPY with recombinant 14-3-3ζ in the presence or absence of the PMA2 phosphopeptide, ETIQQSYpTV. With this experiment, it has been confirmed that 14-3-3ζ was labeled efficiently by 042-BODIPY in the presence of PMA2, whereas no fluorescent transfer occurred when the peptide was absent. Thus the formation of the ternary complex is the determining factor for the labeling reaction. Fluorescent transfer site of 14-3-3ζ was unambiguously clarified to be His164 as designed because fluorescent intensity of the 14-3-3 band was much reduced for a point mutated 14-3-3ζ–His164Ala. Taking advantage of cell-permeability of 042-BODIPY, the phosphorylation-dependent labeling method was successfully applied to selective labeling of 14-3-3 proteins in cells. According to the prediction that the residue at position i + 1 of the phosphopeptides should have a major influence on the stability of the ternary complex, a series of mode 1 type of hexapeptides, RSHpSXP, each containing one of the 20 amino acids at position X (X = i + 1) were evaluated by measuring fluorescent intensity in each case using 042-BODIPY. As shown in Figure 1-14, use of peptides containing Val, Leu, or Ile at position i + 1 resulted in high labeling efficiency, suggesting

that the FC-derived anchor, ISIR-042, well stabilizes the binary complex of 14-3-3ζ with either one of these three phosphopeptides. This result is consistent with the fact that FC/CNs show phyto-hormone like activities towards most of all higher plants of which C-termini of H^+-ATPases are deviated among isoforms as YpTV, HpTV, YpTL or YpTI.[53] Besides in the cases of Val, Leu and Ile, the diterpenic core of ISIR-042 can stabilize 14-3-3 PPIs with hexapeptides having Cys, Met, Thr or unpredictably having Lys and Arg at their *i* + 1 positions, judged from fluorescent transfer efficiencies. In contrast, peptides containing small or bulky side chains, such as Gly, Ala, Ser, Phe, Pro, Tyr, Asn, Gln, Trp, His, Asp or Glu, were not significantly stabilized, suggesting that van der Waals interaction between the diterpenic core of FC derivatives and the side chain of *i* + 1 residue of the client peptide contributes largely to the stability of the ternary complex. These results are consistent with the stabilizing effect of CN-A against two distinct binding sites of c-Raf. As described in section 1–6, CN-A stabilized the inhibitory binding site in c-Raf of which *i* + 1 is Thr but did not stabilize the activating site having Glu at *i* + 1 position.

Taken all of these results together, it can be concluded that FC/CNs have the selectivity intrinsically for medium sized hydrophobic residues at *i* +1 of clients in 14-3-3 PPIs.

1–8. Semi-synthetic Mode 3 Selective Stabilizer

The preceding example demonstrated that designed FC-derivatives can be biological tools to understand physiological events through their stabilizing effects on 14-3-3 PPIs. Another example was reported recently by Higuchi, Daut and Ottmann *et al*.[72]

Previously, the difference of biological activities of CN-A and FC-A towards animal cells were explained hypothetically by possibility that 12-hydroxy group of the latter sterically conflicts with Pro at *i* + 2 position in mode 1 and mode 2 motifs.[54] If this assumption is correct, a FC-derivative that have a sterical bulkiness around its C-ring could be a mode 3 selective stabilizer of 14-3-3 PPIs. Since mode 3 clients in human cells are quite few,[11] such derivative is anticipated to be a good tool to clarify physiological role of the association complexes of 14-3-3 proteins and mode 3 clients. Combined with the intrinsic selectivity of FC/CNs for Val at *i* + 1 position, Higuchi *et al*. selected the 14-3-3/TASK-3 (*vide infra*) PPI as their research target and synthesized FC-THF (Figure 1–15) semi-synthetically from FC-J. As anticipated, FC-THF stabilized the binary complex of 14-3-3σ and the phosphorylated C-terminus peptide, ^{370}RRKpSV^{374}–COOH, of TASK-3. In contrast, but also anticipated, FC-THF did not stabilize any binary complexes of 14-3-3σ with internal binding

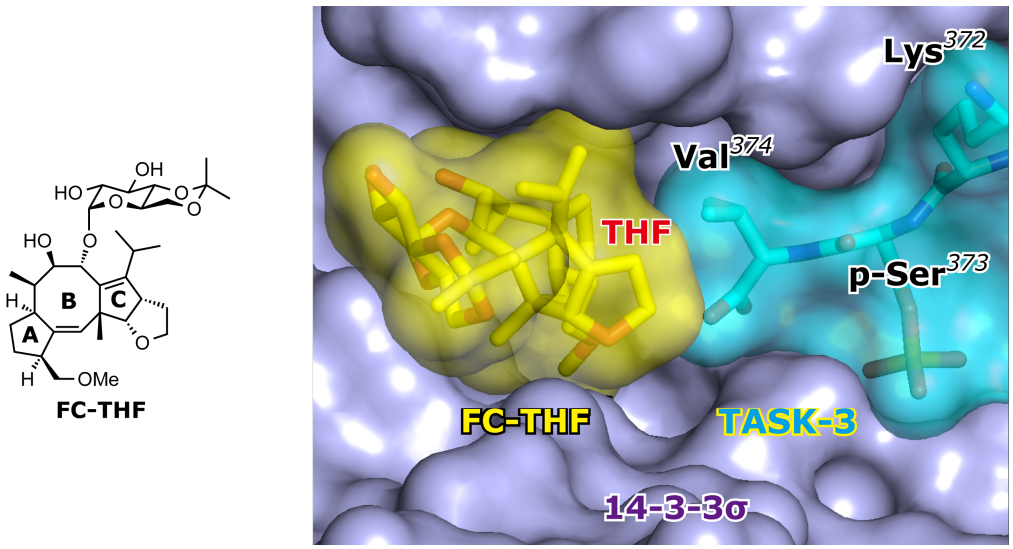

Figure 1−15. Chemical structure of FC-THF and close-up view of the interface of FC-THF (C in yellow and O in red with yellow surface) and C-terminal phosphopeptide of TASK-3 (C in cyan, O in red, N in blue and P in orange with cyan surface) in the binding groove of 14-3-3σ (ζ isoform like mutations; C38V and N166H) with pale purple surface (PDB ID: 3SPR). Figure was created by PyMol.

motifs, such as c-Raf (^{254}SQRQRSTpSTPNVH^{264}), Cdc25B (^{302}QRLFRSPpSMPCSVIR^{316}) and Chibby (^{15}PRKSApSLSNLH^{25}). Rationale for the mode 3 selectivity of FC-THF was given by the crystal structure of the ternary complex. As shown in Figure 1–15, the THF ring fused onto the C-ring of the fusicoccane skeleton overhangs the *i* + 1 Val so that any client peptides that have an *i* + 2 residue are not acceptable with FC-THF.[72]

TASK-3, **T**WIK (**t**andem pore domain **w**eak **i**nward rectifying $\mathbf{K}^+$ channel)-related **a**cid **s**ensitive $\mathbf{K}^+$-channel 3, is a two-pore-domain (K_{2P}) potassium channel[73] and is thought to be involved in cancer development, inflammation, ischemia and epilepsy.[74] And it has been clarified that the association of 14-3-3 protein with TASK-3 promotes the trafficking of the channel to the surface of plasma membrane[75] because the binding of 14-3-3 protein masks a strong endo-plasmic-reticulum (ER) retention signal (^{369}KRR^{371}) overlapped with the 14-3-3 binding site.[76] Therefore, stabilization of the binary complex of 14-3-3 protein and TASK-3 by FC-THF is anticipated to increase functional expression of the channel at the surface of plasma membrane. In fact, FC-THF clearly enhanced the surface expression of TASK-3, which was heterogeneously expressed in oocytes of *Xenopus laevis*, together with increase of outward potassium currents.[72] This is the first example that the rationally designed small molecule gave phenotypic outcome as expected through stabilization of the selected 14-3-3 PPI.

1–9. Research Objective

FC/CNs act as stabilizers of several, if not many, 14-3-3 PPIs as described. This multitarget-nature might be a drawback for drug development and for target-identification of a specific biological activity caused by FC/CNs. However, paradoxically, the mutitarget-nature of natural and/or semi-synthetic fusicoccins could be advantageous for clarification of physiological roles of several, if not many, 14-3-3 PPIs. Since information about SAR of FC/CNs and their client selectivity has been accumulated, rather reliable prediction is now possible to link phenotypes to client features involved in responsible 14-3-3 PPIs. For example, up-regulation of the death receptor (DR5) is observed in combination use of IFN-α with either FC-A or CN-A, but not with ISIR-005. This information makes it possible to predict that mode 3 client is involved in the 14-3-3 PPI and 12-OH in FC-A and 3-OH in CN-A must have additional stabilization effect on the 14-3-3 PPI.

In this research, ISIR-005 was selected as a biological tool. This 3,12-unsubstitued FC-derivative is structurally different from ISIR-021 (12-OH type) and ISIR-050 (3-OH type) in hydroxylation pattern of diterpenic core (*see* Figure 1–13). ISIR-005 alone showed slight cytotoxicity towards solid tumors, whereas ISIR-021 and ISIR-050 did not exhibit cytotoxicity. Therefore, this research deals with identification of the 14-3-3 PPI that is responsible for phenotypic outcome caused only by 3,12-unsubstituted fusicoccin derivatives in conjunction with their characteristic client selectivity in stabilization of 14-3-3 PPIs.

Chapter 2: Characteristic Anti-tumor Activities of ISIR-005, a 3,12-Unsubstituted Fusicoccin Derivative

2–1. Introductory Statements

During structure-activity-relationship (SAR) studies of anticancer activities of FC/CNs, it was recognized that natural/semi-synthetic fusicoccin derivatives can be categorized by the hydroxylation-patterns of their aglycones. As shown in Figure 2–1, they are categorized into three groups; 3-hydroxy derivatives, 12-hydroxy derivatives and 3,12-unsubstituted derivatives.[65] 3-Hydroxy derivatives, such as CN-A and ISIR-050, showed differentiation induction on HL-60 cells and apoptosis induction on solid tumors in the combined use of INF-α through up-regulation of DR5. 12-Hydroxy derivatives, FC-J and ISIR-021, did not show differentiation-inducing activity but showed up-regulation of DR5 in the presence of INF-α. Contrary, 3,12-unsubstituted derivatives, ISIR-005 and ISIR-042, showed differentiation induction on HL-60 cells similar to the cases of 3-hydroxy derivatives. They also suppressed tumor growth with the combination of INF-α.

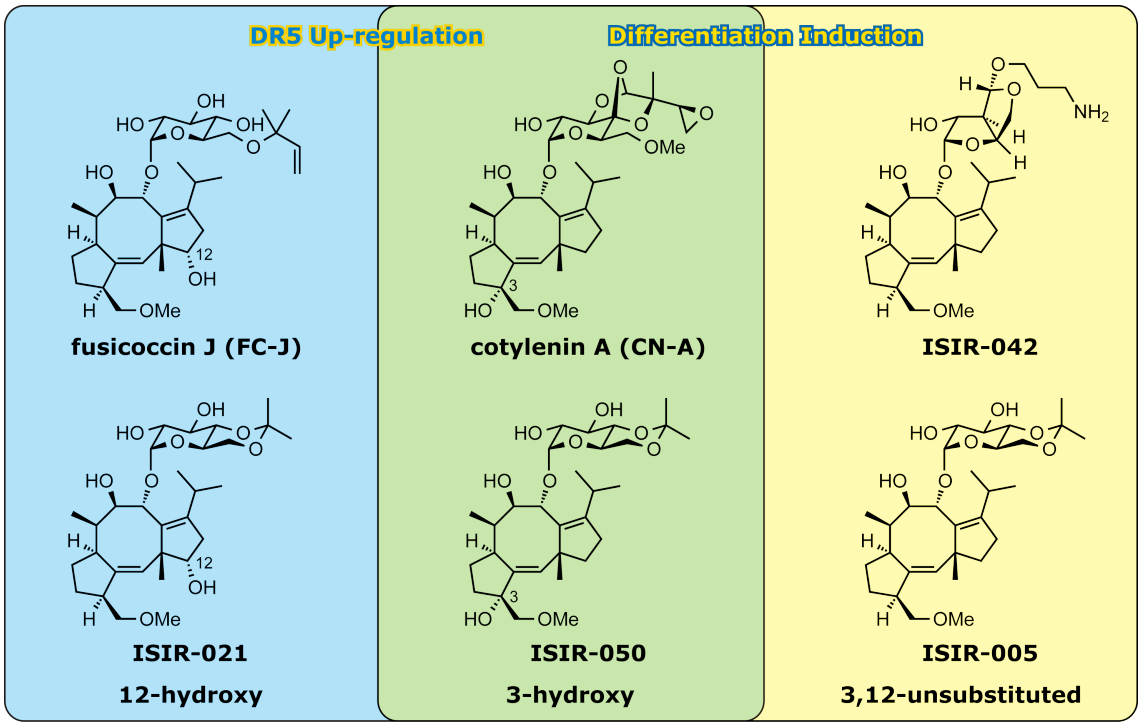

Figure 2–1. Categorization of FC/CN derivatives based on the hydroxylation patterns of aglycones and their characteristic anti-tumor activities.

However, effects of the combination therapy seemed to be only additive effects. These additive effects were clearly different from the synergistic effects caused by the combination of 3-hydroxy derivatives and INF-α. Actually, 3,12-unsubstituted derivatives did not up-regulate DR5 in the presence of INF-α.[65]

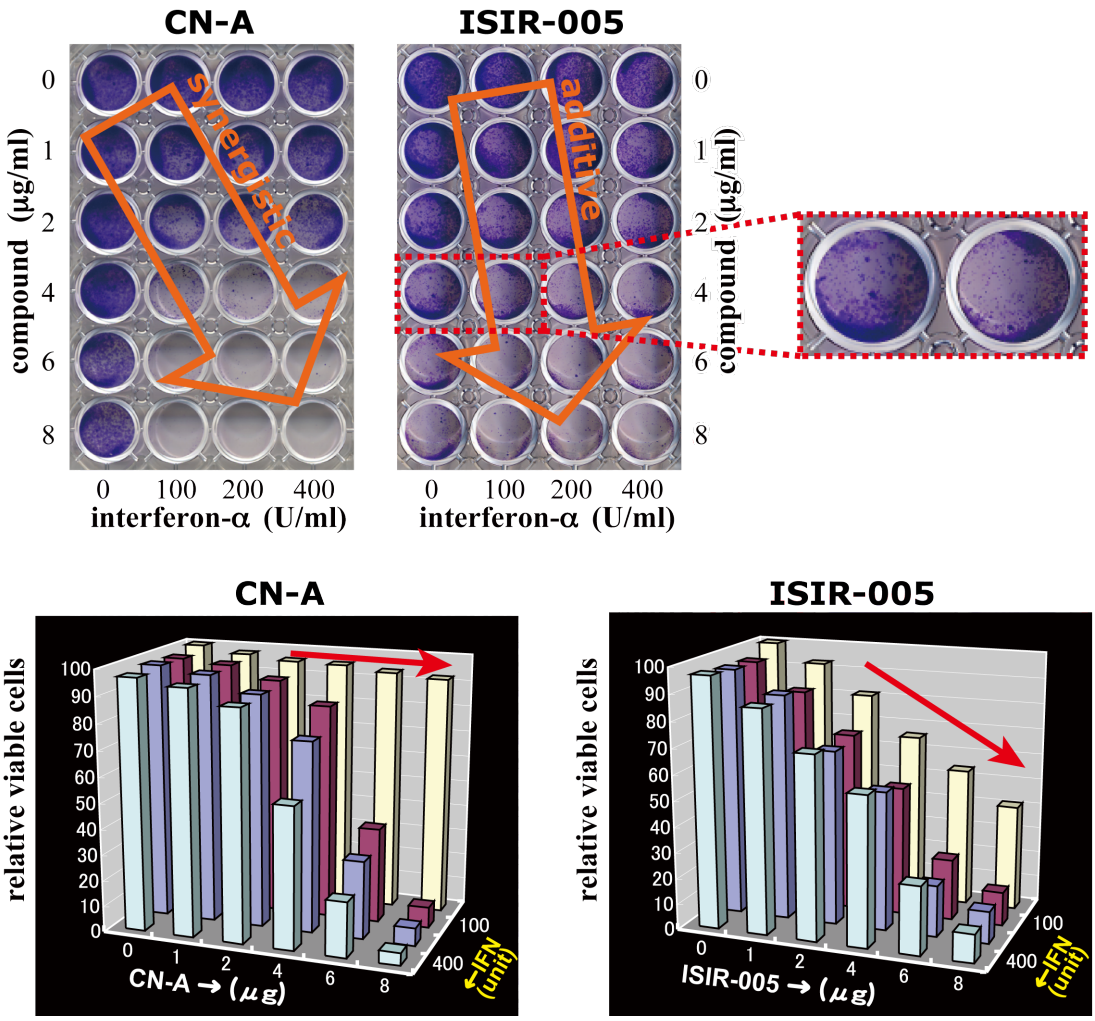

Figure 2−2. The cell growth inhibition of the combined treatment on A549 cells by CN-A or ISIR-005 with IFN-α. A549 cells (1.0×10^4 cells/mL) were cultured with the compound and IFN-α at indicated concentrations for 7 days. After incubation, the cells were stained with Giemsa (upper) or MTS (lower) solution.[65]

Results of Giemsa staining and MTS [3-(4,5-dimethylthiazol-2-yl)-5-(3-carboxymethoxyphenyl)-2-(4-sulfophenyl)-2H-tetrazolium] assays on A549 cells are shown in Figure 2–2. These results show not only the additive effect of ISIR-005 and INF-α but also show that ISIR-005 alone has cytotoxicity against A549 cells. Furthermore, the cytotoxicity of ISIR-005 was clearly enhanced at the central part of wells. This type of cell death is often observed in anoikis (*an-o-EE-kis*; Greek, meaning the state of being without a home)[77] that is known as an anchorage-dependent apoptosis. A549 is a cell line from human lung tumor epithelial cells and is reported to be resistant towards anoikis.[78,79] Anoikis resistance is not A549 specific nature but, in general, is common feature for metastatic tumor cells to invade other organs. Therefore, if cytotoxicity of ISIR-005 is indeed brought by anoikis, it is worth to be investigated in detail to clarify potency of ISIR-005 as an anti-metastatic agent.

2–2. Results

2–2–1. Cell death induced by ISIR-005

As mentioned, A549 cell line was used in this research as an anoikis resistance model. To investigate the effect of ISIR-005 for cell viability, lactate dehydrogenase (LDH) assays were conducted at 5-hrs and 4-days treatments with ISIR-005, FC-A or CN-A. LDH assays can determine the degree of plasma membrane damage by evaluating leakage of LDH form cytoplasm.

ISIR-005 alone induced cell death of A549 cells and the cell death was rescued partially by a caspase-8 inhibitor (CBZ-Ile-Glu(Ome)-Thr-Asp-(Ome)-fluoromethylketone; Z-IETD-FMK)[80] at 4-days (Figure 2–3). CN-A did not induce the cell damage both in 5-hrs and 4-days treatments. FC-A induced cell damage but, contrary to the case of ISIR-005, the caspase-8 inhibitor did not rescue the cell death. Therefore, FC-A seemed to induce not apoptosis but necrosis. In general, anoikis is induced *via* caspase-8 activation by cell-detachment.[81] LDH assays indicated ISIR-005

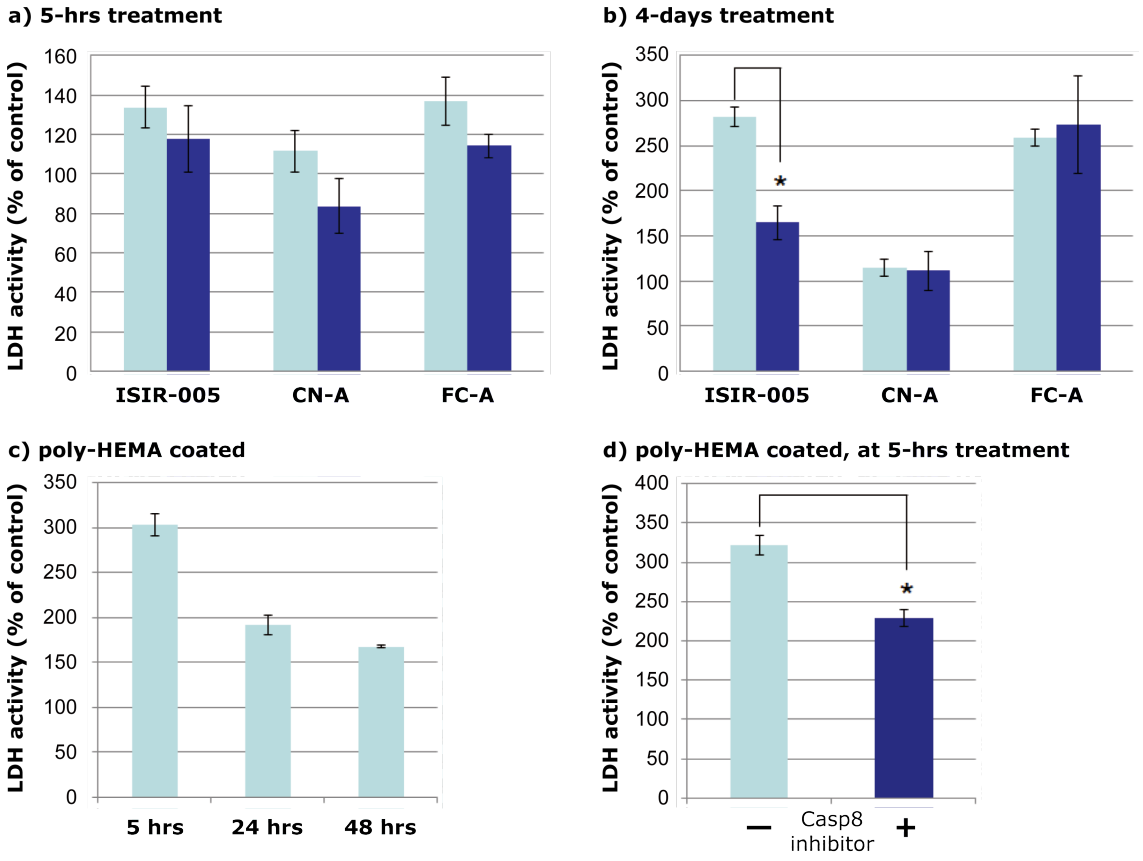

Figure 2–3. The cell death of A549 cells caused by FC/CNs under cell adhesion conditions or floating conditions. a), b) The cell death induction with ISIR-005, CN-A or FC-A at 5-hrs and 4-days treatments. c), d) the cell death induction by ISIR-005 under the adhesion-inhibited conditions. Light and Dark blue bars indicate the degree of LDH leakage with or without Caspase-8 inhibitor, respectively. A549 cells (5.0×10^4 cells/mL) were cultured with compounds (8 μg/mL) for indicated periods on normal plates (a and b) or poly-HEMA coated plates (c and d). Mean ± S.D., n = 3, * $p < 0.05$, t-test, one-sided.

has potential to induce anoikis on A549 cells. Above-mentioned assays were conducted under conditions that cell adhesion processes could be involved. In fact, cell adhesions were observed even after 4-days incubation. Therefore LDH assays under adhesion-inhibited conditions were conducted. To this end, the assay plates were coated with poly 2-hydroxyethyl methacrylate (poly-HEMA) for inhibiting cell adhesions prior to LDH assays.[82] The cell death by ISIR-005 treatment was also confirmed in poly-HEMA coated plates (Figure 2–3). Relative LDH activity of treated wells versus control wells decreased time-dependently (Figure 2–3c). This result, in which difference of LDH activity between with and without ISIR-005 was largest at 5-hrs treatment, was obtained because control cells were gradually deathbed in the floating conditions. Moreover, caspase-8 inhibitor rescued partially from ISIR-005 induced cell death again under the floating conditions (Figure 2–3d). Taken together, it can be concluded that the cell death induced by ISIR-005 is independent of the cell adhesion.

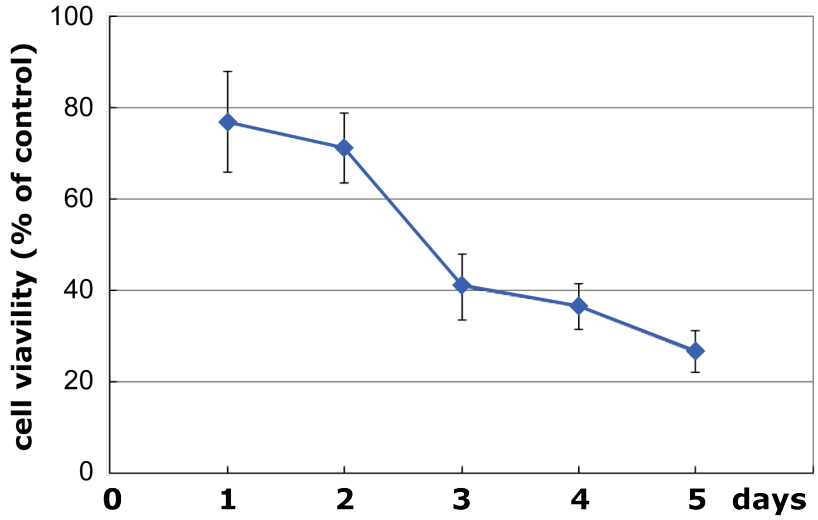

Figure 2−4. Cell viability of A549 cells treated by ISIR-005 in adhesion state. A549 cells (4.0×10^4 cells/mL) were cultured for 12 hrs without compound, and then incubated in the presence of ISIR-005 (4 μg/mL). After indicated periods of incubation, cell viability was evaluated by MTS assays. Mean ± S.D., n=5.

Then it was evaluated whether ISIR-005 also induces cell death against cells in adhesion state. A549 cells were cultured for 12 hrs on 96-well plates until adhesion was completed and, then, were treated with ISIR-005. The amount of cell death was evaluated by MTS assays. As shown in Figure 2–4, the ISIR-005 induced cell death in adhesion state was observed at 2 to 3 days after the treatment. Therefore, the ISIR-005 treatment gives more significant and rapid effects on A549 cells in floating state (less than 5 hrs; Figure 2–3c) than in adhesion state (ca. 3 days; Figure 2–4). These results indicated that ISIR-005 induces the anchorage-dependent apoptosis, *i.e.*, anoikis, on A549 cells and might affect to cell adhesion processes too.

2–2–2. Effects of ISIR-005 on cell–cell adhesion

In general, cell adhesion is classified to two classes, cell–cell adhesion and cell–ECM (extracellular matrix) adhesion. The cell–cell adhesion is achieved by formation of a homo- or hetero-dimer of adhesion molecule/protein on cell surface between a cell and its adjacent cells. This dimerization has selectivity and cell–cell adhesion regulates finely many cell events, such as cell differentiation, embryo formation and immune response.[83] Cadherin is a transmembrane-type adhesion molecule, which forms a homo-dimer depending on Ca^{2+} concentration.[84] Cadherin superfamily is composed of more than 30 subtypes that have been identified in a variety of cell lines.[85] Among them, it was reported that N-cadherin and E-cadherin regulate metastasis of cancer cells.[86] Therefore, cadherin-assay was performed to investigate the effect of ISIR-005 on cell–cell adhesion regulated by cadherin superfamily. ISIR-005 and other FC derivatives did not affect at all on the cell–cell adhesion as shown in Figure 2–5, in which photographs were taken at 7-hrs incubation after treatment with compounds. The similar results were obtained at 0.5, 2, 4 and 10-hrs incubation (data not shown). These results suggested that any of FC/CNs do not affect on cell–cell adhesion mediated by cadherins.

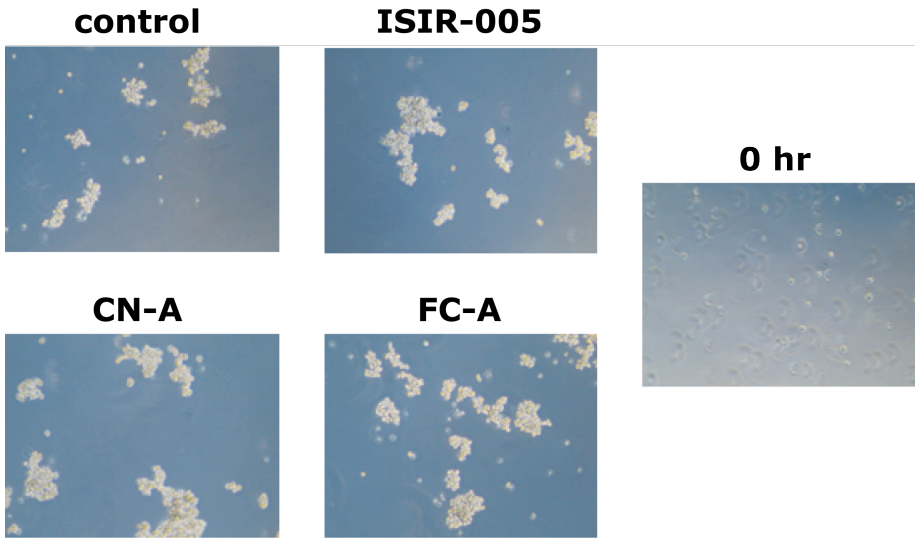

Figure 2−5. The effects of ISIR-005, CN-A and FC-A on cell–cell adhesion of A549 cells. A549 cells (5.0×10^4 cells/mL) were cultured with shaking at 100 rpm for 10 hrs in the presence of indicated compounds at 8 μg/mL. The photographs were taken at 0.5, 2, 4, 7 and 10 hrs. Shown here are those taken after 7-hrs incubation.

2–2–3. Effects of ISIR-005 on cell–ECM adhesion

The extracellular matrix (ECM) consists of a complex mixture of structural and functional macromolecules, and serves several important roles, such as regulation of growth, development,

wound repair, signal transduction and differentiation, and maintenance of cell structure and its function.[87] The cell–ECM adhesion, mediated by integrins and adaptor proteins, provides both physical and regulatory links between the ECM and the cellular microfilament system. The cell–ECM adhesion is also deeply related with events involved in cell migration.[88]

The effects of ISIR-005 and CN-A on cell–ECM adhesion were estimated by evaluating cell numbers attached onto normal plates in the presence of compounds as a simplest model. ISIR-005 significantly inhibited attachment of A549 cells onto the plate at 1-hr incubation with the concentration of 4 μg/mL (Figure 2–6). On the other hand, CN-A showed no inhibitory effects on cell-attachment and even reversely seemed to accelerate cell-attachment on to the plate. These

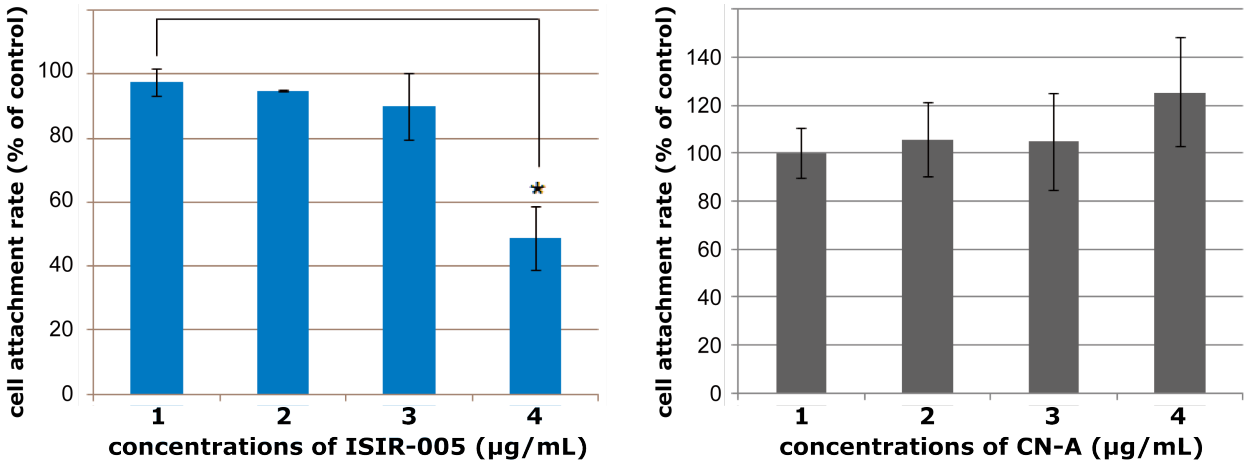

Figure 2–6. Cell attachment assays with ISIR-005 (left) and CN-A (right). A549 cells (3.0×10^5 cells/mL) were cultured with compounds at the indicated concentrations for 1 hr. Attached cells were evaluated by MTS assay. Mean ± S.D., n=3, * $p < 0.05$, t-test, one-sided.

results clearly suggest that ISIR-005 inhibits the cell–ECM adhesion. This inhibitory activity on A549 cells is another characteristic feature of ISIR-005, a 3,12-unsubstituted fusicoccin derivative, as well as the anokis-inducing activity.

By using optical microscope, adhered-cell shapes were observed under treatment of ISIR-005, CN-A and FC-A (Figure 2–7). The cell attachment was observed from 6-hrs incubation in the cases of control, CN-A and FC-A. After 12-hrs incubation, attachment was confirmed only for control and CN-A cases. In contrast, cell attachment on the plate was not observed at any periods of incubation in the case of ISIR-005 and cell death was observed from 6-hrs incubation. The cell death was also observed at 24-hrs incubation in the case of FC-A. Thus ISIR-005 inhibited cell attachment and induced cell death at 6-hrs incubation after treatment, whereas FC-A induced cell death but did not inhibit cell attachment. Consequently, these morphological observations also confirmed that anoikis induction and cell-attachment inhibition are specific activities of ISIR-005.

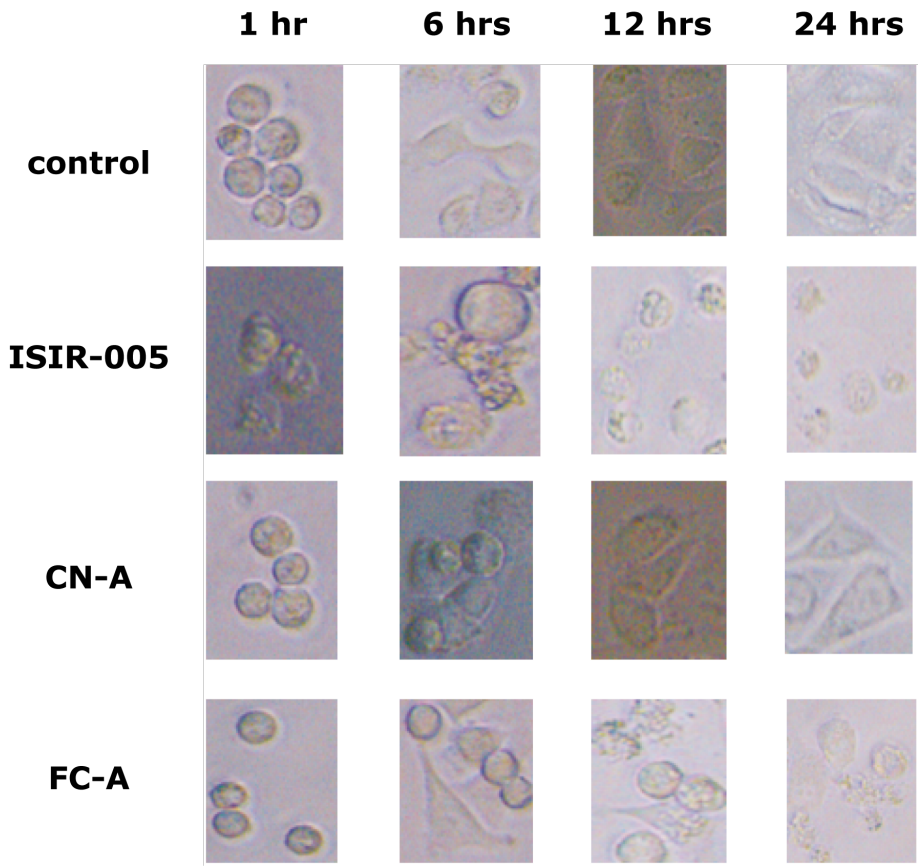

Figure 2−7. The effect and time-course changes of cell adhesion in the presence of ISIR-005 (2nd panels), CN-A (3rd panels) or FC-A (4th panels). ISIR-005 inhibited adhesion even at 24-hrs incubation. A549 cells (5.0×10^4 cells/mL) were cultured with compounds at 8.0 μg/mL. Photographs were taken at indicated periods of incubation.

2–2–4. Involvement of 14-3-3ζ in the effects of ISIR-005

Among isoforms of 14-3-3 proteins, ζ isoform is regarded to have oncogenic characters and is believed to contribute anti-apoptotic nature of many cancer cells.[18,23–28] It has been also reported that 14-3-3ζ is up-regulated in A549 cells,[89] and down-regulation of 14-3-3ζ suppresses anchorage-independent growth of A549 cells through anoikis activation.[19] Furthermore, this isoform is involved in an apoptosis induction caused by CN-A + IFN-α treatment.[65] To investigate the involvements of 14-3-3ζ in cell death and in inhibition of cell attachment, cell damage assay (LDH-assay) and cell adhesion assay (MTS assay) were conducted in the conditions that 14-3-3ζ was knockdowned by *si*RNA (Figure 2–8). After confirming that 30 nM of *si*RNA is enough to down-regulate the expression of 14-3-3ζ (Figure 2–8c), assays were carried out in the presence or absence of ISIR-005. However, *si*RNA itself affected much in these experimental conditions, especially for the cell adhesion assay, probably because 14-3-3ζ is involved in many physiological processes that are inevitable for survival of cancer cell lines. Therefore, although it is difficult to

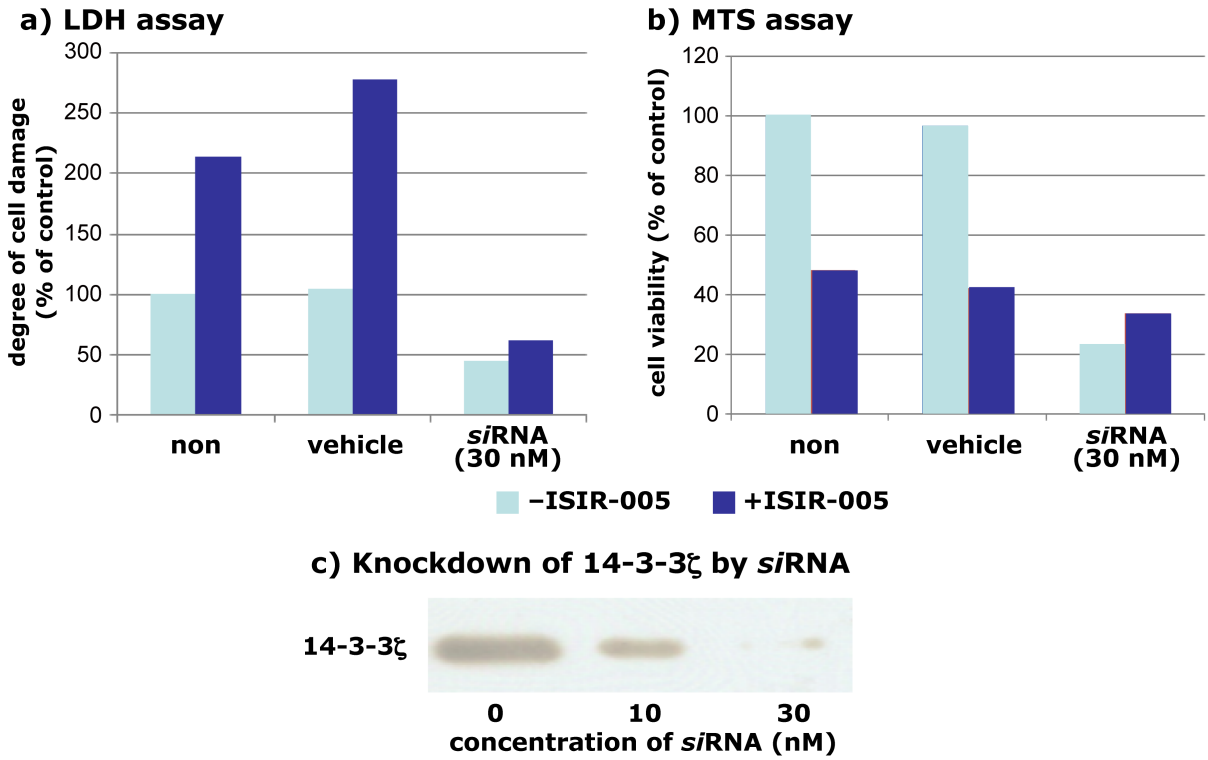

Figure 2−8. The effects of 14-3-3ζ knockdown in cell death and inhibition of cell attachment induced by ISIR-005. 14-3-3ζ was knockdowned for A549 cells with *si*RNA (30 nM), which was used for cell death assay (LDH assay) and cell adhesion assay (MTS assay). The light and dark blue bars indicate the results obtained without or with ISIR-005, respectively. a) LDH assay for cell death detection under 14-3-3ζ knockdown or not at 5-hrs incubation. b) MTS assay for cell adhesion estimation under 14-3-3ζ knockdown or not at 1-hr incubation. c) Western bolt of 14-3-3ζ in the presence of *si*RNA with indicated concentrations. The knockdown was confirmed before assays were conducted. The knockdowned or intact A549 cells (5.0×10^4 cells/mL) were cultured. Concentration of ISIR-005 used is 8.0 μg/mL. Mean, n = 2.

make conclusions with certainty, the knockdown of 14-3-3ζ rescued A549 cells partially from cell death (Figure 2–8a). In the MTS assay, *si*RNA alone affected largely on cell attachment of A549 cells to the plate (Figure 2–8b). Therefore, it was impossible to make a judgment on rescue-effect of *si*RNA toward inhibition of cell adhesion by ISIR-005. This phenomenon suggested that 14-3-3ζ takes an important role for cell adhesion. Nonetheless, the cell death caused by ISIR-005 was canceled by *si*RNA suggesting that 14-3-3ζ was a mediator of ISIR-005 induced cell death signaling in A549 cells.

2–2–5. Inhibition of cell migration by ISIR-005

Wound-healing assay is often used to estimate metastatic nature of cancer cells. Therefore, wound-healing assay was conducted for scratched A549 cells. The confluent cells were scratched,

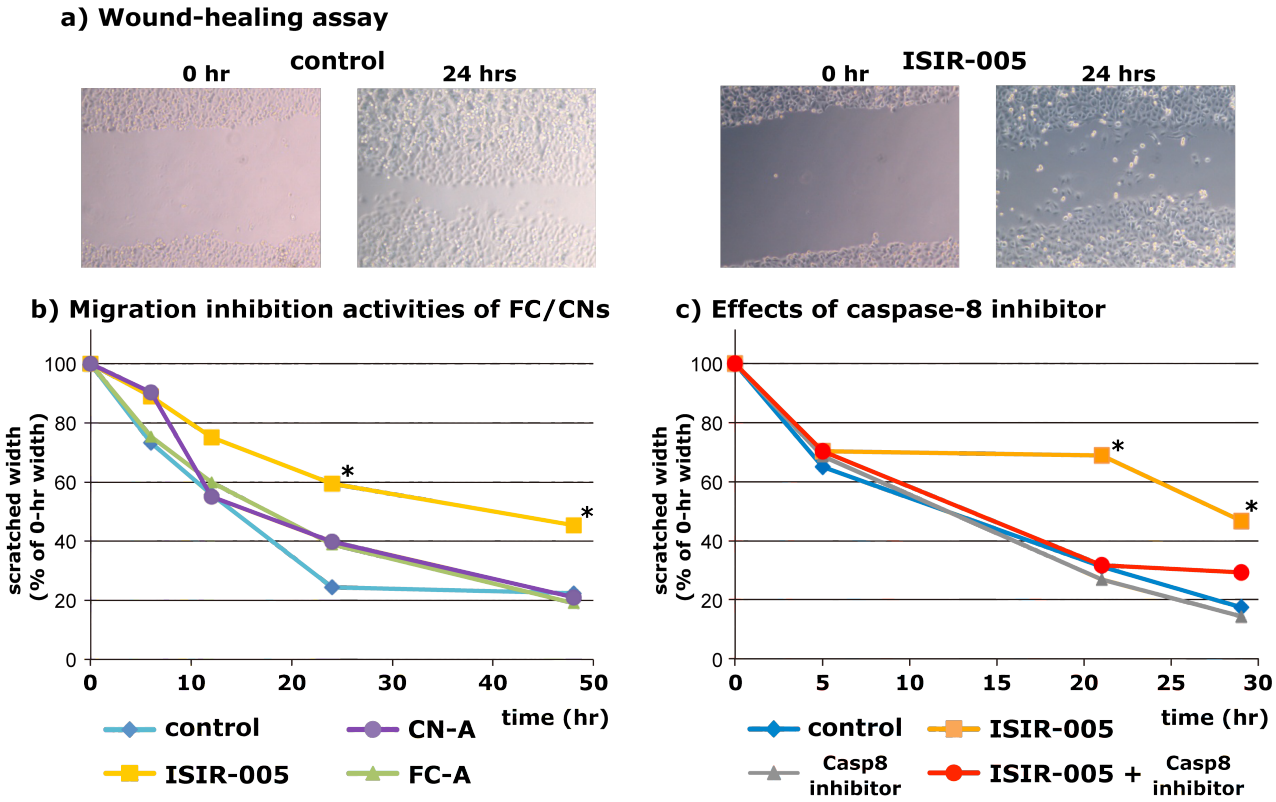

Figure 2−9. The effect on cell migration of FC/CNs evaluated with the wound-healing assay. A549 cells (3.0×10^5 cells/mL) were cultured in the presence of indicated compounds at 8.0 μg/mL. a) photographs of wound-healing assay for control and ISIR-005. b) Time-dependent changes of the scratched width in the presence of ISIR-005, CN-A and FC-A. Mean, n=3, *p < 0.05, turkey-test versus control, one-sided. c) The effect of caspase-8 inhibitor (1.0 μM) for migration-inhibition caused by ISIR-005. Mean, n=3, *p < 0.05, turkey-test versus control, one-sided.

and then treated with compounds. The migration potency was evaluated by measuring the width of unrecovered area of the scratch (Figure 2–9). In the control, scratch was recovered almost completely at 24-hrs incubation. In the cases of FC-A and CN-A, the scratches were fully recovered within 48 hrs indicating that these compounds do not have a significant migration-inhibitory activity for A549 cells. FC-A induced cell death probably by induction of necrosis (*vide supra*), but such activity of FC-A is independent from cell migration. In contrast, ISIR-005 showed inhibitory activity toward cell migration of A549 cells. These results indicated that migration inhibition was a specific character of ISIR-005 among FC/CN derivatives.

One type of anoikis proceeds *via* activation of caspase-8[81] and ISIR-005 induced cell death was partially canceled with the caspase-8 inhibitor (Figure 2–3). Similar to this result, the caspase-8 inhibitor canceled the inhibitory activity of ISIR-005 toward cell migration (Figure 2–9c).

It was revealed that ISIR-005 has potentials such as cell death induction against both of adhered and floating cells, cell–ECM adhesion inhibition and cell migration inhibition. Cell death might be

occurred in floating state, with which cell adhesion was inhibited. Consequently, ISIR-005, a 3,12-unsubstituted fusicoccin derivative, is a unique FC/CN derivative that has anoikis-related and migration-inhibitory activities toward A549 cells.

2–3. Discussion

FC/CNs have a variety of anti-tumor activities. The differentiation induction on HL-60 cells is one of common features for 3-hydroxy derivatives and 3,12-unsubstituted derivatives, whereas the up-regulation of DR5 in the presence of INF-α is commonly observed for 3-hydroxy derivatives and 12-hydroxy derivatives (*vide supra*). These characteristic features gave information about clients of 14-3-3 PPIs involved in the corresponding phenotypes. Since 12-hydroxy derivatives can stabilize binary complex composed of only mode 3 type of clients and 14-3-3 proteins, the client involved in DR5 up-regulation must be a mode 3. Reversely, the client responsible for differentiation induction may be mode 1 or mode 2, because 12-hydroxy derivatives did not afford this phenotypic outcome.

In the above-mentioned context, 3-hydroxy derivatives and 3,12-unsubstituted derivatives should afford similar phenotypic outcome, because both can stabilize binary complexes composed of 14-3-3 proteins and all of mode 1 to 3 clients. Actually, in collaboration with Dr. Kasukabe, Saitama Cancer Center, it has been revealed that both of CN-A (a 3-hydroxy derivative) and ISIR-005 (a 3,12-unsubstituted derivative) inhibit rapamycin-induced phosphorylation of c-Akt in MCF-7 cells and suppress the growth of MCF-7 synergistically with rapamycin.[90] However, as mentioned, ISIR-005 cannot induce DR5 up-regulation in the presence of INF-α. Therefore, there are clearly differences in client selectivity between CN-A and ISIR-005.

This research paid attention to the cytotoxicity of ISIR-005, a 3,12-unsubstituted fusicoccin derivative. By LDH assay, it has been confirmed that ISIR-005 induces cell death of A549 cells *via* apoptosis, because the cell death was partly rescued by a caspase-8 inhibitor (Figure 2–3). The cell death induction by ISIR-005 was more effective toward the floating state than the adhesion state of A549 cells (Figure 2–3) suggesting that ISIR-005 induces anoikis. CN-A, a 3-hydroxy derivative, did not show any cytotoxicity and FC-A, a 12-hydroxy derivative, caused cell death of A549 cells but through necrosis not through apoptosis. Therefore, anoikis induction is one of characteristic activities of ISIR-005. It has been also suggested that 14-3-3ζ is involved in anoikis induction, because *si*RNA for 14-3-3ζ rescued A549 cells from the cell death (Figure 2–8). Cell attachment to the plate as a model of cell–ECM adhesion was also inhibited by ISIR-005 but not by CN-A and

FC-A (Figures 2−6 and 2–7). Probably the inhibition of cell adhesion is related to anoikis induction. ISIR-005 also inhibited cell migration of A549 cells in wound-healing assay. Again this activity is characteristic in ISIR-005 because CN-A and FC-A did not show clear inhibition of the healing.

Thus it has been found that ISIR-005, a 3,12-unsubstituted fusicoccin derivative, induces anoikis-related and migration-inhibited phenotypic outcomes of A549 cell line that was used as an anoikis resistant model. In the following chapters, deeper insights on these characteristic activities of ISIR-005 are discussed.

2–4. Materials and Methods

Materials

Instruments used in this research are as follows; for absorption measurements on 96-well plates, micro plate reader Model 680 (BIO-RAD, Hercules, CA) with filters allowing 490 and 570 nm to transmit; for Western blotting analysis, X-Omat 1000 Processor (KODAK, Rochester, NY) was used to detect chemiluminescence; for optical measurement, microscope Leica DM IL (Leica Microsystems, Wetzlar, Germany) for cell culture, CO_2 incubator MCO-19AICUVH-PJ (Panasonic).

The cultured cell line (A549) was kindly gifted from Prof. Yoshio Honma, Shimane University. RPMI-1640 (Sigma) supplemented with 10% fetal bovine serum (e.g. Dainippon-Sumitomo Pharma) was necessary for cultivation of A549 cells. For the most of assays, a treatment of phosphate buffered saline (D-PBS(–)) was necessary and D-PBS(–) was purchased from Wako or Gibco.

For cell adhesion evaluation, Cell Titer 96® (Promega, Madison, WI) was used. For cell death evaluation, Cytotoxicity Detection Kit^{Plus} (LDH) (Roche) was used. For Giemsa staining, Giemsa solution was purchased from Wako. To extract protein from living cells, protease and phosphatase inhibitor cocktails were purchased form Sigma. For determination of protein concentrations, BCA protein assay kit was obtained from Thermo Scientific. Blocking reagent, coating reagent and bovine serum albumin were purchased from Sigma. For visualization of chemiluminescence, ECL Plus Western blotting detection reagent was obtained from GE healthcare (Buckinghamshire).

Fusicoccin A was isolated from *P. amygdali* as reported before. Cotylenin A was gifted from Prof. Takeshi Sassa, Yamagata University. ISIR-005 was synthesized in Kato Laboratory according to the reported method.[65] These compounds were dissolved in DMSO to be the concentration at 8

μg/mL. Poly (2-Hydroxyethyl Methacrylate) (Poly-HEMA) was purchased from Sigma. *si*RNA for 14-3-3ζ was purchased from Sigma which sequence is shown in Table 2–1.

Table 2–1. The sequences of siRNAs for knockdown of target gene. 'r' means ribose.

Gene name	Sequence
YWHAZ	5'-rGrGUrArCrAUUrGUrGrGrCUUrCrArArATT-3'
(14-3-3ζ)	5'-UUUrGrArArGrCrCrArCrArAUrGUrArCrCTT-3'

Cell culture

A549 cells were regularly maintained in RPMI-1640 supplemented with heat-inactivated 10% FBS and incubated at 37°C in a humidified atmosphere of 5% CO_2 in air. And when cells were grown until nearly 100% confluent, a passage by using the solution containing 0.025% trypsin and 0.01% EDTA and, subsequently, cells were washed, diluted with supplemented basal medium and added into culture flask at concentration of 3500 cells/cm^2.

Poly-HEMA coated plate

Poly-HEMA was solubilized in 95% ethanol at 40°C (120 mg/mL). This solution was added on a 96- or 24-well plate, and evaporated in clean bench at room temperature, and coated plates were stored at 4°C. The wells were washed twice with D-PBS(–) before use.

Cell viability (Giemsa staining)

On a 24-well plate, after cells (1×10^4 cells/mL, 1.0 mL/well) were cultured in the presence or absence of IFN-α and/or indicated compounds at indicated concentrations for 7 days, cells were washed twice with D-PBS(–) and fixed by pre-chilled methanol for 3 min at 0°C. Then, cells were washed with water and were stained with 4% Giemsa solution with water for 2 hrs at room temperature. Finally, supernatant was removed and washed with water again.

Cell death assay (LDH assay)

On a 96-well plate (non-coated or poly-HEMA coated), after cells (5.0×10^4 cells/mL, 0.2 mL/well) were cultured in the presence or absence of a caspase-8 inhibitor (Z-IETD-FMK: 10 μM) and/or indicated compounds at indicated concentrations for indicated periods. The media were separated and centrifuged (4°C, 1000×g, 5 min), and the supernatant (80~100 μL) was added LDH-detection solution. And then the reaction solutions were incubated in dark (at room

temperature) until colorization was completed, and measured absorbance at 490 nm.

Cell adhesion assay (Cadherin assay)

A 24-well plate was incubated with albumin (5% in HEPES(−)) over night, and the well was washed HPES buffer. On the 24-well plate, cells (2.0×10^3 cells/mL, 1.0 mL/well) were cultured in the presence of 1 mM Ca^{2+} and indicated compounds at indicated concentrations for indicated periods with rotary at 80~100 rpm.

Cell adhesion assay (MTS assay)

On a 96-well plate (non-coated or poly-HEMA coated), after cells (3.0×10^5 cells/mL, 0.2 ml/well) were cultured with indicated compound at indicated concentrations for 1 hr, cells were washed twice with D-PBS(–) and exposed to MTS solution. The generated reduced MTS was evaluated by absorbance at 450 nm. Photographs were taken at indicated times in cell culture medium after MTS assay.

Transfection of siRNA

On a 6-well plate, cells (2.5×10^4 cells/mL, 0.5 mL/well) were pre-cultured for 24 hrs, washed with D-PBS(–) twice and RPMI-1640 medium (serum free, 0.5 mL) was added. Besides, to transfect *si*RNA, a mixture including 30 nM of *si*RNA and lipofectamine™ (1.0 μL) in Opti-MEM® (0.1 mL) was added and incubated for 6 hrs at 37°C. After transfection, transfection medium was replaced with complete growth medium (0.5 mL). For confirmation of the effect of *si*RNA, after additional incubation for 24 hrs, cells were lysed and analyzed by immunoblotting according to the Western blotting protocol as described bellow. Meanwhile, to evaluate cell viability, cells were cultured in the presence of indicated compounds at indicated concentrations for indicated periods and were subjected to cell viability assay protocol.

Cell migration assay (Wound-healing assay)

On a 24-well plate, after cells (3.0×10^4 cells/mL, 1.0 ml/well) were cultured for 12 hrs, cells were washed twice with D-PBS(–) and scratched with micropipette chip (for 100 or 200 μL chip was used) in a straight line. Then cells were exposed in the presence or absence of caspase-8 inhibitor (10 μM) and/or indicated compounds at indicated concentrations. Photographs were taken at indicated times (×200). The widths of scratch were measured at three places of unhealed area and the values of their averages were used for the analysis.

Protein extraction

On a 6-well plate, cells (4×10^4 cells/mL, 1.5 mL/well) were incubated in the presence or absence of indicated compounds at indicated concentrations for indicated periods. These cells were washed twice with D-PBS(–) and lysed with buffer 'A' [20 mM Tris·HCl, 140 mM NaCl, 1% (v/v) TritonX-100, pH: 7.4 plus protease inhibitor (complete Mini EDTA-free, Roche) and phosphatase inhibitor (PhosSTOP, Roche)] for 20 min on ice. The resulting suspensions were collected with cell scraper (IWAKI) and centrifuged (15000 ×*g*, 15 min, 4°C) to remove the precipitates, and the supernatant was diluted with 4×Laemmli sample buffer (NuPAGE LDS Sample Buffer, Novex; 4% 2-mercaptoethanol, Wako) and boiled for 5 min at 70°C provided a protein extraction sample. Protein concentration was evaluated with BCA method (Pierce BCA protein assay kit, Thermo).

Western blotting

The protein extraction samples were separated on 4-12% SDS-PAGE (NuPAGE Bis-Tris Gel, Novex; NuPAGE MOPS SDS Running buffer, Novex) with Molecular marker (MagicMark XP, Novex) and transferred onto membrane (Immobilon-P Transfer membrane, Millipore). In the case of using normal primary antibody, membranes were blocked from nonspecific binding by incubation with blocking buffer [5% (v/v) albumin (Albumin from bovine serum, Sigma) in TBST (20 mM Tris·HCl, 140 mM NaCl, pH: 7.4; (BIO-RAD), 0.1% (v/v) Tween-20 (BIO-RAD)] for 12 hrs at 4°C, then incubated with primary antibody diluted with blocking buffer (1: 1000~5000) for 12 hrs at room temperature and washed with TBST three times for 5 min. After a treatment by secondary antibody conjugated with HRP diluted with blocking buffer (1: 5000) for 2 hrs at 4°C, the membrane was washed with TBST three times for 5 min and then visualized by ECL Plus reagent (Pierce Western Blotting Substrate, ThermoFisher Sience).

Chapter 3: Mechanism of Migration Inhibition Induced by ISIR-005

3–1. Introductory Statements and Preliminary Results

In Chapter 2, it was revealed that ISIR-005 induces anoikis of A549 cells. Interestingly, a lot of vacuole or bubble-like structures formed in the cytoplasm from 1-day to 4-days incubation with ISIR-005 treatment (Figure 3–1). These bubble-like structures seemed to be generated through cell blebbing. Cell blebbing is initiated by a combination of events that involve local disruption of membrane–actin cortex interactions, leading to rapid protrusion of the membrane as a result of the cell internal hydrostatic pressure.[91] These cytoskeletal rearrangements are controlled by the Rho

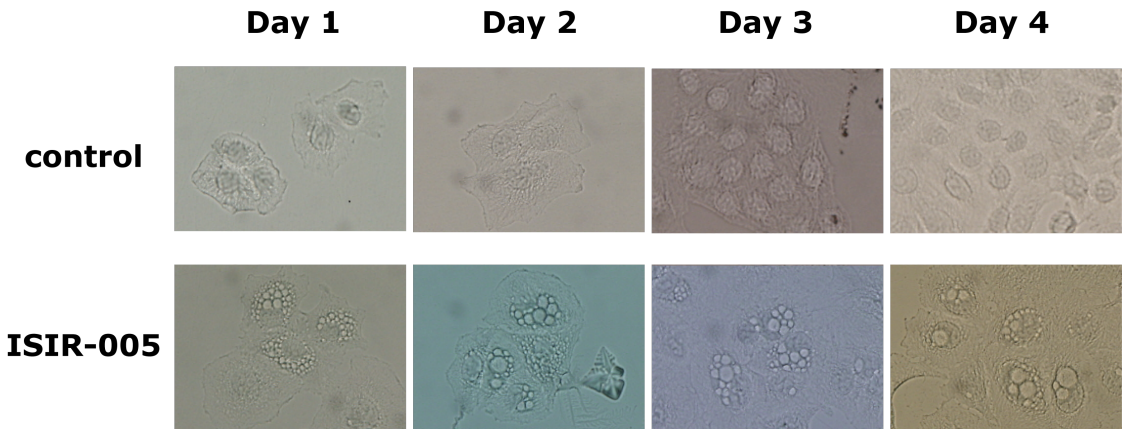

Figure 3–1. The photographs of cell shapes and the blebs in the exposure of transmitted light at 1-, 2-, 3- and 4-days incubation. The upper panel for control cells and the lower panel for ISIR-005 treated cells. The blebs were formed from Day 1 by ISIR-005 treatment. A549 (4.0×10^4 cells/mL) cells were incubated in the presence or absence of ISIR-005 (8 μg/mL) for indicated periods. Cells were fixed with PFA then the photographs were taken under visible light.

family of small GTPases and their downstream signaling cascades, resulting in distinct types of actin-rich invaginations or protrusions such as filopodia, lamellipodia, invadopodia, podosomes,

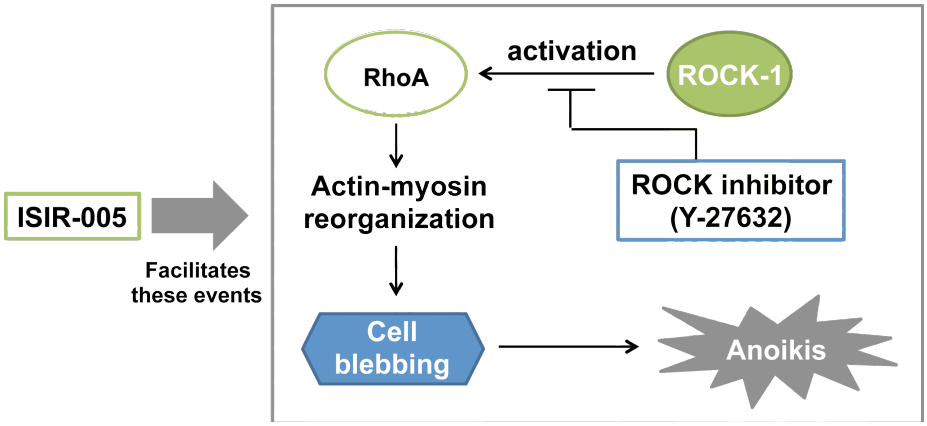

Figure 3–2. A model of anoikis induction by ISIR-005 through RhoA/ROCK-1 induced cell blebbing formation. RhoA induces actin-reorganization following cell blebbing, and then anoikis. ROCK-1 is an effector protein of RhoA.

phagocytic cups, and uropods that serve specialized biological functions.[92] The cell blebbing is primarily regarded as a by-product of apoptotic and necrotic processes.[93–95] Although it has been also proposed that cell blebbing is not essential for the execution of cell death programs,[94,95] experimental resulted here led to a hypothesis that ISIR-005 affected to cytoskeletal remodeling mediated by Rho family, which resulted in the cell blebbing and anoikis (Figure 3–2).

3–2. Results

3–2–1. Cancelation of ISIR-005 effects on A549 cells by a ROCK inhibitor

As proposed in Figure 3–2, it has been suggested that ISIR-005 intervenes in the Rho/ROCK (Rho-associated coiled-coil forming kinase) signaling pathway. If this hypothesis is correct, a ROCK inhibitor should cancel out the cell blebbing and anoikis induction by ISIR-005. As expected, it was confirmed that Y-27632 [(*R*)-(+)-*trans*-*N*-(4-pyridyl)-4-(1-aminoethyl)-cyclohexane-carboxamide], a ROCK inhibitor, canceled significantly the cell blebbing formation in A549 cells induced by ISIR-005 (Figure 3–3).

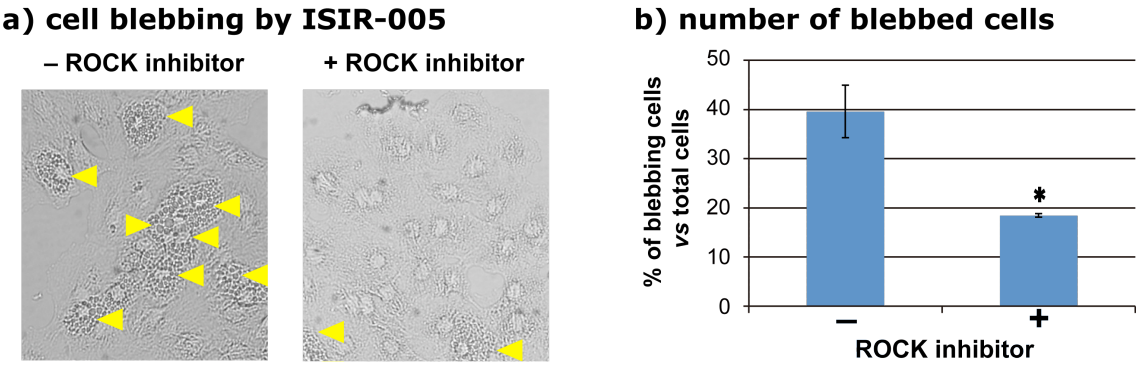

Figure 3–3. The cell blebbing by ISIR-005 in the presence or absence of Y-27632, a ROCK inhibitor, after 4-days incubation. a) Visible light images of cells. The ROCK inhibitor reduced cell blebbing caused by ISIR-005. The yellow triangles indicate the blebbing cells. b) The cell blebbing rate was estimated by counting. The ROCK inhibitor canceled the cell blebbing significantly (n = 3, mean ± S.D., $*p < 0.05$, paired t-test, one-sided). A549 cells (4.0×10^4 cells/mL) were incubated in the presence of ISIR-005 (8 μg/mL) with or without Y-27632 (1 μg/mL). Cells were fixed with PFA (paraformaldehyde) before taking photographs.

Not only the induction of cell blebbing but also the inhibition of the cell adhesion (MTS assay for ECM-attachment cells) and the inhibition of the cell migration (wound-healing assay) induced with ISIR-005 were also canceled partially by the ROCK inhibitor (Figure 3–4 and Figure 3–5, respectively). Therefore, Rho/ROCK signaling pathway may be involved, at least partially, in the anoikis-related and migration-inhibited phenotypic outcomes induced by ISIR-005.

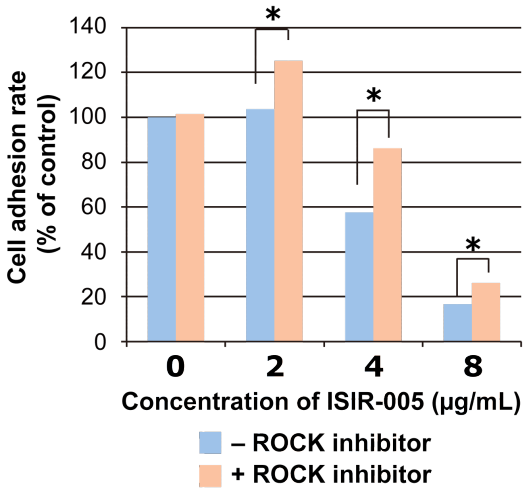

Figure 3–4. The effect of the ROCK inhibitor for cell-adhesion inhibition of ISIR-005. After incubation of A549 cells (3.0×10^5 cells/mL) for 1-hr in the presence or absence of Y-27632 (1.0 μg/mL) with ISIR-005 at indicated concentrations (Mean ± S.D; n = 3, *$p < 0.05$, paired t-test, two-sided).

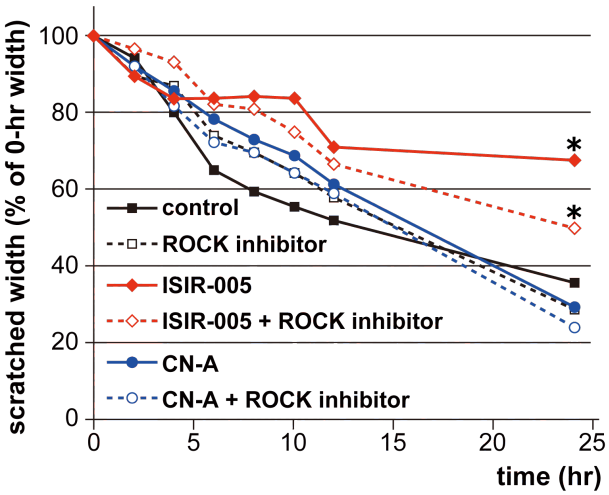

Figure 3–5. The wound healing assay for evaluation of migration-inhibitory activity toward A549 cells. A549 cells (3.0×10^5 cells/ml) were seeded with ISIR-005 or CN (8.0 μg/ml), with/without Y-27632 (1.0 μg/mL) and were incubated. Photographed were taken at 6, 12 and 24-hrs after treatment (Mean; n = 3, *$p < 0.05$, Turkey test) to analyze results.

3–2–2. Effect of ISIR-005 onto localization of Rnd3, an antagonist of RhoA/ROCK-1 signaling

Rnd1, 2 and 3 are proteins belonging to a subfamily of Rho family with unusual properties and functions. Rnd1 and Rnd3 decrease stress fibers, induce cell rounding (hence Rnd for "round") and stimulate cell migration.[96] On the other hand, Rnd2 stimulates cell contraction through activation of RhoA.[97] Among these three members, it has been revealed that Rnd3 (alternative name: RhoE) regulates diverse biological events including actin organization, apoptosis and cell rounding.[98] As one of interesting features, Rnd3 works as an antagonist of RhoA/ROCK-1 pathway.[99] Overexpression of Rnd1 and Rnd3 stimulates p190RhoGAP activity, which reduces the amount of GTP-bound RhoA and decreases stress fibers.[100] Functions and subcellular localization of Rnd3 are regulated by its phosphorylation status and other post-translational modifications. There are multiple phosphorylation sites in Rnd3 by ROCK-1 and PKCα. It is believed that intact Rnd3 is transported into membrane and phosphorylation at Ser210 by PKCα localizes Rnd3 into cytosol.[99,101] Phosphorylation at Ser218 and Ser240 by ROCK-1 is necessary for re-localization of Rnd3 to membrane. Moreover, Rnd3 has another site for post-translational modification; a typical CAAX motif for the farnesyltransferase at its C-terminus. Rnd3 localization is also regulated by farnesylation at Cys241 in the CAAX motif contributing to membrane localization of Rnd3.[101]

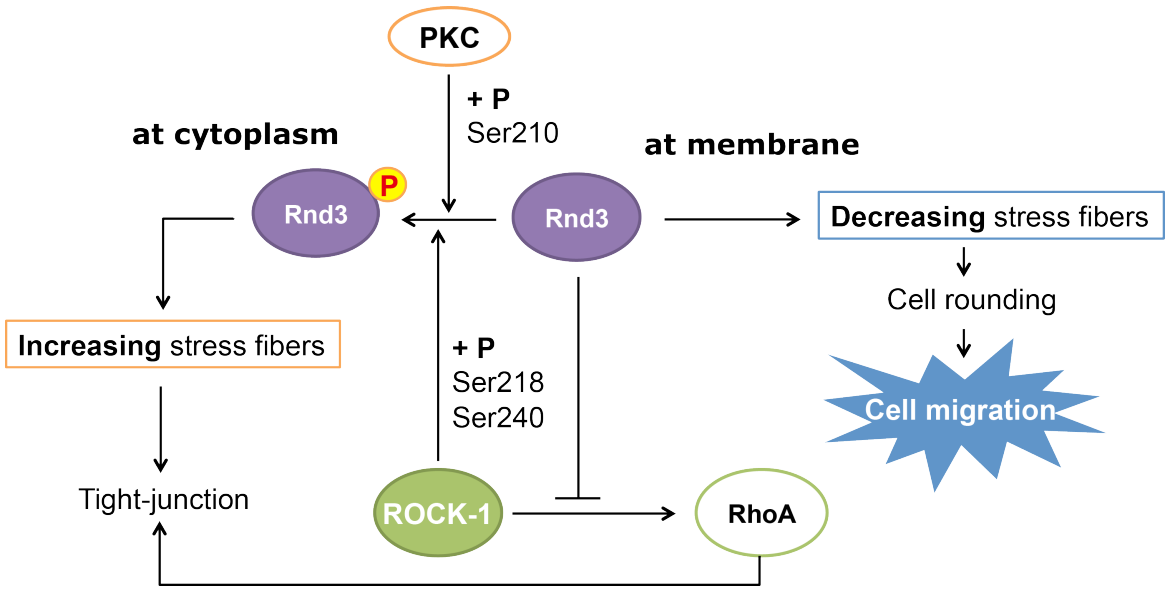

Figure 3–6. The dichotomic character of Rnd3 for the stress fiber formation and the following cell events depending on its subcellular localization. At cytomembrane, Rnd3 deceases stress fibers and increases them at cytoplasm. Activities of Rnd3 are regulated by the post-translational modifications, the phosphorylation and the farnesylation.

Functionally, Rnd3 has a dichotomy in its regulatory characters for stress fiber formation depending on its localization (Figure 3–6). At cytomembrane, Rnd3 induces a loss of actin stress fibers and promotes cell rounding.[102] The cell rounding is known as a step for cell migration. Taken together, Rnd3 facilitates the cell migration *via* the cell rounding in its localization at membrane. On the other hand, Rnd3 induces an increase in stress fibers when it does not localize at membrane.[103] Thus, accumulated information suggests that Rnd3 might be involved in the characteristic migration-inhibition activity of ISIR-005.

Y-27632, a ROCK inhibitor, canceled the migration-inhibition activity of ISIR-005 (Figure 3–5). Therefore, if Rnd3 is involved in these events, it can be speculated that ISIR-005 might affect the expression level and/or the localization of Rnd3, an endogenous ROCK-1 inhibitor. While ISIR-005 did not affect on expression level of Rnd3 in comparison with those of control and CN-A treatment for whole cell proteins (Figure 3–7), the localizations of Rnd3 were greatly altered by ISIR-005 treatment as described below.

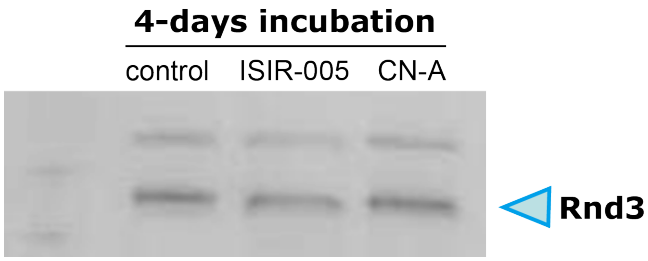

Figure 3–7. The Western blotting of Rnd3 after 4-days incubation of A549 cells in the presence of ISIR-005 or CN-A. A549 cells (4.0×10^4 cells/mL) were incubated with ISIR-005 or CN (8 μg/mL) for 4 days.

A549 cells were seeded in the presence or absence of ISIR-005 (or CN-A used as a reference compound) on non-coated slide glasses. After incubation for certain periods of time, the cells were

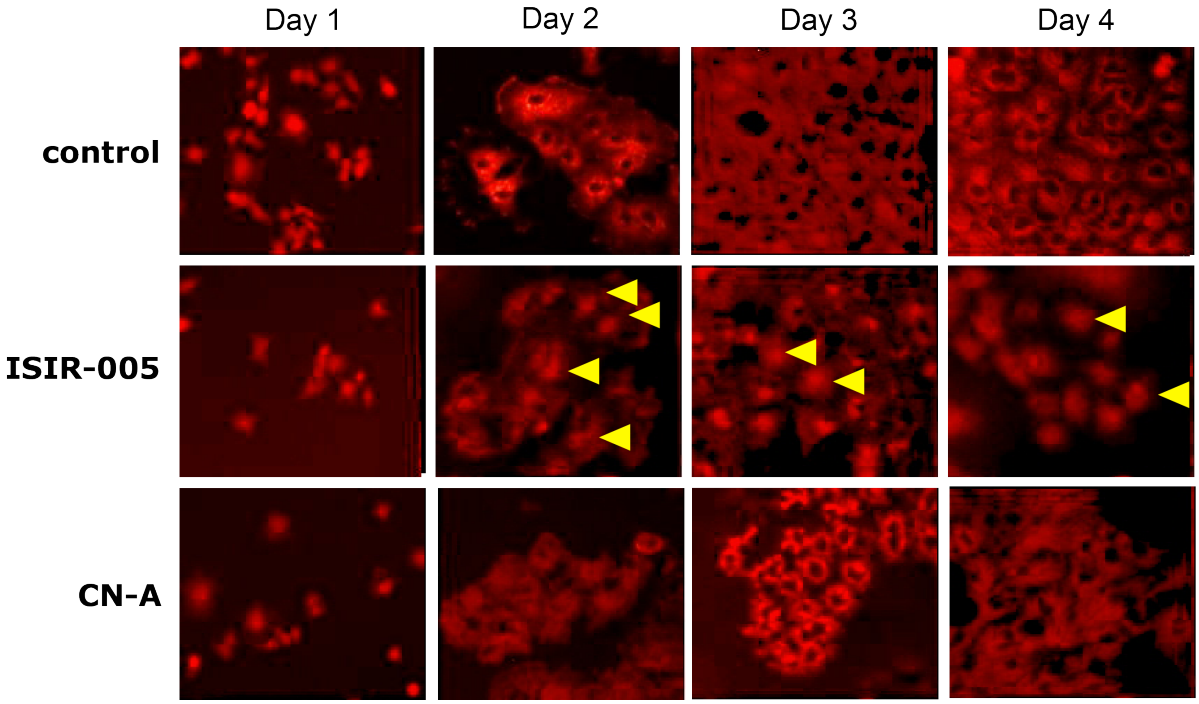

Figure 3–8. The effects of ISIR-005 or CN-A on subcellular localization of Rnd3. At day 1, Rnd3 localized at nuclei in all cells (Left panels). ISIR-005 forced Rnd3 to be retained at nuclei even 4-days incubation (middle panels, yellow triangles). A549 cells (5.0×10^4 cells/mL) were incubated in the presence of ISIR-005 or CN-A (8 μg/mL). After incubation, the cells were fixed with PFA and the protein was stained with 1st antibody and AlexaFluro546 conjugated 2nd antibody (546 nm, ×200).

fixed and the localization of Rnd3 was visualized by immunostaining (Figure 3–8). At the beginning of incubation (Day 1), most Rnd3 localized in the nuclei. After incubation (Day 2 to Day 4), in control and CN-treatment, Rnd3 spread throughout the cell except the nucleus as expected for normal proliferative status. In clear and significant contrast, Rnd3 localized in the nucleus throughout the incubation periods in the presence of ISIR-005. Thus, the Rnd3 mediated dichotomic pathways in Figure 3–6 are switched toward the right-hand side to promote cell migration in control and CN-treatment conditions, whereas, in 005-treatment, the left-hand side pathway is selected at the dichotomous point to prevent the cell-rounding that is necessary prior to the cell migration. Consequently, either by peeling off from membrane or prevention of membrane translocation, ISIR-005 forces Rnd3 to stay in nucleus exhibiting the migration-inhibition activity. Although the role of Rnd3 localization at the nucleus is not clear, the 005-induced cell blebbing might be the result of Rnd3 localization in nucleus.

Interestingly, the nuclear localization of Rnd3 was also confirmed in control cells when existed in the low-density state (Figure 3–9, middle panel) or early phase for adhesion processes (Figure 3–8, Day 1). These indicated that nuclear localization of Rnd3 was a part of normal cell event in early phase of the cell adhesion. On the other hand, Rnd3 localized at cytoplasm and/or membrane in the

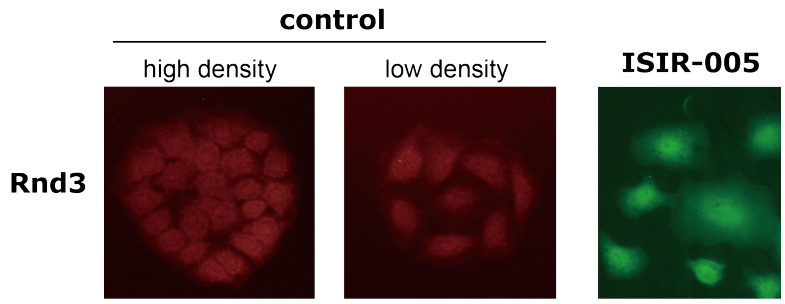

Figure 3–9. Rnd3 localization was affected by the density of cells. Rnd3 located cytoplasm and/or membrane at the high-density state (left panel), on the other hand, Rnd3 localized in nuclei at the low-density state (middle panel). Nuclear localization of Rnd3 was also observed by ISIR-005 treatment (right panel). A549 cells (5.0×10^4 cells/mL) were incubated in the presence or absence of ISIR-005 (8 μg/mL) for 4 days. After incubation, the cells were fixed with PFA and the protein was stained with 1st antibody and AlexaFluoro488 or 568 conjugated 2nd antibody (orange: 586 nm, green: 488 nm, ×300).

high-density state (Figure 3–9, left panel) or after adhesion (Figure 3–8, Day 2 to Day 4). The role of Rnd3 at nuclear localization has not been clear yet, but these results suggested that nuclear Rnd3 might accelerate the cell adhesion. Therefore, it is plausible that ISIR-005 retained the cell state as "pasting" status by localization of Rnd3 at nucleus (Figure 3–9, right panel). Thus the regulation of Rnd3 localization may be a key event in migration-inhibitory activity of ISIR-005.

In the cell migration process, Rnd3 acts as a facilitator, when locates at cytomembrane, by induction of cell rounding and loss of stress fibers (Figure 3–6) and ISIR-005 has an inhibitory activity toward this Rnd3 role, one of its dichotomic roles. If this hypothesis is true, the ROCK

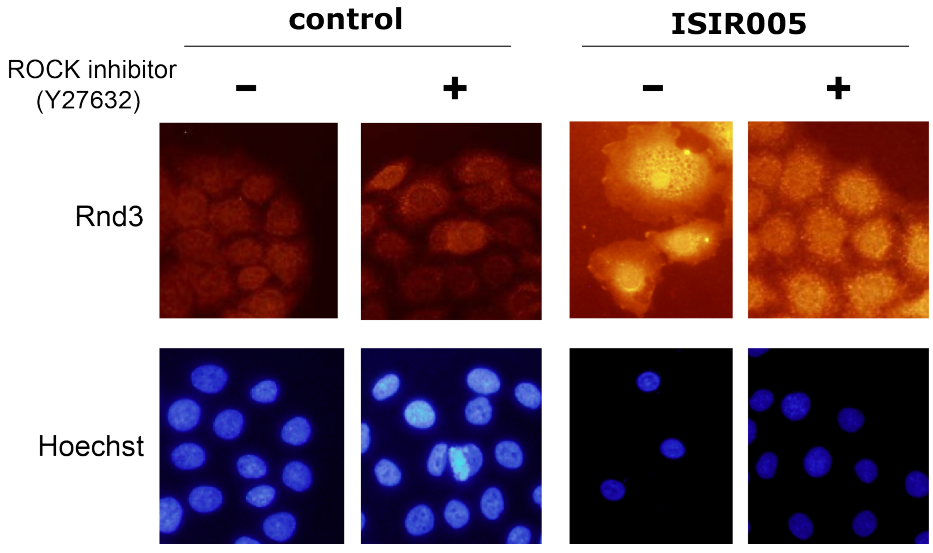

Figure 3–10. Cancelation of the nuclear localization of Rnd3 by Y-27632, a ROCK inhibitor. Y-27632 exported Rnd3 from nuclei to cytosol. A549 cells (5.0×10^4 cells/mL) were incubated in the presence or absence of ISIR-005 (8 μg/mL) with/without Y-27632 (1 μg/mL) for 4 days. The cells were fixed with PFA and Rnd3 was stained wtih its 1st antibody and AlexaFluro546 conjugated 2nd antiboy (546 nm) and nuclei were stained with Hoechst.

inhibitor might show a synergistic or an additive effect with ISIR-005 for inhibition of the cell migration. However, Y-27632 canceled the migration and the cell adhesion inhibition caused by ISIR-005 (Figures 3–4 and 3–5). Moreover, Y-27632 also canceled the Rnd3 localization in nuclei induced by ISIR-005, whereas, in control cells, the ROCK inhibitor exported Rnd3 from nucleus to cytosol (Figure 3–10). It has been reported that the phosphorylation by PKCα is required for translocation of Rnd3 to cytosol from membrane.[104] As its name suggested, the ROCK inhibitor inhibits phosphorylation activity of ROCK. Rnd3 is a phosphorylation target of ROCK-1, and the ROCK inhibitor inhibits this phosphorylation; Ser218 and Ser240 in Rnd3. Therefore, these phosphorylation of Rnd3 by ROCK-1 must be critical for the migration-inhibitory activity of ISIR-005 (Figure 3–11). Strikingly, it has been reported recently that phospho-Ser240 of Rnd3 is required for its interaction with 14-3-3 proteins that could be a target of CN/FCs.[101]

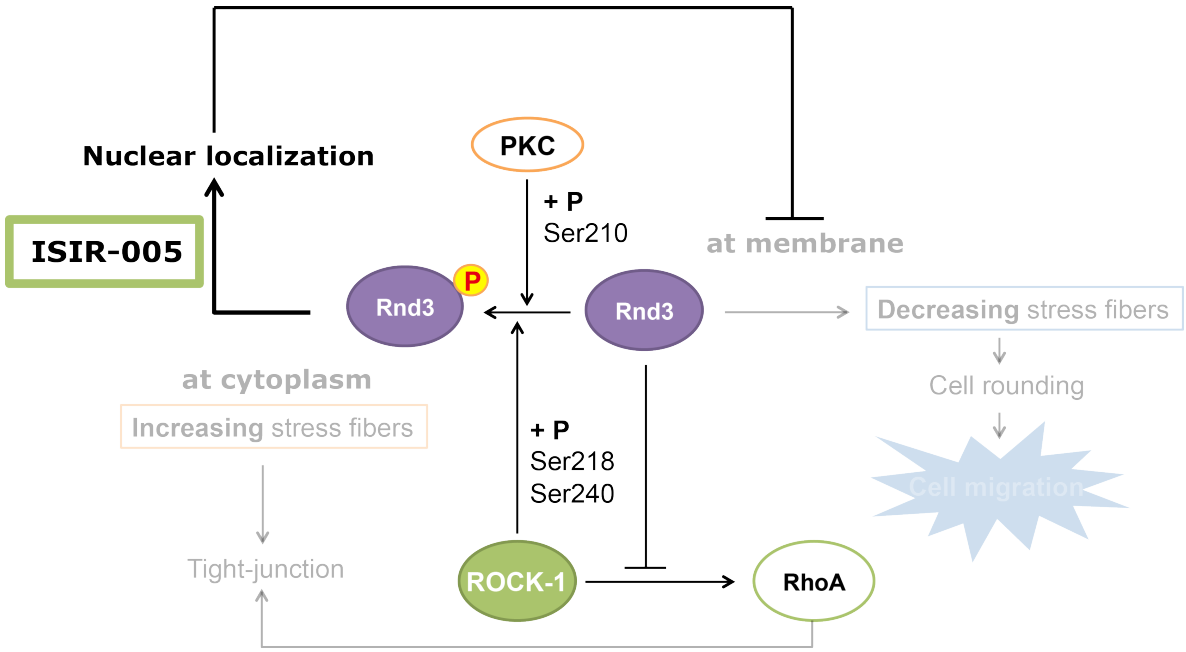

Figure 3–11. The cell migration-inhibition mechanism of ISIR-005. ISIR-005 inhibited cell migration by inducing nuclear localization of Rnd3 depending on its phosphorylation by ROCK. The relationship between the migration inhibition and the cell blebbing and/or anoikis induction has been remained unclear.

3–2–3. Possibility of a binary complex of Rnd3 and 14-3-3 protein as a primary target of ISIR-005

Phosphorylation of Rnd3 at Ser218 and Ser240 by ROCK-1 is essential for the interaction of Rnd3 with 14-3-3 proteins.[101] In other words, Rnd3 is a client of 14-3-3 PPI depending on its phosphorylation status. However, in this case, a simultaneous farnesylation at Cys241 is also

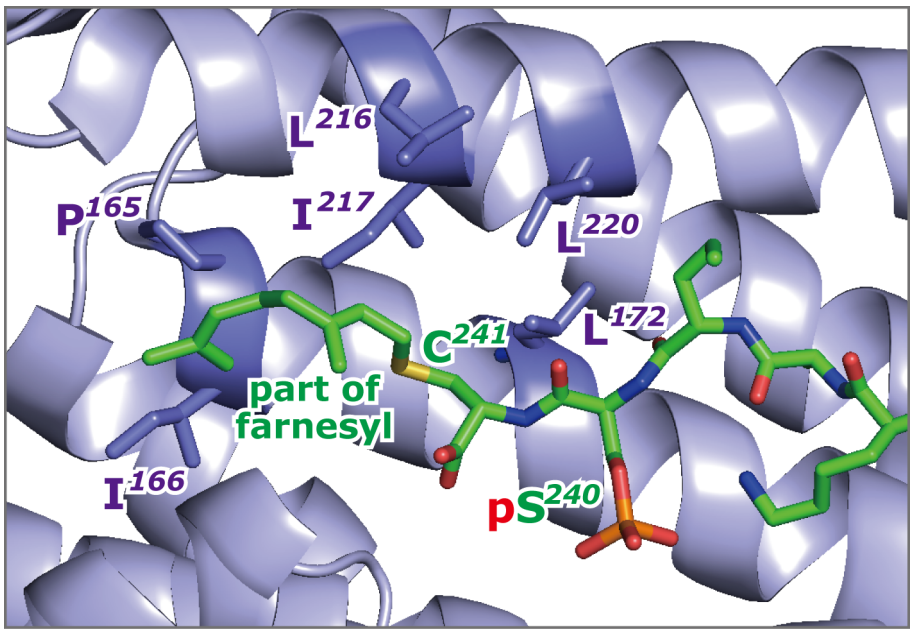

Figure 3–12. The crystal structure of human 14-3-3ζ and the model peptide of the farnesylated Rnd3 (PDB ID: 4BG6)[101]. The former is depicted as pale purple ribbons and the latter is presented as sticks: C in green, N in blue, O in red, S in yellow and P in orange. Residues in 14-3-3ζ contributing hydrophobic interactions with the prenyl chain of Rnd3 are shown in sticks. In this analysis, the terminal is a carboxylate that should be a methyl ester in real post-translational modifications of Rnd3. Figure was prepared by PyMol.

necessary to an effective binding with 14-3-3 proteins. Namely, Rnd3 binds with 14-3-3 proteins at its C-terminal moiety with the post-translational modifications as Asn^{236}–Lys^{237}–Ala^{238}–Lys^{239}–phospho-Ser^{240}–farnesyl-Cys^{241}–COOMe (Figure 3–12).[101] The Cys241 and the farnesyl group attached on this residue make a hydrophobic surface, which interacts with the hydrophobic groove extending from the common binding groove for the phosphorylated client peptides of 14-3-3 proteins. To be modified into the above-mentioned binding motif, Rnd3 is first farnesylated on its consensus motif (so-called CAAX motif; C is the cysteine that is farnesylated, A is any aliphatic amino acid, and X = M, S, Q, A, or C as the C-terminal residue) for the farnesyltransferase, Cys^{241}–Thr^{242}–Val^{243}–Met^{244}–COOH, and then the C-terminal three residues, Thr^{242}–Val^{243}–Met^{244}, are proteolytically removed and finally carboxymethylation of the farnesylated cysteine takes place to provide the binding sequence for 14-3-3 proteins. Therefore, a mode 3 type of C-terminus, phospho-Ser^{240}–Cys^{241}–COOH, is not involved in the post-translational modifications of Rnd3. This fact may be the reason why not only the phosphorylation at Ser240 but also the farnesylation at Cys241 and the truncation of the three C-terminal residues are necessary for the effective binding of Rnd3 with 14-3-3 proteins.[101] The binding of Rnd3 with 14-3-3 proteins alters its localization from membrane to cytosol, and, as a result, the dichotomic roles of Rnd3 is regulated from one side to the

other, *i.e.*, from decreasing stress fibers to increasing stress fibers.

Therefore, if ISIR-005 let Rnd3 to interact effectively with 14-3-3 proteins without farnesylation, it can alter the Rho/ROCK signaling pathway prior to the complete post-translational modifications of Rnd3. From these considerations, it is of worth to investigate the action of mechanism for the migration-inhibition activity of ISIR-005 in conjunction with the behaviors of 14-3-3 proteins.

A. Expression levels of 14-3-3 proteins

14-3-3ζ and 14-3-3σ were reported to contribute to anoikis. The expression level of 14-3-3σ is increased in some cancer cell lines that are resistant to anoikis.[105] Similarly, it was reported that down-regulation of 14-3-3ζ suppresses anchorage-independent growth of lung cancer cells through anoikis activation.[19] Actually, knockdown of 14-3-3ζ with its *si*RNA resulted in the cell death of A549 cells (Figure 2–8). Therefore, at first, effects of ISIR-005 onto expression levels of 14-3-3σ and ζ proteins together with the β isoform as a reference. A549 cells were incubated with ISIR-005 or CN-A for 4 days, and each expression level was evaluated with Western blotting (Figure 3–13). The expression level of 14-3-3σ was very little regardless of presence/absence of FC/CNs. The expression levels of ζ and β isoforms were also not affected by either of ISIR-005 or CN-A. These results led a hypothesis that ISIR-005 affects localizations of 14-3-3 proteins and Rnd3 simultaneously.

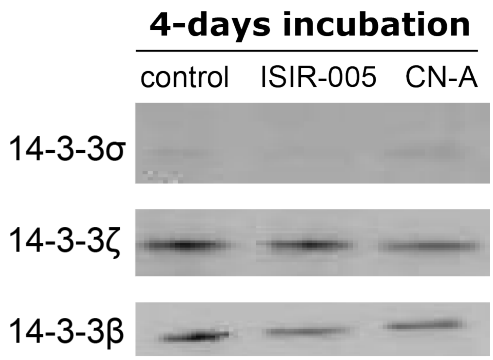

Figure 3–13. Evaluation of expression levels of 14-3-3σ, ζ and β. A549 cells (4.0×10^4 cells/mL) were incubated in the presence or absence of ISIR-005 or CN (8 μg/mL) for 4 days, then the cells were lysed and the proteins were extracted. The proteins were Western blotted on SDS-PAGE.

B. Localization of 14-3-3 proteins in the presence of ISIR-005

Rnd3 was localized to nucleus by ISIR-005 for 4-days incubation (Figure 3–8), which inhibited the cell migration. As shown above, Rnd3 can bind to 14-3-3 proteins depending on its phosphorylation and farnesylation status. Therefore, it is most likely that ISIR-005 stabilizes a binary complex of Rnd3 and 14-3-3 and alters their localization. If this hypothesis is correct, ISIR-005 changes the localization of 14-3-3ζ, which is the 14-3-3 isoform expressed largely in A549 cells. If 14-3-3ζ mediates the localization of Rnd3, these two proteins should be co-localized at nuclei. To validate this working hypothesis, A549 cells were incubated in the presence of

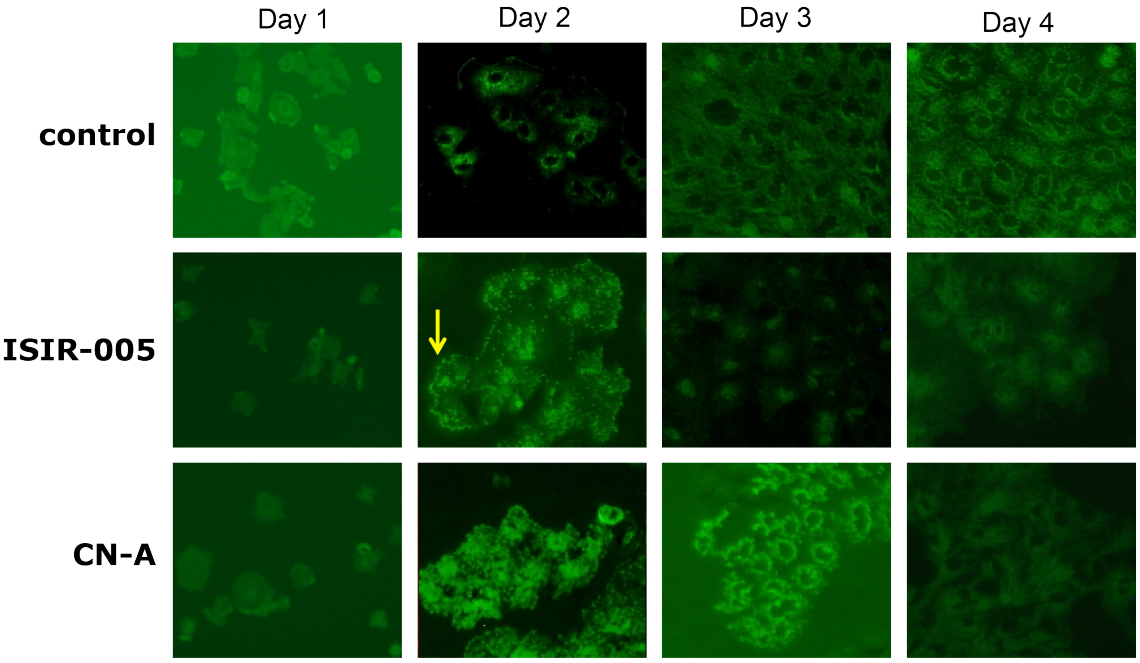

Figure 3–14. The photographs of immunostaining of 14-3-3ζ at Day 1, 2, 3 and 4 after treatment. In ISIR-005 treatment, 14-3-3ζ was localized to nuclei mostly at Day 2 and completely at Day 3 (middle panel). At Day 2, a part of Rnd3 remained at cytomembrane (yellow arrow, 2nd panel). A549 cells (5.0×10^4 cells/mL) were incubated in the presence or absence of indicated compounds (8 μg/mL). After incubation at indicated periods, the cells were fixed with PFA and the protein was stained by 1st and AlexaFluro488 conjugated 2nd antibody (488 nm, ×200).

ISIR-005 and the localization of 14-3-3 was detected by immunostaining. As expected, 14-3-3ζ was also localized to nuclei by ISIR-005 (Figure 3–14) at 2-days and remarkably at 3-days incubation. This localization time course is consistent with that of Rnd3 (Figure 3–8). Therefore, it was strongly suggested that 14-3-3ζ mediates the nuclear localization of Rnd3. Interestingly, Rnd3 remained at cytomembrane at Day 2 by ISIR-005, indicating that ISIR-005 transported the cytoplasmic Rnd3 to nucleus but not Rnd3 in membrane (Figure 3–14, 2nd panel, yellow arrow). In the case of CN-A, the nuclear localization of 14-3-3ζ was also detected in less extent after 2-days incubation. The weaker effect by CN-A might suggest that CN-A recruits some other protein(s) into 14-3-3ζ PPI and localizes them to nuclei.

C. Effects of ISIR-005 on localization of Rnd3 and 14-3-3ζ in pre-adhered A549 cells

In the preceding assays, ISIR-005 was applied to A549 cells simultaneously with the timing of cell-seeding. Namely, the assay evaluates the localization affected not only by the effect of ISIR-005 but also by that of cell-adhesion processes. Thus the localization changes of Rnd3 for pre-adhered A549 cells were investigated. To this end, A549 cells were pre-incubated for 3 days to complete adhesion, and then were treated with ISIR-005. 14-3-3ζ localized both in nuclei and

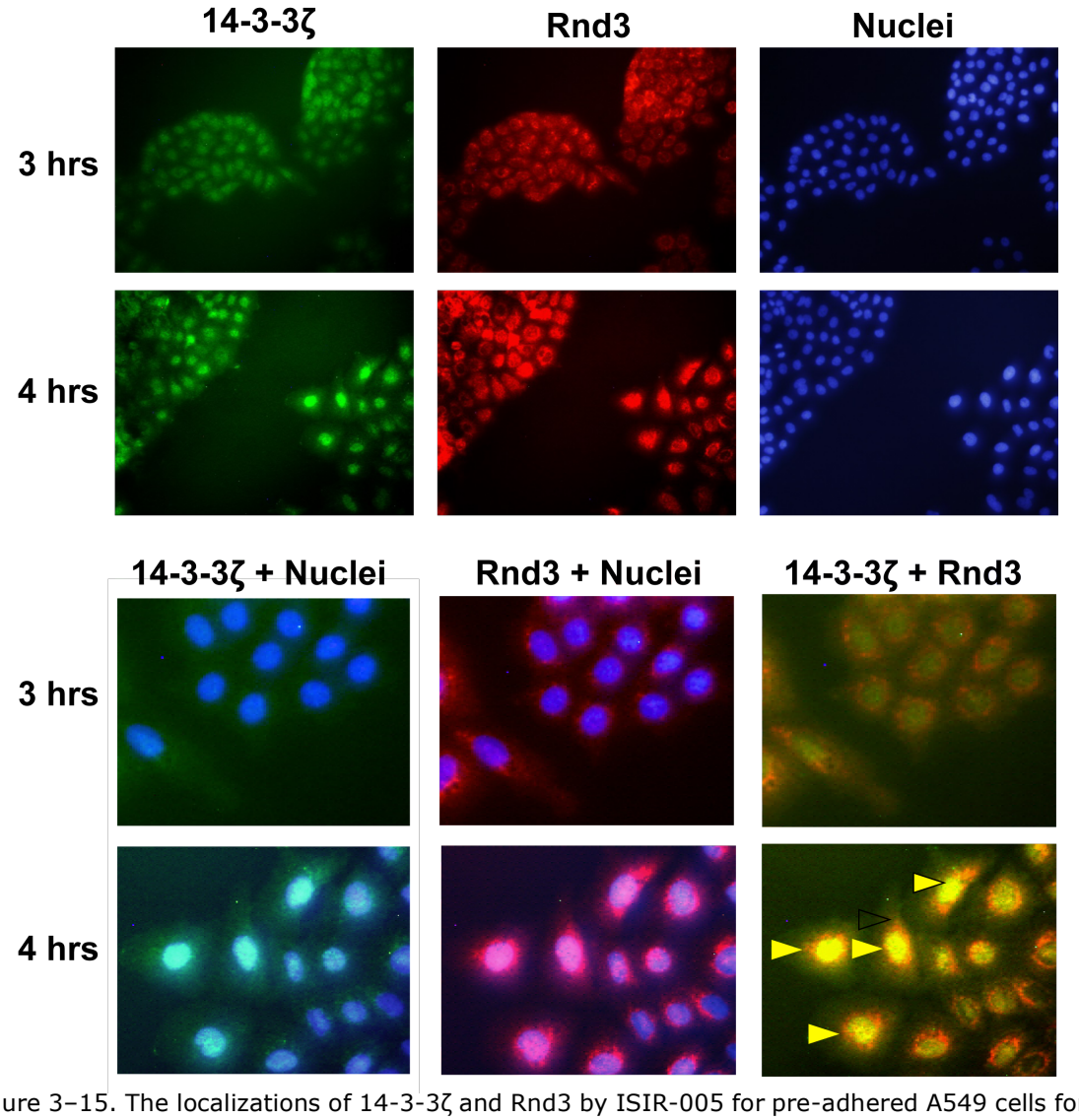

Figure 3–15. The localizations of 14-3-3ζ and Rnd3 by ISIR-005 for pre-adhered A549 cells for 3 and 4 hrs. After 4-hrs treatment by ISIR-005, Rnd3 co-localized with 14-3-3ζ at nuclei. After A549 cells (4.0×10^4 cells/mL) were incubated for 3 days, ISIR-005 (8 μg/mL) was added and after incubation of indicated periods the cells were fixed with PFA. Proteins were then stained with each 1st antibody and fluorescent-conjugated 2nd antibody (488 or 546 nm) and the nuclei were stained with Hoechst.

cytoplasm at 3-hrs incubation after treatment by ISIR-005 (Figure 3–15, upper panels). Rnd3 seemed to locate around the nuclear membrane at that time. At 4-hrs incubation, Rnd3 and 14-3-3ζ co-localized at nuclei (Figure 3–15, yellow triangles, lower panels). Interestingly, the localization of 14-3-3ζ into nuclei occurred slightly faster than that of Rnd3. At 3-hrs incubation, Rnd3 existed around the nuclei where 14-3-3ζ is newly expressed. And at 4-hrs incubation, the cytoplasmic 14-3-3ζ decreased and localized at nuclei accompanying with nuclear localization of Rnd3. These results suggested that the Rnd3 localization by ISIR-005 was mediated by 14-3-3ζ, and 14-3-3ζ might also mediate the nuclear localization of other protein(s), which occurred slightly faster than the Rnd3 localization.

Thus, results obtained for pre-adhered cells showed a difference with those obtained for cells in adhesion processes with regard to the time course of nuclear localization of Rnd3 and 14-3-3ζ. When A549 cells were treated with ISIR-005 from the beginning of their seeding, Rnd3 localized in nucleus at Day 1. Then, a part of Rnd3 was once spread out to cytoplasm and membrane, and re-localization of Rnd3 in nucleus completed at Day 4 (Figure 3–8). In contrast, the nuclear transport of Rnd3 in pre-adhered cells occurred much faster and completed within 4-hrs incubation after treatment by ISIR-005 as shown in Figure 3–15. Namely, the nuclear localization of Rnd3 promoted by ISIR-005 seemed to be effective for the adhered A549 cells but not for the cells in adhesion processes. Similar difference was observed in localization of 14-3-3ζ (Figures 3–14 and 3–15). The cell motility requires localization of Rnd3 in membrane after adhesion. The effect of ISIR-005 toward adhered cells, *i.e*, re-localization of Rnd3 into nucleus from cytoplasm and membrane *via* 14-3-3ζ assistance, retain A549 cells in "pasting" status, which may be responsible, at least partially, for the cell migration-inhibition activity of ISIR-005.

D. Effects of ISIR-005 on localization of Rnd3 in floating A549 cells

From the above-mentioned hypothesis, ISIR-005 may not change the localization of Rnd3 in the floating A549 cells. A549 cells were seeded on poly-HEMA coated plates in the presence of ISIR-005. As shown in Figure 3–16, Rnd3 remained in cytoplasm and membrane, and did not localize to nucleus in floating A549 cells for 3-hrs incubation with ISIR-005. Therefore, the nuclear localization of Rnd3 by ISIR-005 occurs only in the adhered cells, so that cells are forced to retain their "pasting" state.

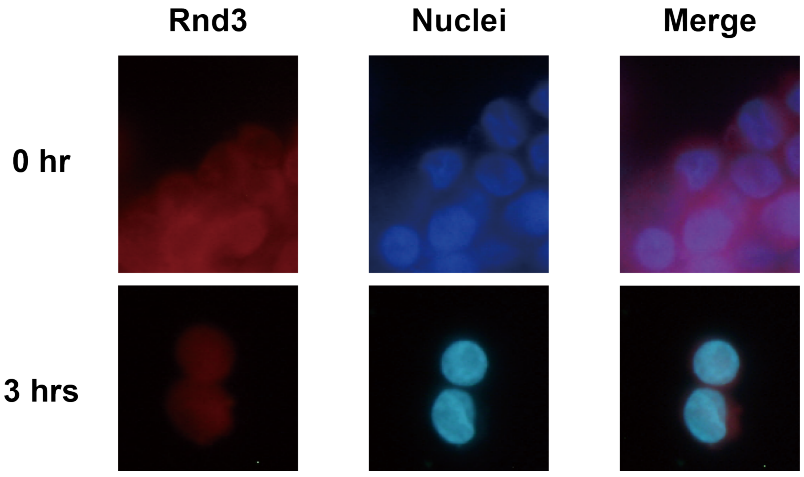

Figure 3–16. Rnd3 localization in floating A549 cells in the presence of ISIR-005. Rnd3 localized not in nucleus but in cytoplasm. A549 cells (50×10^4 cells/mL) were incubated on poly-HMEA coated plates with ISIR-005 (8 μg/mL). After incubation for 3-hrs, the same procedures described in Figure 3–15 were conducted.

3–3. Discussion

In this chapter, details of specific activities of ISIR-005, a 3,12-unsubstituted fusicoccin derivative, have been investigated. ISIR-005 afforded anoikis-related phenotypic outcomes on A549 cells, which did not obtained by 3-hydroxy and 12-hydroxy derivatives of FC/CNs. Since ISIR-005 induced formation of bubble-like structures in A549 cells (Figure 3–1), Rho/ROCK signaling pathway has been suspected to be involved in the anoikis-related events caused by ISIR-005. Because the formation of bubble-like structures seemed to be resulted from cytoskeletal rearrangement mediated by Rho/ROCK signaling. Actually, Y-27632, a ROCK inhibitor, significantly suppressed the formation of bubble-like structures in A549 cells even in the presence of ISIR-005 (Figure 3–3). The ROCK inhibitor also canceled the inhibitory activities for the cell adhesion (Figure 3–4) and the cell migration (Figure 3–5), both of which are another characteristic activities of ISIR-005.

These rescue effects of the ROCK inhibitor strongly suggested the involvement of Rho/ROCK signaling pathway in the events caused by ISIR-005; the formation of bubble-like structures that must be closely related to the cell blebbing and anoikis, inhibition of cell adhesion and inhibition of cell migration. At first, the latter two activities of ISIR-005, inhibition of the cell-adhesion and the cell-migration, have been investigated further. Because, recently, knowledge about the cell adhesion and migration has been greatly accumulated in conjunction with Rnd proteins within Rho superfamily.[96–100] Furthermore, attention has been focused on Rnd3 among Rnd subfamily, since it has been recently reported that the localization and function of Rnd3 are regulated by 14-3-3 PPI.[101] Namely, there is a possibility that ISIR-005 alters Rnd3 functions through stabilization of interaction between Rnd3 and 14-3-3 protein.

To validate above-mentioned hypothesis, localization of Rnd3 and 14-3-3ζ in the presence or absence of ISIR-005 has been intensively investigated. Before making further discussions, one should notice that the sub-cellular localization of Rnd3 is regulated by its post-translational modifications. Rnd3 is known to receive phosphorylation at Ser210 by PKCα and at Ser218 and Ser240 by ROCK-1 as the post-translational modification. It is also farnesylated at Cys241 in its C-terminal CAAX motif. The post-translational prenylation on cysteine in the CAAX motif, followed by proteolytic removal of the AAX part and carbomethylation of the cysteine, is common event in regulation of localization and function of GTPases. Normally, these irreversible modifications mediate the interaction of the GTPases with membranes and are generally required for their functions. The farnesylation of Rnd3, together with phosphorylation at Ser218 and/or

Ser240, recruits 14-3-3 protein onto the post-translationally modified C-terminus of Rnd3 (Figure 3–12). However, contrary to most cases, the 14-3-3 association re-localizes farnesylated Rnd3 into cytoplasm from membrane.[101] Therefore, experimental observations on the localization of Rnd3 should be discussed in correlation with these post-translational events on Rnd3.

Before adhesion of cells (Figure 3–8, control, Day 1) or in low-density conditions (Figure 3–9, control, low-density), Rnd3 localized in nucleus in the absence of ISIR-005. After completion of adhesion, it localized in cytoplasm and cytomembrane (Figure 3–8, control, Day 2 to Day 4; Figure 3–9, control, high-density). In treatment with ISIR-005, Rnd3 remained in nucleus (Figure 3–8, ISIR-005, Day 1 to Day 4) in normal incubation conditions and re-localized into nucleus from cytoplasm in pre-adhered cells (Figure 3–15, Rnd3, 4-hrs). Faster effect in the latter conditions suggested that ISIR-005 can affect only on the adhered cells. This was further confirmed by checking ISIR-005 effect onto the floating cells. No effects of ISIR-005 on the localization of Rnd3 were observed in the floating A549 cells (Figure 3–16, Rnd3, 3-hrs).

The localization of 14-3-3ζ, which is up-regulated in A549 cells and is known to bind to the post-translationally modified C-terminus of Rnd3, was coincident with that of Rnd3 in the presence of ISIR-005. In the normal incubation conditions, 14-3-3ζ was transported gradually into nucleus by ISIR-005 treatment (Figure 3–14, ISIR-005, Day 3) and more quickly in the pre-adhered cells (Figure 3–15, 14-3-3ζ, 4-hrs). These results are consistent with the working hypothesis that the nuclear localization of Rnd3 is mediated by 14-3-3ζ with assistance of ISIR-005. Actually, co-localization of 14-3-3ζ with Rnd3 in nucleus was confirmed by immunostaining (Figure 3–15,

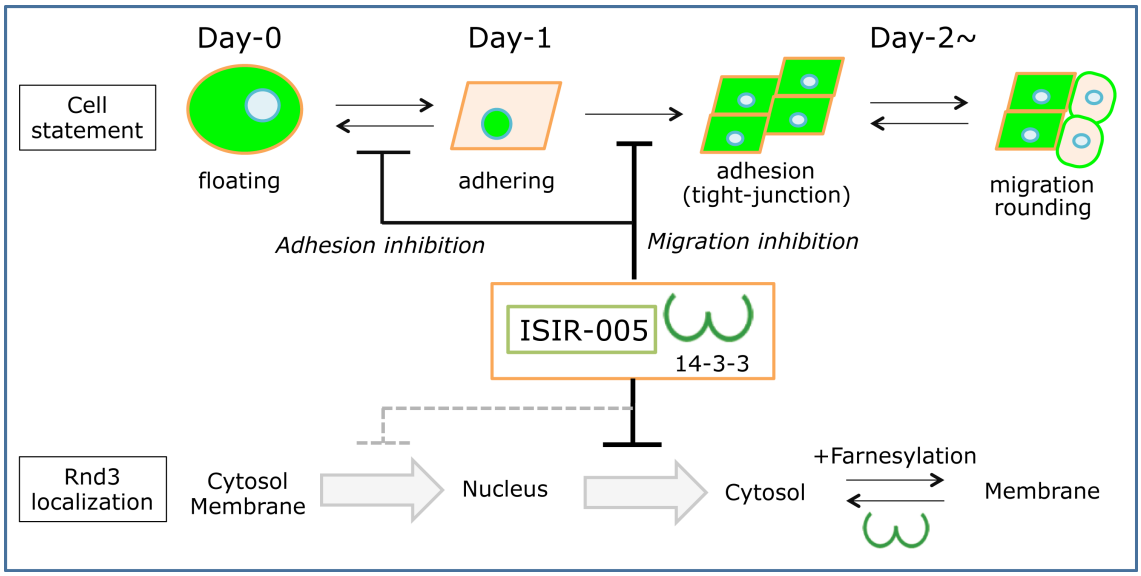

Figure 3–17. Schematic representation of subcellular localization of Rnd3 and cytoskeletal status of A549 cells. ISIR-005 retained cells as "pasting" status by the nuclear localization of Rnd3 *via* 14-3-3 (ζ isoform) PPI with Rnd3.

14-3-3ζ + Rnd3, 4-hrs). Consequently, it is most plausible that ISIR-005, together with 14-3-3ζ, prevents cytoplasmic localization of Rnd3 as shown in Figure 3–17.

As discussed above, Rnd3 was transported by ISIR-005 *via* 14-3-3ζ PPI from cytoplasm to nucleus (Figure 3–17). It has been reported that the complexation of Rnd3 and 14-3-3ζ requires both of phosphorylation at Ser240 and farnesylation at Cys241. And the inhibition of farnesylation localizes Rnd3 from membrane to cytosol and nucleus.[101] Since the farnesyl moiety introduced by post-translational modifications of Rnd3 occupies the hydrophobic groove of 14-3-3 proteins (Figure 3–12) where FC/CNs use in the ternary complex formation (Figures 1–12 and 1–15), it must be impossible that ISIR-005 interacts with farnesylated Rnd3. Therefore, it is most plausible that ISIR-005 forms a ternary complex with 14-3-3 protein and Rnd3 of which Ser240 is phosphorylated but Cys241 is not farnesylated. With the same reason, if ISIR-005 promotes the association of Rnd3 and 14-3-3 through ternary complex formation, farnesylation at Cys241 must be inhibited and, therefore, Rnd3 is transported into nucleus. Taken reported knowledge and results obtained together, plausible relationships between post-translational modifications and cell events mediated by Rnd3 can be summarized as Figure 3–18.

In this research, attention was focused on specific activities induced by ISIR-005, a 3,12-unsubstituted fusicoccin derivative. Actually, CN-A (3-hydroxy derivative) and FC-A (12-hydroxy derivative) did not show the migration-inhibition activity against A549 cells. This

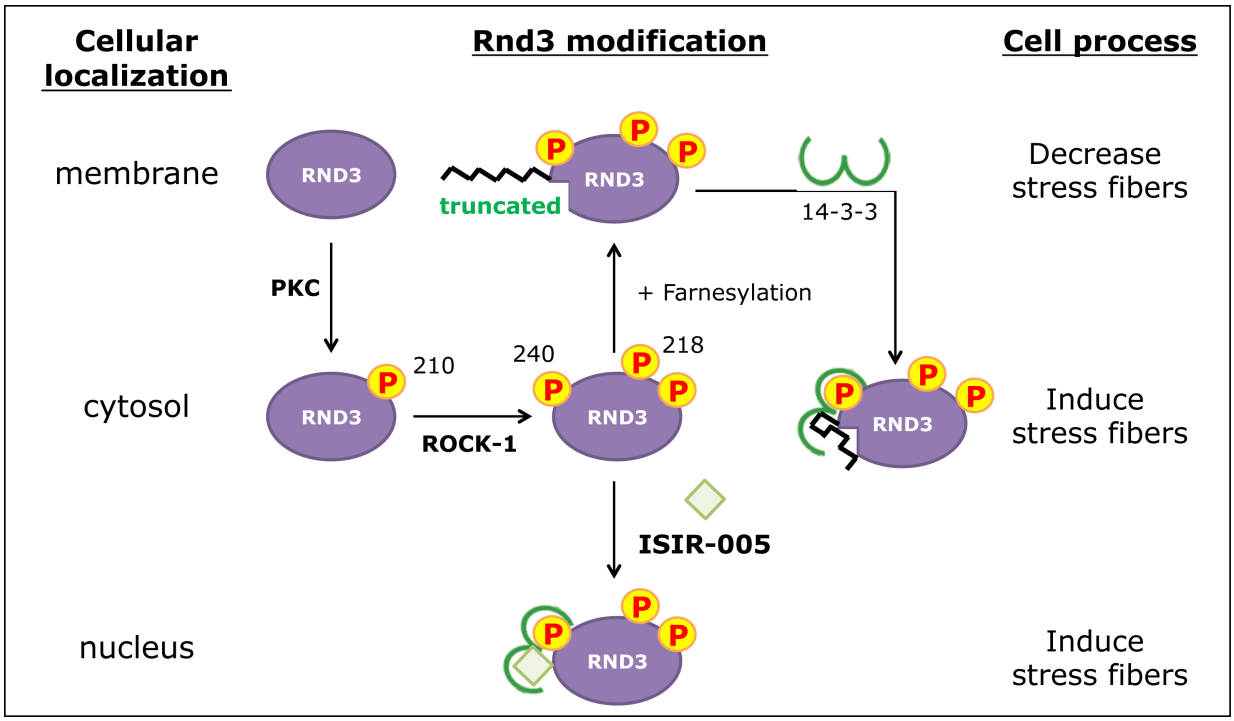

Figure 3–18. Relationships of subcellular localization of Rnd3, its post-translational modifications and the corresponding events mediated by Rnd3.

specificity should be correlated with the selectivity of FC/CNs toward the clients of 14-3-3 proteins. If the ternary complex formation 14-3-3/Rnd3/ISIR-005 is responsible for the nuclear localization of Rnd3, the client sequence must be the C-terminus of Rnd3 that is pSer^{240}– Cys^{241}–Thr^{242}–Val^{243}–Met^{244}–COOH. FC-A, a 12-hydroxy derivative, is not compatible with this motif, because residues beyond the *i* + 1 position conflict sterically, as descried in Chapter 1, with the 12-hydroxy group on the aglycone of FC-A. On the other hand, it is anticipated that ISIR-005, a 3,12-unsubstituted derivative, can stabilize the hypothetical binary complex of 14-3-3/Rnd3, because it has been already revealed that ISIR-042 having the same aglycone structure with that of ISIR-005 could be compatible with this sequence of which *i* + 1 is cysteine (Figure 1–14).[71] To predict compatibility of CN-A with cysteine at *i* + 1 position of the client peptide, a model study has been carried out. As a simplest model, the crystal structure of the ternary complex of 14-3-3ζ/c-Raf peptide/CN-A (PDB ID: 4IHL)[62] set to an initial structure. Then the Thr^{260} at *i* + 1 position of the c-Raf peptide was mutated into Cys *in silico* (Schrödinger Suite 2013). As a result, a sterical collision was developed between 3-hydroxy group of CN-A and the mutated cysteine because of longer length of C–S bond than those of C–C and C–O bonds (Figure 3–19). Therefore, CN-A may not be able to stabilize the Rnd3 peptide within 14-3-3 PPI and this may be a rationale for inactiveness of CN-A for migration inhibition.

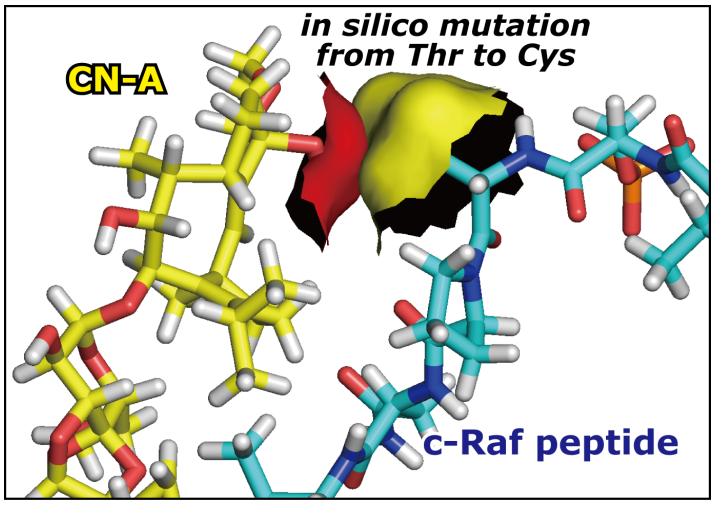

Figure 3–19. Interface of CN-A and a model peptide of Rnd3 in the binding groove of 14-3-3 protein. The initial structure was adapted from the ternary complex of 14-3-3ζ/c-Raf peptide/CN-A (PDB ID: 4IHL).[62] The *i* + 1 residue was mutated in silico from Thr to Cys. Red surface is for the 3-OH of CN-A and yellow surface is for the thiol group of the cysteine. 14-3-3ζ is omitted for clarity.

Accumulated knowledge including results obtained by this research now leads to the conclusion described as follows. The Rnd3 presumably localizes at nucleus when adhesion processes are progressing. Phosphorylation at Ser210 by PKCα induces cytosol localization of Rnd3 and promotes stress fiber and tight-junction formations that are necessary for the cell-adhesion. Further phosphorylation at Ser218 and Ser240 by ROCK-1 enables Rnd3 to be an endogenous Rho/ROCK inhibitor accompanying membrane localization of Rnd3. The inhibition of Rho/ROCK signaling results in decreasing stress fiber formation and, therefore, promotes cell rounding and cell migration.

Adhesion and migration of cells must be regulated correctly in growth of tumors. The farnesylation of Rnd3 at Cys241 takes this regulating role with the assistance of 14-3-3 PPI. The binding of 14-3-3 protein causes re-localization of Rnd3 in cytosol and, therefore, Rnd3 looses the inhibitory nature against Rho/ROCK signaling. ISIR-005 intervenes these cellular events by capturing Rnd3 before the farnesylation takes place. Although the role of Rnd3 in nucleus has not been clear yet, it is obvious that nuclear-localized Rnd3 cannot take the role as an inhibitor of Rho/ROCK signaling pathway. Therefore, stress fiber formation is continuously activated and the cell-migration is prevented. This effect is named as "pasting" effect in this research. With this "pasting" effect, ISIR-005 inhibited the cell migration (Figure 3–20). Nuclear localization of Rnd3 by ISIR-005 was canceled by Y-27632, a ROCK inhibitor, because direct inhibition of ROCK diminishes phosphorylation status on Ser240 of Rnd3 that is necessary for 14-3-3 PPI and, therefore, ISIR-005 looses its target to be stabilized.

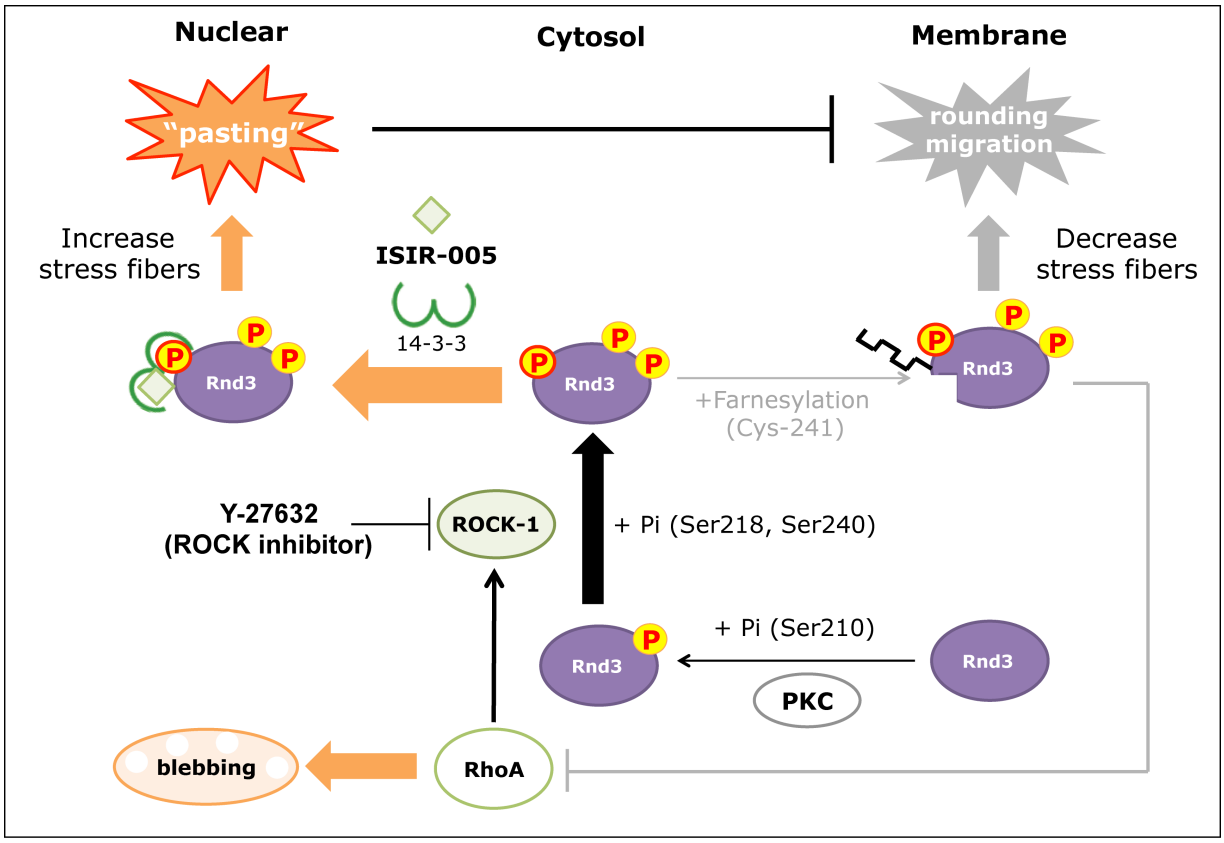

Figure 3–20. The summarized mechanism of migration inhibition by ISIR-005 through Rnd3 localization *via* 14-3-3ζ PPI. Rnd3 is phosphorylated by ROCK-1 at cytoplasm. Then Rnd3 is farnesylated and is translocated to membrane. The farnesylated Rnd3 is localized into cytoplasm by 14-3-3 proteins. In floating state, Rnd3 was expressed throughout the cells, and ISIR-005 could not change the localization. On the other hand, in hi-density adhered cells (tight-junction), Rnd3 was located in cytoplasm and membrane. ISIR-005 transported phosphorylated but not farnesylated Rnd3 into nucleus *via* 14-3-3ζ PPI.

Thus, ISIR-005 alters localization of Rnd3 by affecting its interaction with 14-3-3 protein. Results obtained here strongly suggest that ISIR-005 forms a ternary complex with 14-3-3 protein and Rnd3 of which translational modification is not completed. Although further validation is necessary to prove the ternary complex formation, this is the first example that alteration of a certain 14-3-3 PPI by fusicoccin derivatives is directly correlated with an apparent phenotypic outcome. Interestingly, ISIR-005 did not change the localization of Rnd3 toward cells in ongoing adhesion processes. Therefore, there should be a different mechanism that is responsible for the adhesion-inhibition activity of ISIR-005.

3–4. Materials and Methods

Materials

Instruments used in this research are as follows; for absorption measurements on 96-well plates, Multidetection microplatereader POWERSCAN HT DynaBook Satellite J50 (DS Pharm Biomedical); for Western blotting analysis, ChemiDOC XRS (BIO-RAD), QuantityOne ver 4.5 (BIO-RAD), PowerPacTM HC (BIO-RAD), High-speed refrigerated microcentrifuge MX-300 (TOMY); for immunofluorescence analysis, Fluorescence microscope Olympus BX-51 (Olympus), 100W High Pressure Mercury Burner Olympus BH2-RFL-T3 (Olympus); for cell culture, CO_2 incubator MCO-19AICUVH-PJ (Panasonic).

The antibodies were purchased and used as follows: polyclonal anti Rnd3 in rabbit (abcam), polyclonal anti 14-3-3ζ in mouse (Imgene), polyclonal anti 14-3-3ζ in rabbit (Santa Cruz), polyclonal anti 14-3-3σ in goat (Santa Cruz) and polyclonal anti 14-3-3β in rabbit (Santa Cruz) as primary antibodies; HRP-conjugated anti-mouse, rabbit and goat IgG (Santa Cruz), FITC-conjugated anti-rabbit IgG (Santa Cruz, CA), AlexaFluoro405/488/546 conjugated anti-mouse and rabbit IgG (Invitrogen) as secondary antibodies; Hoechst33258 (Dojindo) as nuclear staining reagent; D-PBS(–) was purchased from Gibco or Wako.

Cell blebbing detection

On 6-well plates, A549 cells (5×10^4 cells/mL, 1.5 mL/well) were incubated in the presence or absence of ISIR-005 (8.0 μg/mL) at indicated concentrations for 1, 2, 3 and 4 days with or without Y-27632 (1.0 μg/mL, Wako). These cells were washed twice with D-PBS(–) and fixed with 5% PFA. The photographs were taken and blebbed cells and normal cells were counted.

Adhesion assay

As described in Materials and Methods of Chapter 2.

Wound healing assay

As described in Materials and Methods of Chapter 2.

Protein extraction

On 6-well plates, cells (4×10^4 cells/mL, 1.5 mL/well) were incubated in the presence or absence of compounds at indicated concentrations for indicated periods. These cells were washed twice with D-PBS(–) and lysed with buffer 'A' [20 mM Tris·HCl, 140 mM NaCl, 1% (v/v) TritonX-100, pH: 7.4 plus a protease inhibitor (complete Mini EDTA-free, Roche) and a phosphatase inhibitor (PhosSTOP, Roche)] for 20 min on ice. The resulting suspensions were collected with cell scraper (IWAKI) and centrifuged (15000 ×g, 15 min, 4°C) to remove the precipitates, and the supernatant was diluted with 4 × Laemmli sample buffer (NuPAGE LDS Sample Buffer, Novex; 4% 2-mercaptoethanol, Wako) and boiled for 5 min at 70°C providing a protein extraction sample. Protein concentration was estimated with BCA method (Pierce BCA protein assay kit, Thermo).

Western blotting

The protein extraction samples were separated on 4-12% SDS-PAGE (NuPAGE Bis-Tris Gel, Novex; NuPAGE MOPS SDS Running buffer, Novex) with Molecular marker (MagicMark XP, Novex) and transferred onto membrane (Immobilon-P Transfer membrane, Millipore). In the case of using normal primary antibody, membranes were blocked from nonspecific binding by incubation with blocking buffer [5% (v/v) albumin (Albumin from bovine serum, sigma) in TBST (20 mM Tris·HCl, 140 mM NaCl, pH: 7.4; (BIO-RAD), 0.1% (v/v) Tween-20 (BIO-RAD)] 12 hrs at 4°C, then incubated with primary antibody diluted with blocking buffer (1: 1000~5000) for 12 hrs at room temperature and washed with TBST three times for 5 min. After a treatment by secondary antibody conjugated with HRP diluted with blocking buffer (1: 5000) for 2 hrs at 4°C, the membrane was washed with TBST three times for 5 min and then visualized by ECL Plus reagent (Pierce Western Blotting Substrate, ThermoFisher Sience).

Immunofluorescence detection-1

Cells (5×10^4 cells/mL for 4 days, 5.0×10^5 cells/mL within 1 day, 1.5 mL/well) were grown in

6-well plates or non-coated slide glasses (18×18 mm) in 6 well plates or poly-HEMA coated 6 well plates for indicated periods, and then washed twice with D-PBS(–) and fixed with paraformaldehyde (Wako) 20 min at room temperature. Then permeabilization by T-PBS (0.5% (v/v) TritonX-100 (Nacalai) in D-PBS(–), pH: 7.4) for 5 min at room temperature was conducted. Nonspecific binding was blocked with blocking buffer (5% (v/v) Albumin in T-PBS) for 2 hrs at 4°C. Primary antibody diluted with blocking buffer (1: 100) was incubated for 12 hrs at 4°C and then cells were washed with T-PBS three times. FITC, AlexaFluro405 or AlexaFluore548 conjugated secondary antibody diluted with blocking buffer (1: 500) was treated for 2 hrs at 4°C and cells were washed three times with T-PBS. Additionally, nuclei were stained with Hoechst solution diluted with PBS (1: 500). The cells were washed with T-PBS and mounted by anti-fade reagent (PrologGold, Invitrogen). Finally, stained cells were monitored by a digital camera at suitable wavelength for each chromophore.

Immunofluorescence detection-2

A549 cells (4.0×10^4 cells/mL, 1.5 mL/well) were seeded in 6 well plates and cultured for 3 days. After pre-culture, ISIR-005 (8 μg/mL) was added and incubated for indicated periods. The following procedures were conducted as described above.

Chapter 4: Effect of ISIR-005 onto Stress Fibers and Cell Detachment

4–1. Introductory Statements

Actin is a molecule to participate in many important cellular processes including muscle contraction, cell motility, cell division, and so on. It forms microfilaments that contribute as components of the cytoskeletal scaffoldings and are involved in the processes of cell adhesion and cell migration. Actin is expressed in eukaryotes and six isoforms are identified such as α1~4, β and γ. α-actin is expressed in the muscle cells and β- and γ-actins are expressed in non-muscle cells. The actin fiber (F-actin) is formed by polymerization of actin molecules. Since this process is reversible, the polymerization and de-polymerization of actins are repeatedly regulated in cells. As one of the actin fibers, stress fibers are known to be involved in the process of cell adhesion and migration.[106] The stress fibers bridge focal adhesions, which rise tensional force in the cell and accelerate cell adhesion and migration. In the cell migration, actin polymerization is accelerated and forms cytoskeletal structures, such as filopodia and lamellipodia. filopodia and lamellipodia that makes the "grip" for migration, and the tensional force drives cell body toward to the grip position.

As discussed in Chapter 3, ISIR-005 changed Rnd3 localization *via* 14-3-3ζ PPI (Figures 3–18 and 3–20). It has been reported that Rnd3 influences the actin stress fiber formation depending on its localization, as shown in Figure 3–6. Rnd3 is phosphorylated by ROCK-1 at cytoplasm, which induces cytosol localization of Rnd3 and induces stress-fiber formation, and a ROCK inhibitor, H1152 {(*S*)-(+)-2-Methyl-1-[(4-methyl-5-isoquinolinyl)sulfonyl]-hexahydro-1*H*-1,4-diazepine}, inhibits induction of stress fibers by Rnd3.[103] Therefore, it is plausible that phosphorylation of Rnd3 by ROCK-1 is required to induce stress fibers. On the other hand, Rnd3 localizes at cytomembrane after receiving farnesylation on its CAAX motif. Rnd3 localization at cytomenbrane induces loss of stress fibers.[101] Moreover, Rnd3 co-localizes with actin at the cell periphery and leads to the formation of highly sealed tight junctions.[107] As described in Chapter 3, ISIR-005 induced nuclear localization of Rnd3 (Figure 3–8), which inhibited cell migration. Therefore, ISIR–005 might affect the actin status accompanied with Rnd3 localization.

4–2. Results

4–2–1. Effect of ISIR-005 onto β-actin and actin filaments

At first, it was investigated the effect of ISIR-005 for non-fibered β-actin. A549 cells were

incubated in the presence or absence of ISIR-005 or CN-A for 4 days. ISIR-005 did not show any remarkable influence for localization of β-actin (Figure 4–1). The viable cell number was decreased because of cell death induction by ISIR-005. Similar to the case of control, β-actin existed at cytoplasm and membrane with treatment of ISIR-005 or CN-A. β-Actin was not transported into nucleus under these conditions.

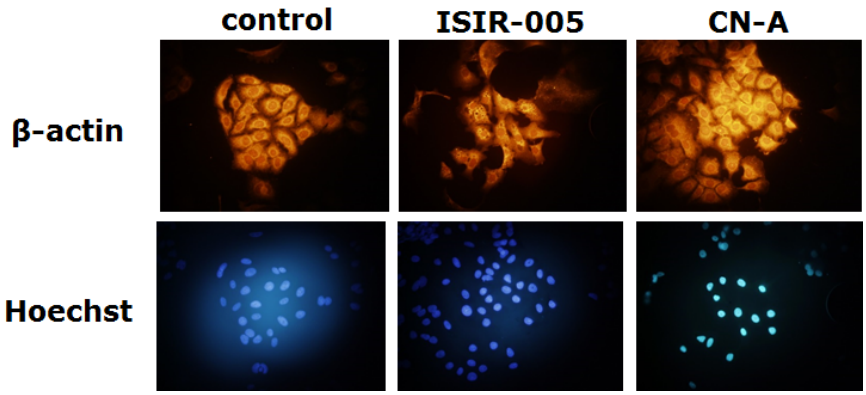

Figure 4−1. The effects of ISIR-005 and CN-A on localization of β-actin. A549 cells (4×10^4 cells/mL) were incubated in the presence of ISIR-005 or CN-A (8 μg/mL) for 4 days. Then the cells were fixed with PFA and stained with its 1st antibody and AlexaFluro546 conjugated 2nd antibody (upper panels, orange, 546 nm). The nuclei were stained with Hoechst (lower panels, blue, 352 nm).

Next, the effect of ISIR-005 on F-actin, which has a filamentous structure, was investigated. F-actin was stained with fluorescent (FITC)-conjugated phalloidin that is used as a staining agent

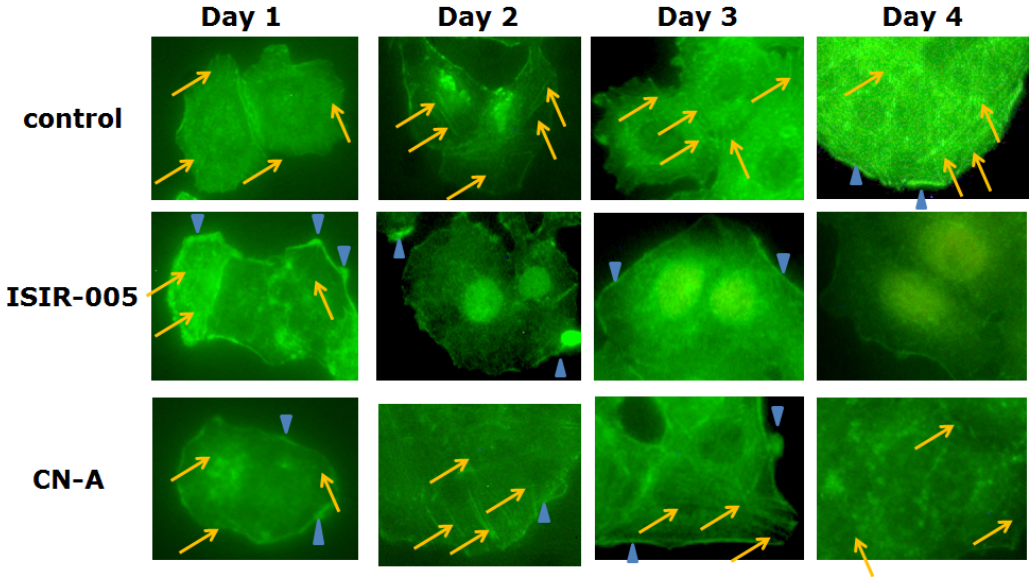

Figure 4−2. The effects of ISIR-005 (2nd panels) or CN-A (3rd panels) on F-actin localization and stress fiber formation. Yellow arrows indicate stress fibers and blue triangles indicate lamellipodia. A549 cells (4.0×10^4 cells/mL) were incubated in the presence or absence of ISIR-005 or CN-A (8 μg/mL). The cells were fixed with PFA and stained with Acti-stain 488 and observed at 488 nm.

for F-actin. After incubation of indicated periods, cells were fixed and stained. At Day-1, formation of the stress fibers was confirmed in all conditions (Figure 4–2, left panels, yellow allows). In the case of ISIR-005 treated cells, remarkable formation of lamellipodia was observed in periphery of the cells. The lamellipodia, which has actin filament–rich structure (Figure 4–2, blue triangles), is at leading-edge in cell migration. In the processes of lamelipodia formation, Rac1 protein plays an important role to construct the lamelipodia structure.[108] Surprisingly, at Day-2, nuclear localization of F-actin was induced by ISIR-005 treatment. The transportation of F-actin into nucleus was not observed in control and CN-A treated cells. Therefore, induction of nuclear localization of F-actin seemed to be a specific effect of ISIR-005. Simultaneously with the nuclear localization of F-actin, stress fibers were diminished in ISIR-005 treated cells. These changes were retained by Day-4. Since the loss of stress fibers decreases cell motility, this phenomenon must contribute to migration-inhibitory effect of ISIR-005 in addition of the nuclear localization of Rnd3. In control and CN-A treated cells, the cell shapes were looked like "rigid" and "tense", but those of ISIR-005 treated cells were looked like "loosened" and "extended". Thus, ISIR-005 clearly affected cytoskeletal maintenance of A549 cells.

4–2–2. Effect of ISIR-005 onto focal adhesion

Focal adhesion was strained with vinculin, an adaptor protein, which is known as a molecular marker of focal adhesion.[109] The focal adhesions (yellow arrows) were observed as spots in control cells (Figure 4–3a, left panels). As expected, staining by vinculin revealed that the number of red

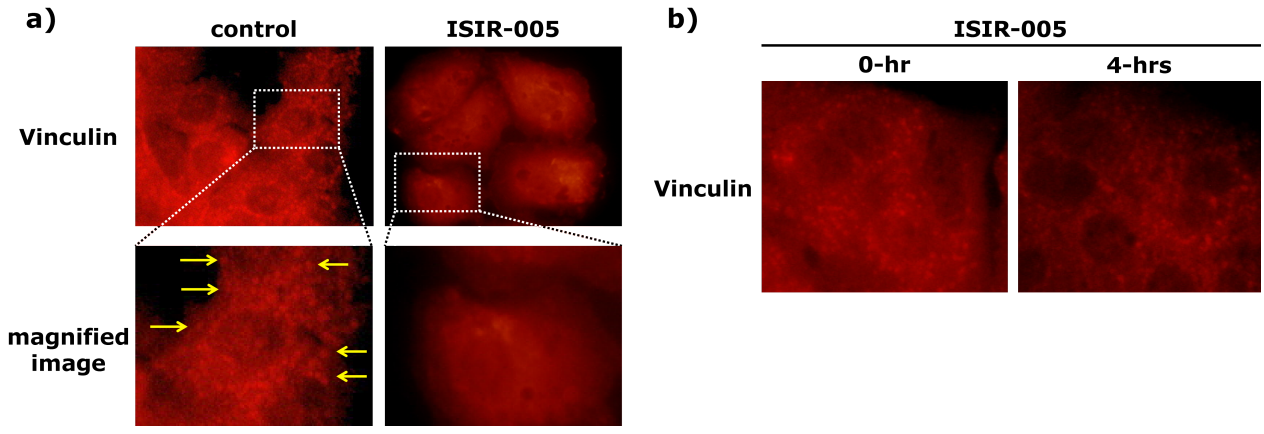

Figure 4–3. Effect of ISIR-005 on vinculin localization and focal adhesion. a) A549 cells (4.0×10^4 cells/mL) were incubated in the presence or absence of ISIR-005 (8 μg/mL) for 4 days. b) A549 cells (4.0×10^4 cells/mL) were incubated for 3 days to complete adhesion. Then ISIR-005 (8 μg/mL) was added to pre-adhered A549 cells and incubated for 4 hrs. Cells were fixed with PFA and stained with vinculin antibody (1st) and AlexaFluor546 (2nd) antibody and observed at 546 nm.

spots is significantly decreased with ISIR-005 treatment, confirming decrease of focal adhesions (Figure 4–3a, right panels). On the other hand, the remarkable decrease of focal adhesions was not observed for pre-adhered A549 cells even in ISIR-005 treated cells (Figure 4–3b).

4–2–3. Effect of ISIR-005 onto tight-junction

Next, the effect of ISIR-005 for tight-junction formation was investigated. Tight-junction is a type of cell–cell junction and contributes to cell adhesion and barrier both to the passage of ions and molecules. This structure is rich in epithelial cells. ZO-1 (Zonula Occluden protein 1) is known as a molecular marker of tight-junction. ZO-1 has the actin-binding region and links actin to transmembrane proteins.[110,111] Therefore, the effect of ISIR-005 was inspected by ZO-1 staining. In control cells, tight-junctions were observed clearly at cell–cell surfaces (Figure 4–4, left panels, yellow triangles). In contrast, ISIR-005 remarkably induced loss of tight-junction after 4-days incubation. Therefore, ISIR-005 inhibited the formation of focal adhesion and tight-junction. For pre-adhered A549 cells, remarkable effect of ISIR-005 on tight-junction was not observed by 4-hrs incubation. Rearrangement in tight-junction may require a long-term incubation with ISIR-005. Thus, it was revealed that ISIR-005 reduced cell–ECM and cell–cell adhesions. It is plausible that, with these effects, ISIR-005 shows not only the inhibition of cell-migration but also induction of cell detachment and anoikis.

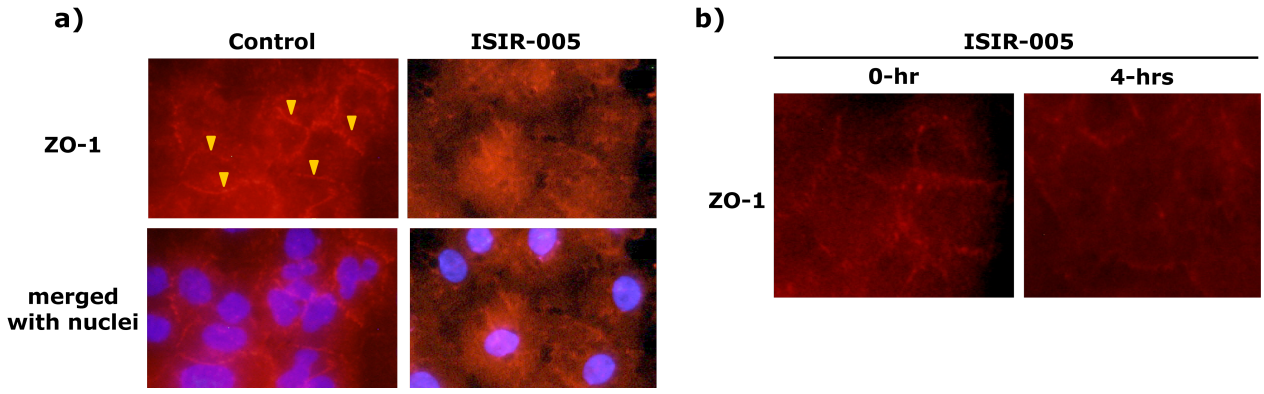

Figure 4–4. Effect of ISIR-005 on tight-junction. a) A549 cells (4.0×10^4 cells/mL) were incubated in the presence or absence of ISIR-005 (8 μg/mL) for 4 days. Yellow triangles indicate tight-junctions. b) A549 cells (4.0×10^4 cells/mL) were incubated for 3 days to complete adhesion. Then ISIR-005 (8 μg/mL) was added to pre-adhered A549 cells and incubated for 4 hrs. Cells were fixed with PFA and stained with ZO-1 antibody (1st) and AlexaFluor546 (2^{nd}) antibody. Hoechst33342 was used for staining of nuclei. Images were observed at 546 or 352 nm.

4–3. Discussion

F-actin staining revealed that stress fibers were increased at Day-1 and then decreased by ISIR-005 treatment. It has been reported that Rac1 activates RhoA *via* Dbs protein,[112] and Rho/ROCK pathway induces formation of stress fibers and lamellipodia.[108] At Day-1, Rnd3 is transported into nucleus and its antagonistic activity toward Rho/ROCK signaling pathway is prevented (Chapter 3). Namely, it is plausible that formations of lamellipodia and stress fibers are caused by loss of Rnd3 function resulting in activation of RhoA/ROCK-1 signaling at Day-1 (Figure 4–5). However, contrary to expectation, stress fibers were decreased gradually and almost completely diminished in cytoplasm at Day-4 (Figure 4–2), because the nuclear localization of F-actin depletes cytosolic F-actin and, therefore, decreases stress fibers (Figure 4–5). Nevertheless, at Day-2, since stress fibers are still remained, cells are kept in the pasting state, caused by nuclear localization of Rnd3, which mainly contributed to the migration-inhibitory activity of ISIR-005 in Day-1 to Day-2.

At Day-3 to Day-4, the cell shape looked "loosened" and F-actin accumulated in nuclei. Depletion of cytosolic F-actin by its nuclear accumulation leads loss of stress fibers. It was easily predicted that loss of F-actin and stress fibers leads loss of focal adhesions and tight-junctions as well. Thus vinculin was used as a molecular marker for detection of focal adhesions. Vinculin localizes at focal adhesion and acts as an intermediate of the linkage between integrin and actin with binding to the actin stress fibers.[113] Therefore, focal adhesions can be detected as spots or dot-like images with vinclin antibody and AlexaFluor546® as a second antibody (Figure 4–3). While these spots could be clearly detected in control cells, ISIR-005 de-localized vinculin and spread it throughout cells in 4-days incubation (Figure 4–3). These observations suggested that ISIR-005 induces loss of focal adhesions through loss of cytoplasmic F-actin. In the migration processes, focal adhesion must be required at the edge of cell to make an anchor for migration. Thus, loss of focal adhesion contributed to migration inhibition at Day-3 to Day-4.

While focal adhesion is a main contributor for cell–ECM interaction, tight-junction is another element for cell–cell adhesion. As mentioned above, ZO-1 bridges actin and transmembrane proteins. Therefore, it can be used as a maker for tight-junction. As expected, since ISIR-005 induced nuclear localization of F-actin, ZO-1 could not bind to F-actin at the cell surface and, therefore, tight-junctions are lost by ISIR-005 treatment (Figure 4–4). Thus, at Day-3 to Day-4, the cytosolic F-actin was depleted, which resulted in loss of focal adhesion and tight-junction. Loss of focal adhesion and tight-junction may be proposed as a putative mechanism of cell detachment.

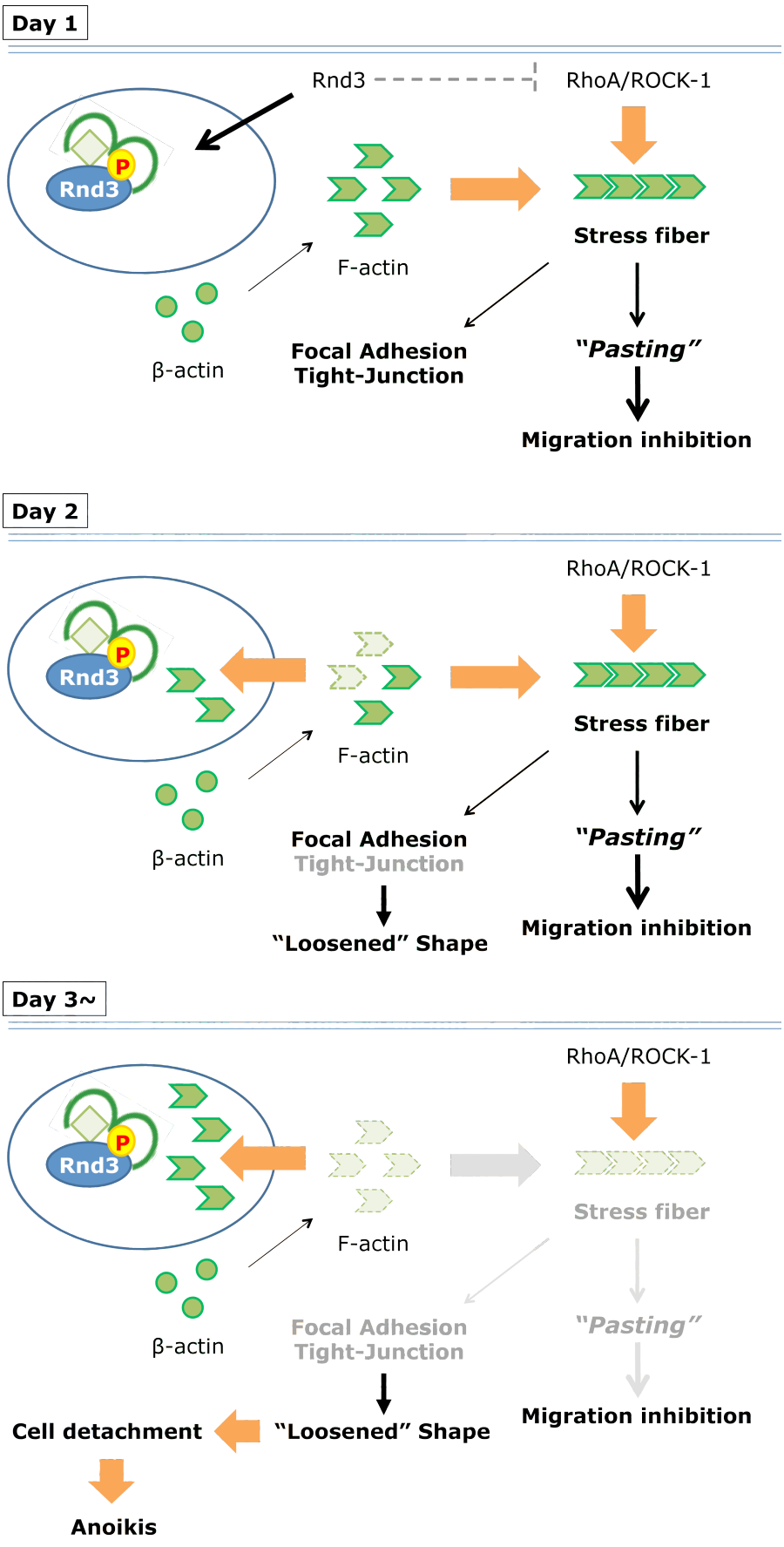

Figure 4−5. A putative model for localization and structures of F-actin induced by ISIR−005.

Day 1:
ISIR-005 localizes Rnd3 to nucleus *via* 14-3-3ζ PPI, resulting in activation of RhoA/ROCK-1 and induction of formation of stress fibers. The nuclear Rnd3 forces cells to be pasting state and, therefore, inhibits cell migration.

Day 2:
F-actin starts to be accumulated into nucleus, which depletes cytosolic F-actin. The cell shape becomes loosened because of decreasing cytosolic F-actin.

On and after Day 3:
Nuclear accumulation of F-actin induces depletion of cytosolic F-actin and then loss of stress fibers, focal adhesion and tight-junction, and pasting state may be released. After these events take place, cell detachment is induced at Day 3 or later and then cell death (anoikis) is resulted.

Coincidently, cell death induction was observed after 3-days incubation for pre-adhered cells as discussed in Chapter 2. This coincidence led a hypothesis that cell detachment caused by loss of cytosolic F-actin triggered anoikis induction that was also brought by ISIR-005 treatment (Figure 4–6). Details on anoikis induction will be discussed in Chapter 5 in conjunction with this hypothesis.

The mechanism of nuclear localization of F-actin has not been revealed yet. Since ISIR-005 did not affect on the localization of β-actin, ISIR-005 probably does not change the expression levels of actin and its localization as a monomer. Furthermore, since F-actin could be observed in nuclei, the equilibrium of polymerization and de-polymerization of actins may not affected by 005-treatment. Therefore, main effect of ISIR-005 on F-actin localization is suggested to be brought either by

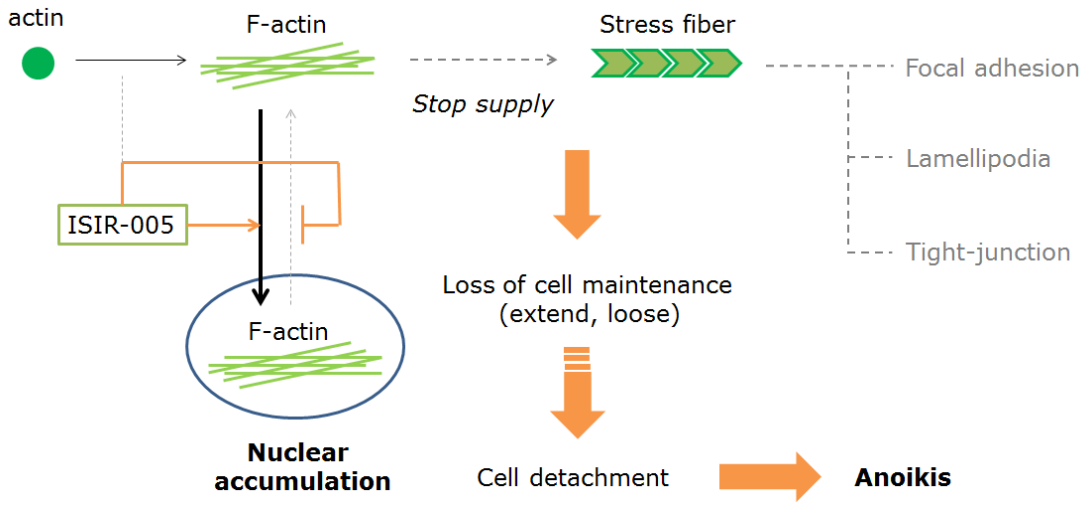

Figure 4–6. A putative mechanism of the nuclear accumulation of F-actin and induction of cell detachment by ISIR-005. ISIR-005 induces the nuclear localization of F-actin followed by loss of stress fibers, focal adhesions and tight-junctions. These losses of cytoskeletal structures decrease cytoskeletal maintenance and change cell morphology to "loosened". As a result of these events, ISIR-005 induces cell detachment from ECM that triggers to initiate anoikis.

acceleration of nuclear import or inhibition of nuclear export of F-actin.

ISIR-005 also inhibited cell adhesion processes of floating cells (Chapter 2). Since F-actin accumulation in nuclei (started at Day-2) was a delayed event compared with the nuclear localization of Rnd3 (Day-1 event), cell adhesion inhibition on cells in adhering processes has a different mechanism from those for cell migration inhibition and cell detachment induced by F-actin translocation into nucleus.

Thus, it has been revealed that ISIR-005 induces depletion of cytosolic F-actin by its nuclear accumulation, which leads loss of stress fibers, focal adhesions and tight-junctions at Day-3 to

Day-4. These contributed partially to migration-inhibition activity of ISIR-005 together with the "pasting" effect induced by the nuclear localization of Rnd3 at Day-1 to Day-2. Depletion of the cytosolic F-actin also induces the loss of cytoskeletal scaffoldings and, therefore, also induces cell detachment. The cell detachment can be a trigger for anoikis as discussed in Chapter 5.

4–4. Materials and Methods

Materials

Instruments used in this research are as follows; for Fluorescence microscope Olympus BX-51 (Olympus), 100W High Pressure Mercury Burner Olympus BH2-RFL-T3 (Olympus), Net FrameWok (Microsoft) and DPControl (Distalpia).

The antibodies were purchased and used as follows: polyclonal anti β-actin in mouse (Santa Cruz), polyclonal anti ZO-1 in rabbit (invitrogen), monoclonal anti vinculin in mouse (sigma) as primary antibodies; AlexaFluoro488 and 546 conjugated anti-mouse IgG and AlexaFluoro546 conjugated anti-rabbit IgG (Invitrogen) as secondary antibodies; Hoechst33342 (Dojindo) for nuclear staining, Acti-stain 488 Palloidin for F-actin staining (cytoskeleton).

Cell culture

As described in Materials and Methods of Chapter 2.

Immunofluorescence detection

As described in Materials and Methods of Chapter 3.

Chapter 5: Mechanism of Cell Death Induction by ISIR-005

5–1. Introductory Statements and Preliminary Results

ISIR-005, a 3,12-unsubstituted fusicoccin derivative, induced anoikis for A549 cells and this anoikis induction was canceled partially by a caspase-8 inhibitor (Figures 2–2 and 2–3). Therefore, caspase-8 activation seemed to be involved in ISIR-005 induced cell death mechanism. The FADD (Fas-associated death domain protein),[114] Fas ligand, Fas receptor (as a trimer) and procaspase-8 make up the complex called death-inducing signaling complex (DISC)[115] and lead activation of caspase-8.[116] Therefore, it can be postulated that ISIR-005 facilitates DISC formation in the death process (Figure 5–1).

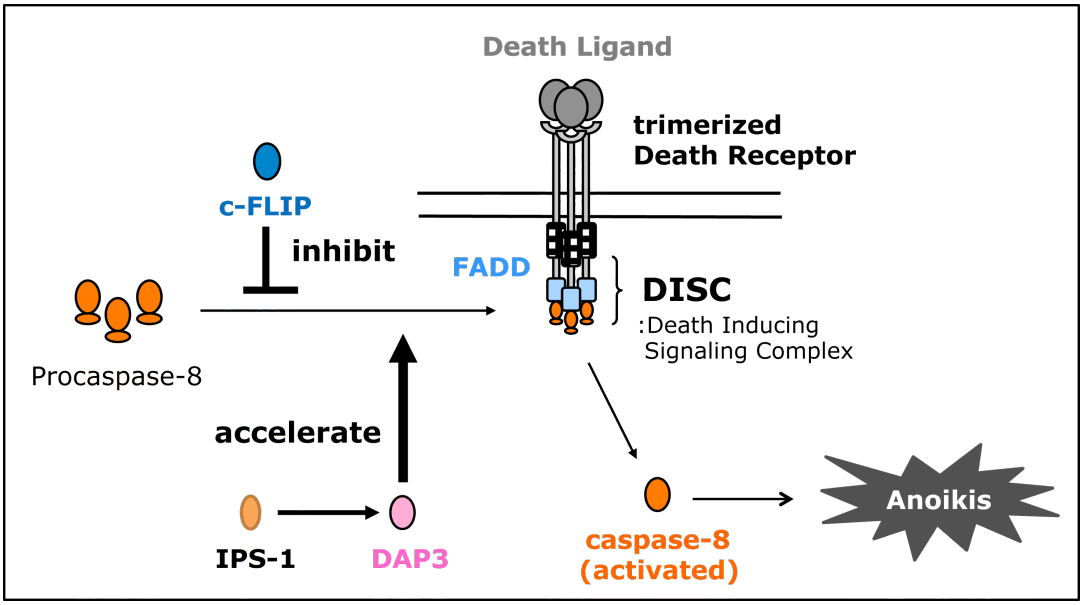

Figure 5−1. The balance of cell death and survival mediated by DISC formation. Caspase-8 is activated *via* formation of DISC, which is inhibited with c-FLIP by complex formation between c-FLIP and procaspase-8 and/or FADD. DAP3 and IPS-1 accelerate DISC formation and induce anoikis. DAP3 binds to procaspase-8 and FADD, and accelerates DISC formation. IPS-1 binds to DAP3 and mediates DISC formation.

Various endogenous inhibitors are known against the apoptotic process. Among them, the cellular-FLICE inhibitory protein (c-FLIP) is known to block the apoptotic cascade at various levels. c-FLIP, an inhibitor of the pathway activated by the death receptor, binds to FADD and inhibits the signal transduction, *e.g.* TRAIL induced apoptosis.[117] At the DISC, c-FLIP inhibits caspase-8 activation because c-FLIP can bind to both of FADD and procaspase-8.[118] It has been reported that the expression level of c-FLIP is up-regulated in cancer cells and supports metastasis of cancer cells through its anti-apoptotic activity.[119]

Death-associated protein 3 (DAP3) was identified as a proapoptotic protein.[120] DAP3 is involved in the ligand dependent apoptosis induction, such as TNFα and Fas ligand.[121,122] Kissil *et al*. also reported that the antisense of DAP3 rescued tumor cells from cell death induced by above-mentioned death ligands.[121] DAP3 interaction with FADD is induced by cell detachment leading to activation of caspase-8 and anoikis.[123] Miyazaki *et al*. showed that DAP3 accelerates the formation of DISC by recruitment of FADD and caspase-8 *via* binding to DR4 or DR5 in a GTP-dependent manner.[122] Interferon-β promoter stimulator 1 (IPS-1), known as a mitochondrial antiviral signaling protein, has a caspase recruitment domain (CARD).[124] In addition, IPS-1 contains a transmembrane region with which IPS-1 is localized at the mitochondrial outer membrane. The mitochondrial localization of IPS-1 is essential for triggering downstream signals, in which FADD and caspase-8 are involved.[125] Li *et al*. reported that IPS-1 binds to DAP3 and activates caspase-8 leading to anikis.[126]

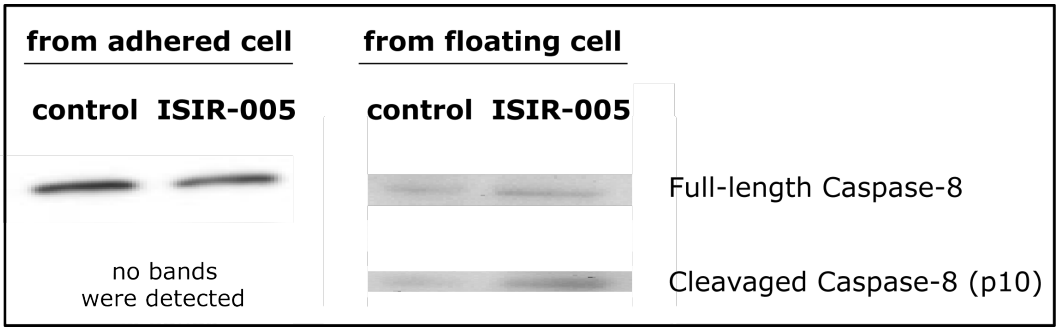

Figure 5−2. Effect of ISIR-005 to caspase-8 activation in adhered cells (left lanes) or floating cells (right lanes). A549 cells (4.0×10^4 cells/mL) were incubated in the presence or absence of ISIR-005 (8 μg/mL) for 4 days, and then adhered cells and floating cells were corrected, separately. Then fractionated cells were lysed independently, and analyzed on SDS-PAGE (8 μg/lane).

With the above-mentioned background in mind, as preliminary experiments, the possibility of caspase-8 activation by ISIR-005 was inspected. A549 cells were incubated with ISIR-005 for 4 days, and floating cells and adhered cells were collected separately. In adhered cells, no cleavage of caspase-8 was observed (Figure 5–2, left lanes). On the other hand, in the lysate obtained from floating cells, cleavage of caspase-8 was enhanced with ISIR-005 treatment (Figure 5–2, right lanes). Although the detachment of cells induces activation of caspase-8 and caspase-3,[81] caspase-8 activation was not significant in detached cells without ISIR-005. Therefore, preventing mechanism for anoikis is working in A549 cells. Taken together, it is plausible that ISIR-005 intervenes the preventing mechanism through affecting the DISC related proteins, such as c-FLIP (inhibitory for anoikis), DAP3 and IPS-1 (activatory for anoikis). Studies on the effects of ISIR-005 toward these DISC related proteins are reported in this chapter (Figure 5–3).

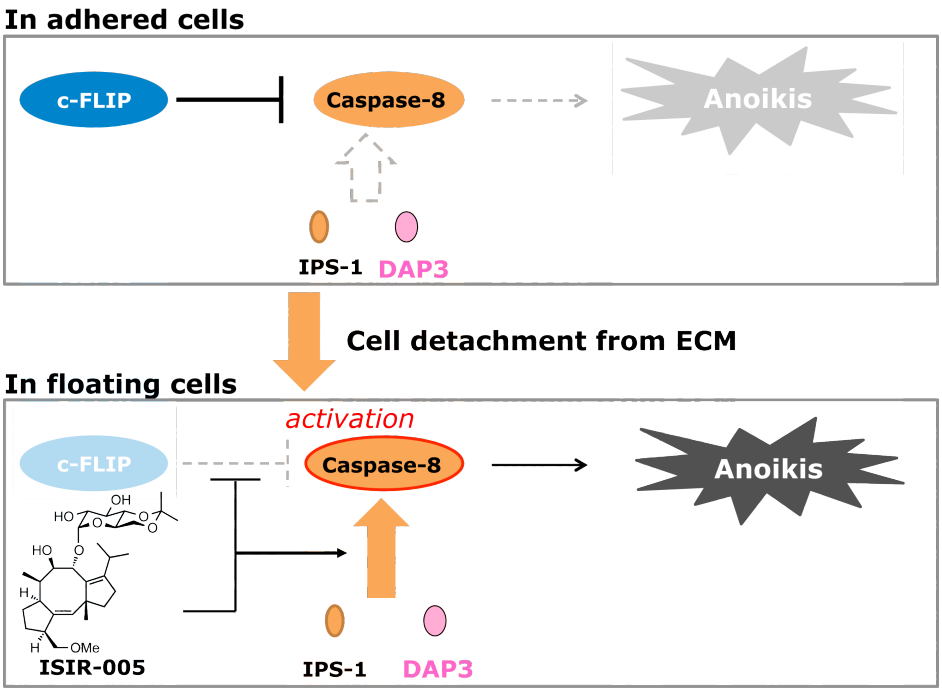

Figure 5–3. The plausible mechanism of anoikis induction by ISIR-005. In adhered cells, anoikis-preventing action is working in A549 cells and ISIR-005 does not intervene in this process. In floating cells, ISIR-005 either inhibits c-FLIP by promotion of its degradation or assists the activating function of DAP3 and/or IPS-1 to lead activation of caspase-8. From obtained results (Figure 5–2), anoikis induction by ISIR-005 requires cell detachment.

5–2. Results

5–2–1. Effect of ISIR-005 onto c-FLIP expression and localization

Firstly, the effect of ISIR-005 onto c-FLIP amount in A549 cells was evaluated by Western blotting at 6-hrs, 24-hrs and 4-days incubation of A549 cells in the presence or absence of ISIR-005 (Figure 5–4). Without ISIR-005, amount of c-FLIP was increased by trypsin treatment for seeding

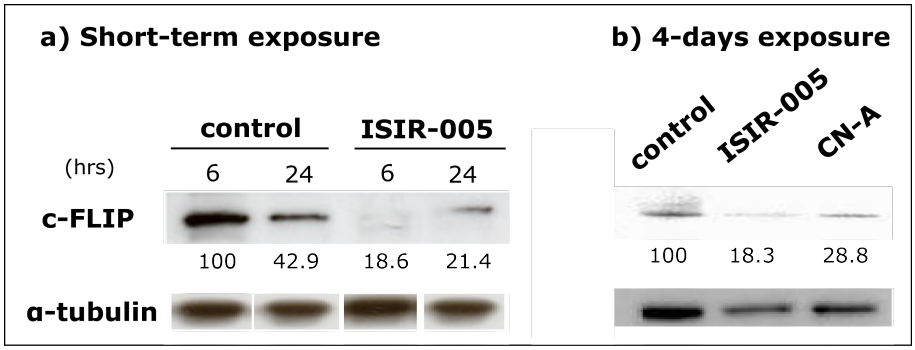

Figure 5–4. The effect for degradation c-FLIP by treatment of ISIR-005. a) 6- and 24-hrs incubation in the presence or absence of ISIR-005 (8 μg/mL). b) 4-days incubation in the presence of ISIR-005 or CN-A (8 μg/mL). The amounts of c-FLIP were detected by Western blot. α-Tubulin was used as a control. The amounts of proteins were evaluated with ImageJ (% of control). After incubation, cells were lysed and separated with SDS-PAGE.

of cells (6-hrs) and reached the steady state at 24-hrs which is enough time to be needed for cell adhesion. In contrast, ISIR-005 decreased c-FLIP amount (about 20% vs. control at 6-hrs) remarkably.

Because caspase-8 is activated through the interaction with FADD at the membrane, c-FLIP should inhibit this event at/near the membrane (Figure 5–1). To inspect this possibility, subcellular localization of c-FLIP was detected with immunostaining in the presence or absence of ISIR-005 or CN-A. At 4-days incubation after treatment with ISIR-005, c-FLIP seemed to be localized only at nucleus. In control and CN-A treated cells, c-FLIP was detected not only at nucleus but also at cytosol (Figure 5–5).

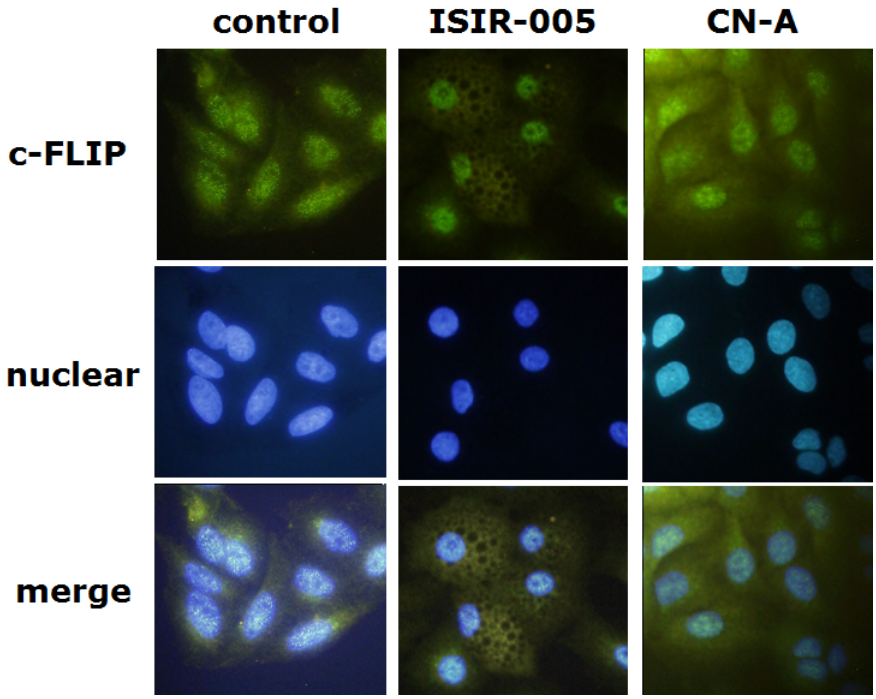

Figure 5−5. The change of c-FLIP localization by ISIR-005 (center panels) or CN-A (right panels). Photographs are immunostaining images of c-FLIP (upper panels), nucleus (middle panels) and merge of them (lower panels). After incubation for 4 days in the presence or absence of ISIR-005 or CN-A, the cells were fixed with PFA and stained c-FLIP with its 1st antibody then FITC conjugated 2nd antibody (green, 488 nm). Nuclei were stained with Hoechst33342 (blue, 352 nm).

As shown in Chapter 3, Y-27632, a ROCK inhibitor, rescued A549 cells from cell blebbing and cell death triggered by ISIR-005 (Figures 3–3 and 3–4). There are two possibilities for the rescue effect of Y-27632; prevents either degradation or nuclear localization of c-FLIP induced by ISIR-005. As anticipated, Y-27632 induced cytosolic localization of c-FLIP from nuclear in ISIR-005 treated cells (Figure 5-6a). On the other hand, the amount of c-FLIP was not changed remarkably by Y-27632 regardless of ISIR-005 treatment (Figure 5–6b). Thereby, the ROCK inhibitor, Y-27632, rescued cells from anoikis triggered by ISIR-005 through translocation of

c-FLIP from nucleus to cytoplasm.

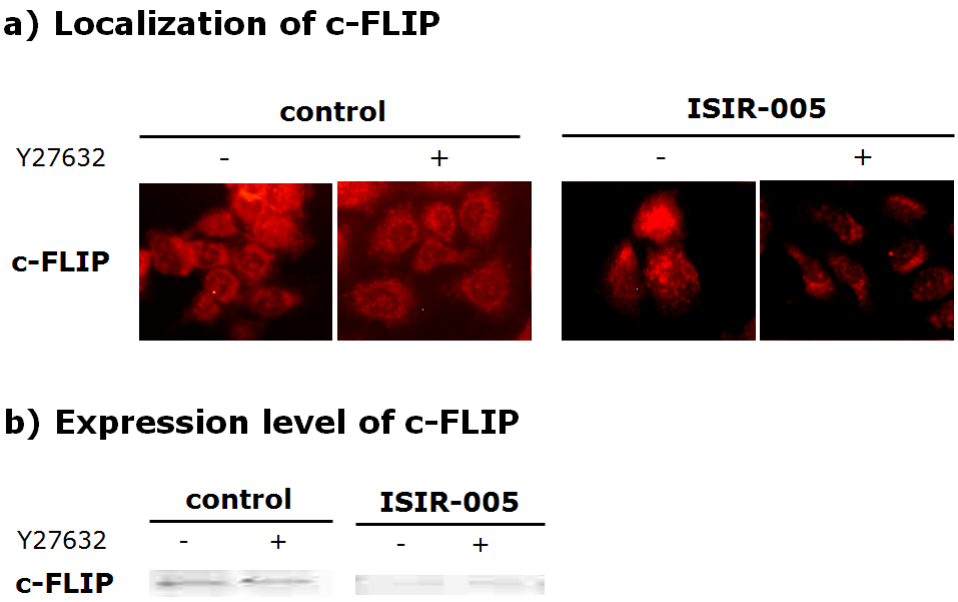

Figure 5−6. Effect of Y-27632 onto localization and expression level of c-FLIP with or without ISIR-005. a) The images of immunostaining of c-FLIP. ISIR-005 induced the nuclear localization of c-FLIP (3rd panel). Y-27632 induced translocation of c-FLIP from nuclear to cytoplasm in ISIR-005 treated cells (3rd and 4th panels). b) The images of Western blotting of c-FLIP. Y-27632 did not change the expression levels remarkably. After incubation for 4 days in the presence or absence of ISIR-005 (8 μg/mL) ± Y-27632 (1 μg/mL), the cells were lysed or fixed with methanol. In the fixed cells, c-FLIP was stained with its antibody then AlexaFluoro546 conjugated 2nd antibody (orange, 546 nm). The lysate were separated with SDS-PAGE (8 μg/lane).

5–2–2. Effects of ISIR-005 onto DAP3 and IPS-1

c-FLIP is a "defense" protein for cell death. In the preceding section, it has been revealed that ISIR-005 weakens the defense protein. Then, how does ISIR-005 affect on the "offense" mechanism for cell death? Since caspase-8 activation was detected in detached cells by ISIR-005, the proteins related to DISC formation were investigated. DAP3 and IPS-1, as "offense" proteins, accelerate DISC formation, caspase-8 activation and anoikis.

A549 cells were treated by trypsin to unify them to be detached status and re-seeded to culture plates with ISIR-005 and incubated for 6 and 24 hrs. Amounts of DAP3 and IPS-1 were evaluated by Western blotting. In control A549 cells, none of DAP3 could be detected. The very few of DAP3 may be contributing to anoikis-resistant nature of A549 cell line. ISIR-005 induced up-regulation of DAP3 from 6-hrs incubation (Figure 5–7, upper panels). On the other hand, IPS-1 is expressed in detached A549 cells and is gradually increased with progression of cell adhesion. ISIR-005 clearly stimulated up-regulation of IPS-1 in this event (Figure 5–7, middle panels). Consequently, it has

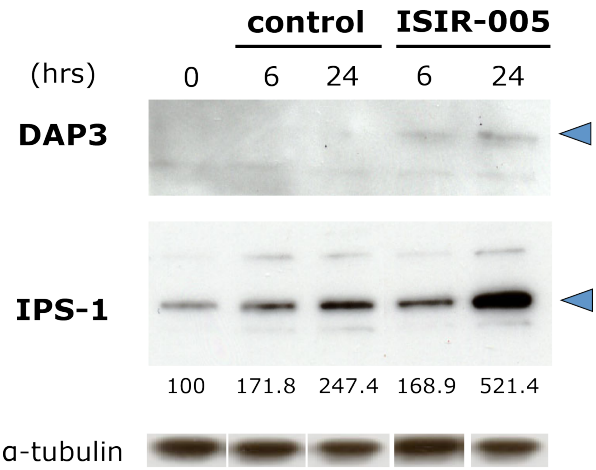

Figure 5−7. Effects of ISIR-005 on expressed levels of DAP3 (1st panels) and IPS-1 (2nd panels). A549 cells (4.0×10^4 cells/mL) were incubated in the presence or absence of ISIR-005 (8 μg/mL), and then, after 6 and 24-hrs incubation, cells were lysed and the lysate was separated with SDS-PAGE (10 μg/lane). The expression levels of proteins were evaluated with ImgaeJ®.

been revealed that ISIR-005 strengthens also the offensive mechanism for anoikis through induction of up-regulation of both DAP3 and IPS-1.

5–2–3. Effect of ISIR-005 onto activities of p53

A. Working hypothesis

The *p53* is known as a tumor suppressor gene and a representative transcriptional factor. As one of many physiological roles, p53 influences the degradation of c-FLIP protein *via* the ubiquitination-proteasome processes, which has been confirmed in colon cancer cells.[127,128] p53 is degradated by proteasome system through ubiqutination by Mdm2.[129] A type of apoptosis induced by CN-A plus IFN-α was mediated through the activation of p53.[65] In this process, the expression level of p53 was decreased probably because of a negative feedback mediated by Mdm2.[130] In fact the p53 degradation was inhibited by MG-132, a proteasome inhibitor. These results suggested that CN-A plus IFN-α induces the proteasome activation in the processes of apoptosis.[65] It has been reported that the nuclear import or nuclear retention of p53 is essential for exhibition of its function in growth inhibition[131] or induction of apoptosis.[132] Furthermore, in some type of tumor that has wild-type p53, loss of p53 activity is associated with its localization at cytoplasm (Figure 5–8).[133] Cytoplasmic accumulation of p53 leads loss of its responsive nature to genome stress.[134] IRTKS (**I**nsulin **r**eceptor **t**yrosine **k**inase **s**ubstrate) binds directly to p53 and increases p53 ubiquitination and cytoplasmic localization.[135] Moreover, some proteins are known to induce nuclear localization

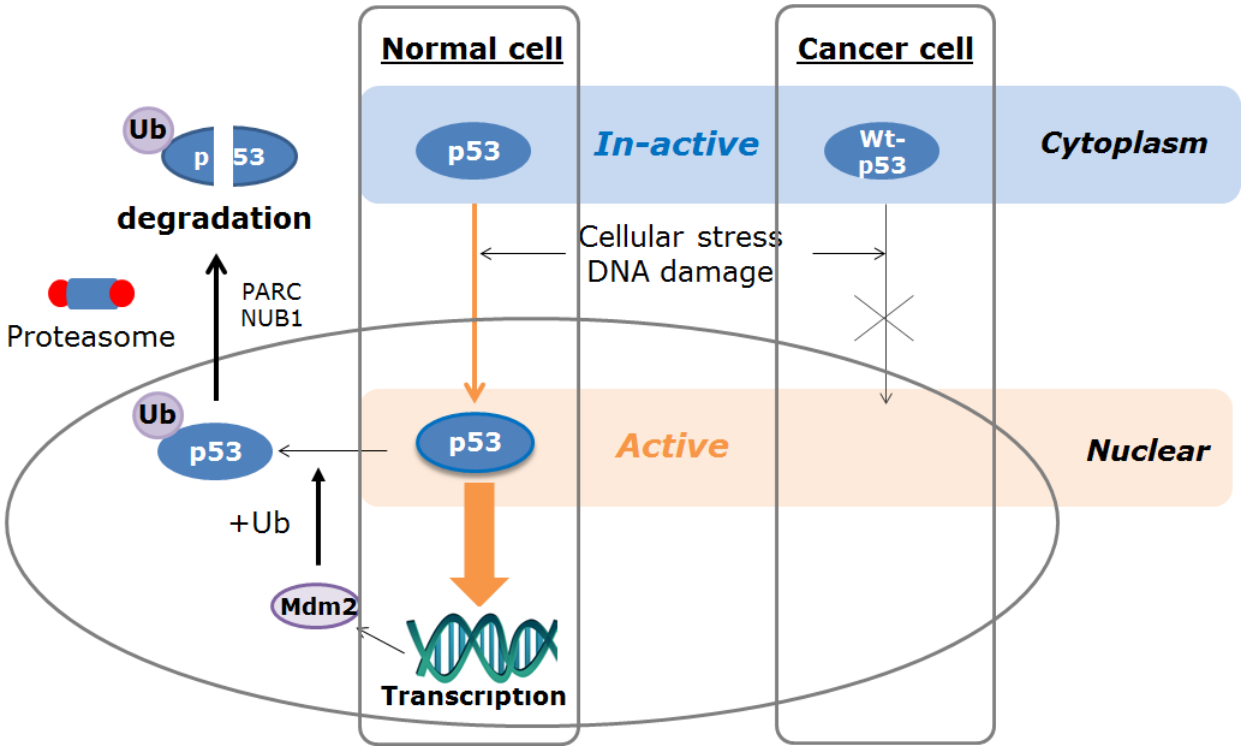

Figure 5–8. The relationships between the activity and localization of p53 in normal or cancer cells. Cellular stress or DNA damage induces nuclear localization of cytoplasmic p53, which is in inactive stage. The nuclear localization of p53 activates its transcriptional activity in normal cells, which leads several cellular processes including apoptosis. In some cancer cells retaining wt-p53, p53 does not localize to nucleus by cellular stress or DNA damage.

of p53, such as PARC (Parkin-like ubiquitin ligase),[136] and NUB1 (NEDD8 ultimate buster 1)[137] (Figure 5–8). Both of c-FLIP and p53 are degradated by proteasome, and p53 is activated in CN-A plus INFα induced apoptosis.[65] Taken together, it can be hypothesized that ISIR-005 promotes degradation of c-FLIP by activation of p53.

B. Results

A549 cells were incubated with ISIR-005 for 4 days and the proteins were extracted, and their expression levels were evaluated by Western blotting (Figure 5–9). In cells treated with ISIR-005, p53 was decreased remarkably at 4-days incubation (Figure 5–9, top panels). Moreover, the expression and the phosphorylation level of Mdm2 were up-regulated by treatment with ISIR-005 (Figure 5–9, middle and bottom panels). These results indicated that ISIR-005 stimulated transcriptional activation of p53 and subsequent activation of proteasome that leads to the negative-regulation of p53. Because of both p53 activation (Figure 5–9) and c-FLIP decomposition (Figure 5–6) were confirmed at the same period of incubation (4-days), it was inferred that p53 activation by ISIR-005 might be responsible for the acceleration of c-FLIP degradation.

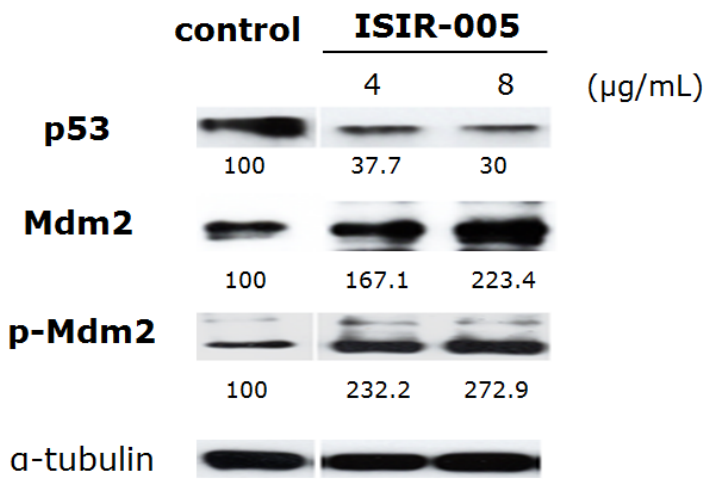

Figure 5−9. The effects of ISIR-005 for the expression levels of p53 and Mdm2, and the phosphorylation status of Mdm2. The expression levels of p53 (1st panels), Mdm2 (2nd panels) and p-Mdm2 (pSer166, 3rd panels) were detected by Western blotting. α-Tubulin was used as control (4th panels). The p53 was down-regulated with up-regulation of Mdm2 expression and phosphorylation in ISIR-005 treated cells. A549 cells (4.0×10^4 cells/mL) were incubated in the presence of ISIR-005 (4 or 8 μg/mL) for 4 days, and then cells were lysed, separated with SDS-PAGE (10 μg/lane). The expression levels of proteins were evaluated with ImgaeJ®.

As mentioned earlier, the localization of p53 is important for its transcriptional activity. Transcriptional activity of p53 was accelerated by treatment of ISIR-005 accompanying with its degradation (Figure 5–8). Moreover, up-regulations of DAP3 and IPS-1 may be interpreted by activation of the transcriptional activity of p53. To clarify this possibility, the localization of p53 after treatment of ISIR-005 was inspected by immunostaining method.

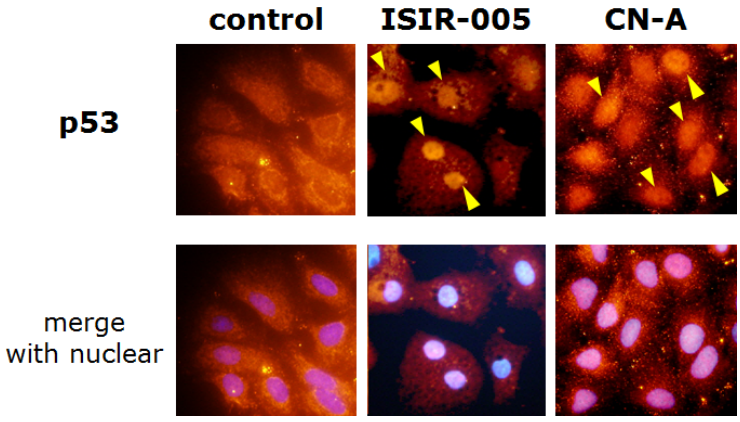

Figure 5−10. Immuno-fluorescent staining of p53 in A549 cells treated by indicated compounds for 4 days. The p53 localized at nuclei with ISIR-005 (2nd panels) or CN-A (3rd panels) treatments. In control cells, p53 existed in cytoplasm (1st panel), which is negative status for its activity. A549 cells (4.0×104 cells/mL) were incubated with or without indicated compounds (8 μg/mL), and then fixed with PFA and stained p53 with its 1st antibody and AlexaFluor546 conjugated 2nd antibody (Top panels, orange, 546 nm). The nuclear was stained with Hoechst33342 (blue, 352 nm) and merged with the image of p53 (lower panels).

A549 cells were seeded with or without ISIR-005 and incubated for 4 days. As expected, ISIR-005 localized p53 to nucleus at 4-days incubation (Figure 5–10), whereas p53 localized mainly at cytoplasm in control cells (Figure 5–10, 1st panels). It has been reported that the ubiquitination of p53 by Mdm2 occurs mainly in the cytoplasm, and Mdm2 ubiquitin ligase activity is required for p53 nuclear export.[138] Thus, down-regulation (Figure 5–9, top panels) and nuclear localization (Figure 5–10, 2nd panels) of p53 were confirmed to be induced by ISIR-005.

5–3. Discussion

ISIR-005 induces several anoikis-related events as follows; 1) degradation and nuclear accumulation of c-FLIP, 2) up-regulation of DAP3 and IPS-1, and 3) p53 activation by nuclear localization and its negative-feedback *via* Mdm2. Although the preparation to death is completed in the adhered cells with ISIR-005, caspase-8 activation is confirmed only in floating cells. These results indicated that the cell detachment progressed after above events to initiates anoikis.

The c-FLIP degradation induced by ISIR-005 was confirmed in the adhered cells (Figure 5–4). The cell death induction (Figure 2–8) and the c-FLIP down-regulation (Figure 5–4, right lanes) by ISIR-005 were induced coincidently (5~6 hrs after treatment). Therefore, this down-regulation of c-FLIP is considered to be a key step for the cell death by ISIR-005. In addition to the degradation, c-FLIP is accumulated in nucleus. By comparison of control and ISIR-005 treated cells, the expression levels in the nuclear localization of c-FLIP seemed to be similar in both cells. To confirm this, the concentrations of c-FLIP in the nucleus were evaluated by the fluorescence intensity obtained from ImageJ® analysis (Figure 5–11). This analysis showed that the nuclear abundance of c-FLIP was not changed by ISIR-005 ($p > 0.05$, $n = 3$, paired t-test). Therefore, it is most plausible that c-FLIP in cytoplasm

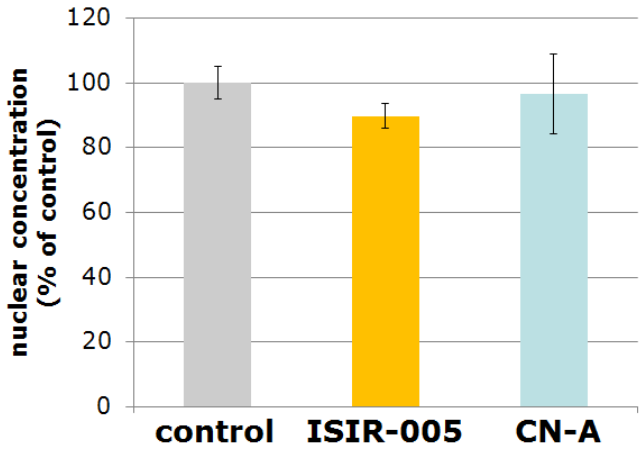

Figure 5–10. The expression level of c-FLIP at nucleus. Although total amount of c-Flip decreased in ISIR-005 treated cells (Figure 5–4), no significant changes were observed in its nuclear amounts. Therefore, ISIR-005 decreased cytoplasmic c-FLIP. This analysis was performed using images shown in Figure 5–5 by use of ImageJ®. There were no significant differences as shown (paired t-test, $p < 0.05$, one-sided).

was degradated selectivity by ISIR-005 treatment. This degradation antagonizes the caspase-8 inhibitory activity of c-FLIP and induces caspase-8 activation after cell detachment. Together with c-FLIP degradation, ISIR-005 induces up-regulation of DAP3 and IPS-1, which accelerate DISC formation and apoptosis/anoikis (Figure 5–12). As mentioned in Chapter 4, nuclear accumulation of F-actin might be responsible for induction of cell detachment accompanying with loss of stress fibers, focal adhesion and tight-junction.

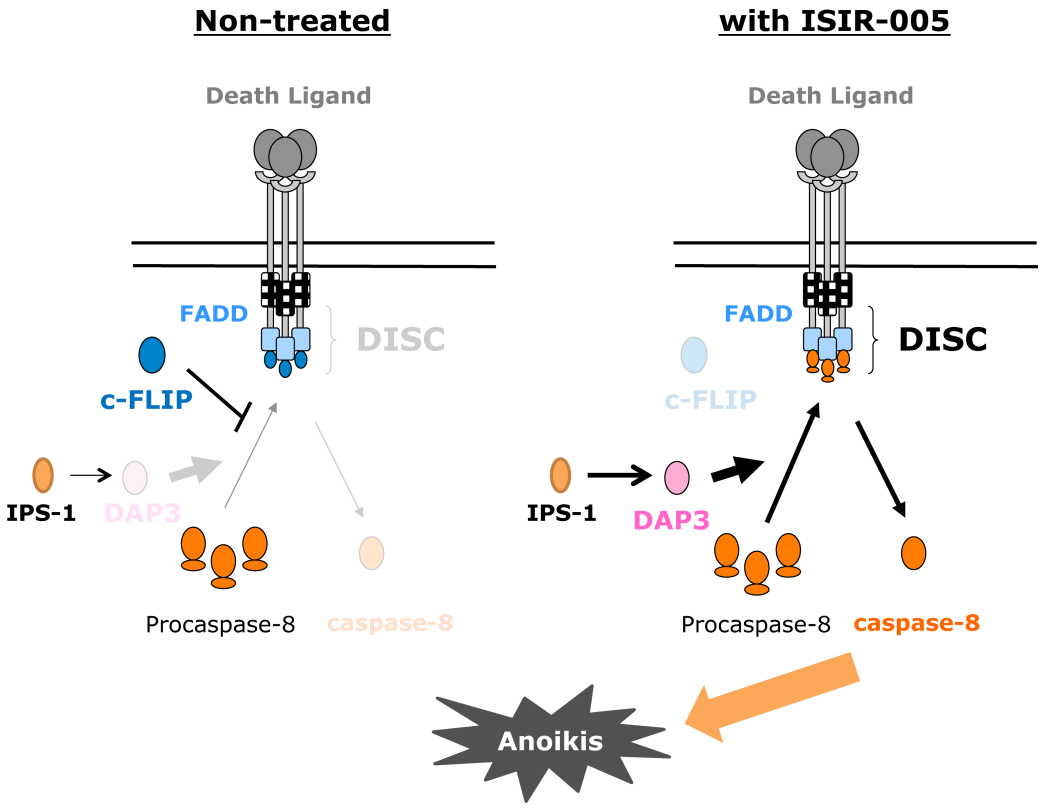

Figure 5−11. The putative mechanism of caspase-8 activation *via* DISC formation by ISIR-005 in A549 cells. ISIR-005 induces that degradation of c-FLIP (defensive) and increase DAP3 and IPS-1 (offensive). These induce acceleration of DISC formation and anoikis *via* caspase-8 activation.

Degradation of p53 was observed by ISIR-005 treatment (Figure 5–9). In this process, Mdm2, a transcriptional target of p53, increased at 4-days incubation. As mentioned above, since Mdm2 is a negative-regulator of p53, degradation of p53 seemed to be progressed by its negative-feedback *via* Mdm2. These results may be explainable as follows; cytoplasmic p53 is transported into nucleus by ISIR-005 treatment and exhibits its transcriptional role to up-regulate Mdm2. Then Mdm2 ubiquitinates cytoplasmic p53 leading to its degradation by the proteasome system. By these chain events, p53 localized at nucleus and cytoplasmic p53 was degradated in ISIR-005 treated cells. Activation of p53 by ISIR-005 was also supported by up-regulation of DAP3. DAP3, which is also a transcriptional target of p53,[139] increased at 24-hrs incubation with ISIR-005 (Figure 5–7).

Therefore, it is most likely that ISIR-005 facilitates the transcriptional activity of p53 by forcing its nuclear accumulation or localization.

Interestingly, F-actin was localized at nuclear after 4 days as describe in Chapter 4. Okorokov *et al*. reported that nuclear F-actin associates with p53 and retains it at nuclear under DNA-damage conditions.[140] Since the nuclear import of p53 is required for its transcriptional activity, it was suggested that the co-localization of p53 and F-actin retains the activity and the expression level of p53. Indeed, expression level of p53 remained in a steady state for 4 days (Figure 5–9). Therefore, ISIR-005 induces co-localization of p53 and F-actin at nucleus with which effects transcriptional activity of p53 was retained (Figure 5–12).

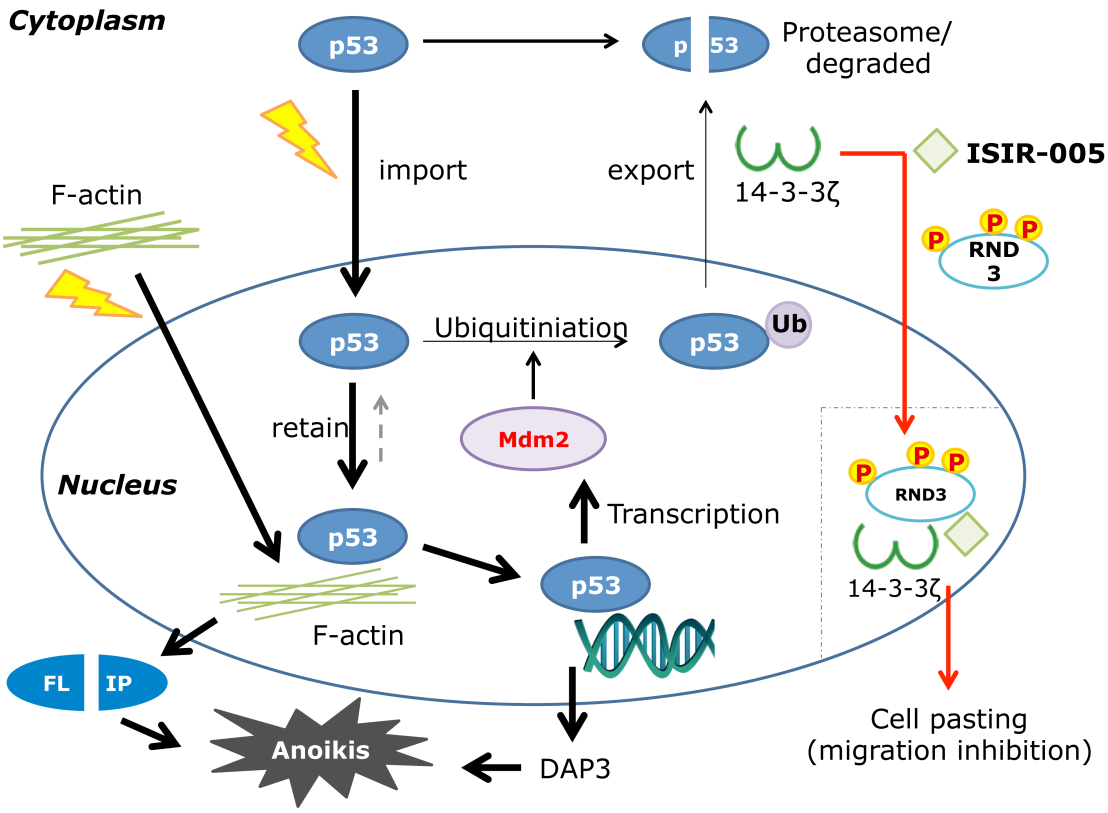

Figure 5−12. The putative model of ISIR-005 induced modulation of p53 localization and activity. ISIR-005 induced the nuclear localization of p53, which associated with F-actin and retained the nuclear localization and its activity. The transcriptional products of p53, Mdm2 and DAP3 were up-regulated by ISIR-005. The DAP3 induction and c-FLIP degradation accelerate anoikis mediated by activated caspase-8. 14-3-3ζ imports Rnd3 into nucleus with the complexation, which inhibits cell migration.

It was reported that overexpression of 14-3-3ζ deceases p53 in mammary epithelial cells.[141] More importantly and interestingly, it has been reported that the phosphorylated extreme C-terminus of p53 is the client of 14-3-3 proteins and this 14-3-3 PPI is important for the formation of the active

p53 tetramer.[142–144] Therefore, one may anticipate that ISIR-005 stabilizes the p53/14-3-3 PPI as a primary target for the activation of p53. However, this hypothesis has a critical defect. The 14-3-3 interacting C-terminus of p53 is Lys^{386}–phospho-Thr^{387}–Glu^{388}–Gly^{389}–Pro^{390}–Asp^{391}–Ser^{392}–Asp^{393}–COOH. Namely, the *i* +1 residue is Glu that is not compatible with any types of FC/CNs (Figure 1–14). Actually, a binary complex of the residues 385–393 of p53 (pT387) and 14-3-3 could not be stabilized by any fusicoccin derivatives.[145] Therefore, ISIR-005 cannot enhance p53/14-3-3 PPI directly. It is more plausible that ISIR-005 indirectly contributes to the formation of p53/14-3-3 PPI. The primary target(s) could exist in the upstream signaling pathways for adjusting the phosphorylation status of p53 suitable for 14-3-3 PPI.

Interestingly, p53-null H1299 cells were also induced adhesion-inhibition and cell-death by ISIR-005 at 6-hrs incubation (Figure 5–13 a) and b), respectively). Adhesion inhibition may be caused by a similar mechanism with that on A549 cells (Chapter 4). At present, it is not clear that p53 is involved in the adhesion inhibition. Although it has been revealed that p53 plays a central role in the induction of cell death caused by ISIR-005, the mode of action for the cell death remains unclear. Further investigations are necessary for clarification of the primary target responsible for this phenotypic outcome.

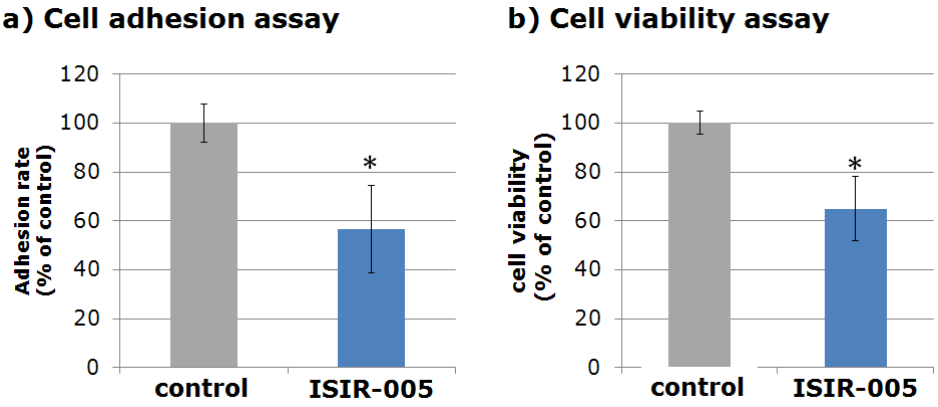

Figure 5−13. The effect of ISIR-005 on cell adhesion and cell viability of H1299 cells. ISIR-005 exhibited the similar effect both on A549 and H1299 cells that does not express p53 protein. H1299 cells (10×10^4 cells/mL) were incubated with or without ISIR-005 (8 μg/mL) for 6 hrs on the culture plates (a, adhesion assay) or poly-HEMA coated plates (b, cell viability assay). Adhesion rate and viability were estimated by MTT assay (Mean ± S.D., n = 3, $*p < 0.05$, paired *t*-test, one-sided).

5–4. Materials and Methods

Materials

Instruments used in this research are as follows; For absorption measurements on a 96-well plate, micro plate reader Model 680 (BIO-RAD, Hercules, CA) with filters allowing 490 and 570 nm to transmit. For Western blotting analysis, X-Omat 1000 Processor (KODAK, Rochester, NY) was used to detect chemiluminescence; for Fluorescence microscope Olympus BX-51 (Olympus), 100W High Pressure Mercury Burner Olympus BH2-RFL-T3 (Olympus).

The antibodies were purchased and used as follows: polyclonal anti c-FLIP in rabbit (cell signaling Inc.), polyclonal anti p53 in mouse (Calbiochem Inc.), polyclonal anti p21 in mouse (Santa Cruz Inc.), monoclonal anti-Mdm2 in rabbit (Cell Signaling Technology Inc.), monoclonal anti phosphor-Mdm2 in rabbit (Cell Signaling Technology Inc.) and polyclonal anti α-tubulin in mouse (Santa Cruz, CA; or Sigma) as primary antibodies; horseradish peroxidase (HRP)-conjugated anti-mouse, rabbit and goat IgG (Santa Cruz, CA), FITC-conjugated anti-rabbit IgG (Santa Cruz, CA), AlexaFluoro405 anti-mouse IgG and AlexaFluoro568 anti-rabbit IgG (Invitrogen) as secondary antibodies; Hoechst33342 (dojindo) for nuclear staining.

For cell adhesion and viability evaluation, Cell Titer 96® (Promega, Madison, WI) was used. To extract protein from living cells, protease and phosphatase inhibitor cocktails were purchased form Sigma. For determination of protein concentrations, BCA protein assay kit was obtained from Thermo Scientific. As blocking reagent and coating reagent, bovine serum albumin was purchased from Sigma. For visualization of chemiluminescence, ECL Plus Western blotting detection reagent was obtained from GE healthcare (Buckinghamshire).

The statistical analysis was performed with Microsoft Excel (paired student t-test).

Cell culture

H1299 cell line was obtained from the American Type Culture Collection (ATCC). The culture conditions were the same to those for A549 cells (See Chapter 2).

Protein extraction

On a 6-well plate, cells (5×10^4 cells/mL, 1.5 mL/well) were incubated in the presence or absence of compounds at indicated concentrations for indicated periods. These cells were washed twice with D-PBS(–) and lysed with buffer ‘A’ [20 mM Tris·HCl, 140 mM NaCl, 1% (v/v) TritonX-100, 2 mM NaF, protease and phosphatase inhibitor cocktails, pH: 7.4] for 20 min on ice. The resulting

suspensions were collected and centrifuged (15000×g, 15-mins, 4°C) to remove the precipitates, and the supernatant was diluted with 2×Laemmli sample buffer and boiled for 5 min at 95°C provided a protein extraction sample.

Western Blotting

As described in Materials and Methods of Chapter 3.

Immunofluorescence detection

As described in Materials and Methods of Chapter 3. The localization was ditected by ImageJ®. The nuclear areas were selected and calculated their area and mean values. The figure showed mean values (Figure 5–10).

Chapter 6: Conclusion

This research revealed that ISIR-005, a 3,12-unsubstituted fusicoccin derivative, has specific biological activities that are related to anoikis. In this research, A549 cells are used as an anoikis resistant model and it has been revealed that 1) ISIR-005 induces anoikis-like cell death; 2) ISIR-005 significantly inhibits cell migration and adhesion; 3) The nuclear translocation of Rnd3 by ISIR-005 is required for inhibition of cell migration; 4) The nuclear accumulation of F-actin by ISIR-005 induces loss of stress fibers, focal adhesions and tight-junctions resulting in both migration inhibition and cell-detachment induction; 5) The acceleration of DISC formation is the key step in the capase-8 dependent anoikis caused by ISIR-005.

These anti-tumor activities are specific in ISIR-005. CN-A, a 3-hydroxy derivative, and FC-A, a 12-hydroxy derivative, do not show these activities. Thus, the biological activity of FC/CNs is depending on the hydroxylation-patterns of aglycone moiety in them. The 3,12-unsubstitution on the aglycone is the structural feature of ISIR-005 among other FC/CNs such as CN-A and FC-A. Therefore, this structural characteristics should take resposibility for the specific biological activities of ISIR-005.

In this research, attension was focused onto Rnd3 in conjunction with the migration-inhibition activity of ISIR-005. Because, it has been recently reported that 14-3-3 proteins regulate subcellular localization of Rnd3 and FC/CNs have a potential to stabilize such 14-3-3 PPIs. In intact cells, subcellular localization of Rnd3 is regulated by post-translational modifications such as phosphorylation at Ser210, Ser218 and Ser240 and farnesylation onto Cys241. Antagonistic activity of Rnd3 toward Rho/ROCK signaling pathway is achieved by farnesylation that translocates Rnd3 to cytomembrane. On the other hand, simultaneous modifications of phosphorylation at Ser240 and farnesylation at Cys241 localize Rnd3 into cytoplasm through a binary complex fromation with 14-3-3 protein resulting in activation of Rho/ROCK signaling. These subcellluar localizations of Rnd3 must be regulated correctly for tumor growth. From experimental results, it has been revealed that ISIR-005 prevents these events by forcing nuclear localization of Rnd3. Involvement of 14-3-3ζ was confirmed by observing co-localization of Rnd3 and 14-3-3ζ at nuclei in the presence of ISIR-005. The phosphorylation at Ser240 by ROCK-1 was required for the nuclear localization of Rnd3 because a ROCK inhibitor canceled the nuclear import of Rnd3 induced by ISIR-005. Taken together, it has been strongly suggested that ISIR-005 formed a ternary complex with 14-3-3ζ and Rnd3 of which Ser240 is phosphorylated but Cys241 is intact. Since the farnesylation

of Cys241 is required for membrane localization of Rnd3 and fanesylation must be steriacally prohibited in the ternary complex due to 14-3-3 binding at the adjacent Ser240, the ternary complex formation completely inhibits translocation of Rnd3 into cytomembrane and, therefore, brings continuous activation of Rho/ROCK signaling. FC-A cannot make the ternary complex due to steric conflict between its 12-hydroxyl and the *i* + 2 residue (Thr242) in the binding motif of Rnd3. CN-A might not be able to form the ternary complex due to incompatibility of its 3-hydroxyl with the i + 1 Cys241 as suggested by model studies (Figure 3–19). These considerations supported the ISIR-005 specific nuclear import of Rnd3. Although further validation including a direct proof of the ternary complex formation must be necessary to confirm the mode of action, it can be concluded that the nuclear localization of Rnd3 directly brings the earliest phenotypic outcome, *i.e.*, "pasting" state of A549 cells.

The nuclear accumulation of F-actin seemed to contribute not only for migration inhibition but also for cell detachment, although the primary target has not been identified yet. Degradation of c-FLIP and the increase of DAP3 and IPS-1 suggested the activation of p53. These events should accelerate the DISC formation. The p53 activation was supported by up-regulation of its target gene products, DAP3 and Mdm2. It is plausible that the combination of p53 activation and cell detachment caused by loss of cytoplasmic F-actin induces caspase-8 activation resulting in anoikis. In other words, both of the DISC formation and cell detachement are the critical events for cell death induction by ISIR-005.

Although mode of actions of above-mentioned phenotypic outcomes are not fully clarified yet, all of the migration-inhibition, the adhesion-inhibition, induction of cell detachment and induction of apoptosis are desirable biological activities for ISIR-005 potentially being an anti-metastatic agent.

This research identified Rnd3 as a most probable candidate of the primary target of ISIR-005 in migration inhibitory activity. The new migration inhibition mechanism, which is named as "pasting" effect, has been also revealed by this research. This new mechanism could lead a new strategy for cancer therapy. ISIR-005, a 3,12-unsubstituted fusicoccin derivative, has many kinds of anti-tumor activities. Although this multitarget-nature may be a drawback for drug development based on ISIR-005, this 3,12-unsubstituted fusicoccin derivative, as exemplified with this research, can be a useful tool to clarify several physiological roles of 14-3-3 PPIs.

References

1. Aitken, A.; 14-3-3 proteins: a historic overview. *Semin. Cancer Biol.*, **2006**, *16*, 162–172.
2. Moore, B. E.; Perez, V. J.; in "Physiological and biochemical aspects of nervous integration", Carlson, F. D., ed., Prentice-Hall, **1967**, p. 343–59.
3. Ichimura, T.; Isobe, T.; Okuyama, T.; Yamauchi, T.; Fujisawa, H.; Brain 14-3-3 protein is an activator protein that activates tryptophan 5-monooxygenase and tyrosine 3-monooxygenase in the presence of Ca^{2+}, calmodulin-dependent protein kinase II. *FEBS Lett.*, **1987**, *219*, 79–82.
4. Wilker, E. W.; Grant, R. A.; Artim, S. C.; Yaffe, M. B.; A structural basis for 14-3-3sigma functional specificity. *J. Biol. Chem*., **2005**, *280*, 18891–18898.
5. Yang, X.; Lee, W. H.; Sobott, F.; Papagrigoriou, E.; Robinson, C. V.; Grossmann, J. G.; Sundström, M.; Doyle, D. A.; Elkins, J. M.; Structural basis for protein-protein interactions in the 14-3-3 protein family. *Proc. Natl. Acad. Sci. USA*., **2006**, *103*, 17237–17242.
6. Obsil, T.; Ghirlando, R.; Klein, D. C.; Ganguly, S.; Dyda, F.; Crystal structure of the 14-3-3zeta:serotonin *N*-acetyltransferase complex. A role for scaffolding in enzyme regulation. *Cell*, **2001**, *105*, 257–267.
7. Muslin, A. J.; Tanner, J. W.; Allen, P. M.; Shaw, A. S.; Interaction of 14-3-3 with signaling proteins is mediated by the recognition of phosphoserine. *Cell*, **1996**, *84*, 889–897.
8. Yaffe, M. B.; Rittinger, K.; Volinia, S.; Caron, P. R.; Aitken, A.; Leffers, H.; Gamblin, S. J.; Smerdon, S. J.; Cantley, L. C.; The structural basis for 14-3-3:phosphopeptide binding specificity. *Cell*, **1997**, *91*, 961–71.
9. Coblitz, B.; Wu, M.; Shikano, S.; Li, M.; C-terminal binding: an expanded repertoire and function of 14-3-3 proteins. *FEBS Lett*., **2006**, *580*, 1531–1535.
10. Petosa, C.; Masters, S. C.; Bankston, L. A.; Pohl, J.; Wang, B.; Fu, H.: Liddington, R. C.; 14-3-3zeta binds a phosphorylated Raf peptide and an unphosphorylated peptide via its conserved amphipathic groove. *J. Biol. Chem*., **1998**, *273*, 16305–16310.
11. Johnson, C.; Crowther, S.; Stafford, M. J.; Campbell, D. G.; Toth, R.; MacKintosh, C.; Bioinformatic and experimental survey of 14-3-3-binding sites. *Biochem. J*., **2010**, *427*, 69–78.
12. Ottmann, C.; Yasmin, L.; Weyand, M.; Veesenmeyer, J. L.; Diaz, M. H.; Palmer, R. H.; Francis, M. S.; Hauser, A. R.; Wittinghofer, A.; Hallberg, B.; Phosphorylation-independent interaction between 14-3-3 and exoenzyme S: from structure to pathogenesis. *EMBO J*., **2007**, *26*, 902–913.
13. Morrison, D. K.; The 14-3-3 proteins: integrators of diverse signaling cues that impact cell

fate and cancer development. *Trends Cell Biol.*, **2009**, *19*, 16–23.

14. Lee, J. A.; Park, J. E.; Lee, D. H.; Park, S. G.; Myung, P. K.; Park, B. C.; Cho, S.; G1 to S phase transition protein 1 induces apoptosis signal-regulating kinase 1 activation by dissociating 14-3-3 from ASK1. *Oncogene*, **2008**, *27*, 1297–305.
15. Dong, S.; Kang, S.; Gu, T. L.; Kardar, S.; Fu, H.; Lonial, S.; Khoury, H. J.; Khuri, F.; Chen, J.; 14-3-3 Integrates prosurvival signals mediated by the AKT and MAPK pathways in ZNF198-FGFR1-transformed hematopoietic cells. *Blood*, **2007**, *110*, 360–369.
16. Obsilová, V.; Silhan, J.; Boura, E.; Teisinger, J.; Obsil, T.; 14-3-3 proteins: a family of versatile molecular regulators. *Physiol. Res.*, **2008**, *57* (Suppl. 3), S11–S21.
17. Masters, S. C.; Subramanian, R. R.; Truong, A.; Yang, H.; Fujii, K.; Zhang, H.; Fu, H.; *Biochem. Soc. Trans.*, **2002**, *30*, 360–365.
18. Neal, C. L.; Yao, J.; Yang, W.; Zhou, X.; Nguyen, N. T.; Lu, J.; Danes, C. G.; Guo, H.; Lan, K. H.; Ensor, J.; Hittelman, W.; Hung, M. C.; Yu, D.; 14-3-3zeta overexpression defines high risk for breast cancer recurrence and promotes cancer cell survival. *Cancer Res.*, **2009**, *69*, 3425–3432.
19. Li, Z.; Zhao, J.; Du, Y.; Park, H. R.; Sun, S. Y.; Bernal-Mizrachi, L.; Aitken, A.; Khuri, F. R.; Fu, H.; Down-regulation of 14-3-3zeta suppresses anchorage-independent growth of lung cancer cells through anoikis activation. *Proc. Natl. Acad. Sci. USA*, **2008**, *105*, 162–167.
20. Ge, F.; Lu, X. P.; Zeng, H. L.; He, Q. Y.; Xiong, S.; Jin, L.; He, Q. Y.; Proteomic and functional analyses reveal a dual molecular mechanism underlying arsenic-induced apoptosis in human multiple myeloma cells. *J. Proteome Res.*, **2009**, *8*, 3006–3019.
21. Yang, X.; Cao, W.; Lin, H.; Zhang, W.; Lin, W.; Cao, L.; Zhen, H.; Huo, J.; Zhang, X.; Isoform-specific expression of 14-3-3 proteins in human astrocytoma. *J. Neurol. Sci.*, **2009**, *276*, 54–59.
22. Liu, Y.; Tian, R. F.; Li, Y. M.; Liu, W. P.; Cao, L.; Yang, X. L.; Cao, W. D.; Zhang, X.; The expression of seven 14-3-3 isoforms in human meningioma. *Brain Res.*, **2010**, *1336*, 98–102.
23. Bajpai, U.; Sharma, R.; Kausar, T.; Dattagupta, S.; Chattopadhayay, T. K.; Ralhan, R.; Clinical significance of 14-3-3 zeta in human esophageal cancer. *Int. J. Biol. Markers*, **2008**, *23*, 231–237.
24. Lin, M.; Morrison, C. D.; Jones, S.; Mohamed, N.; Bacher, J.; Plass, C.; Copy number gain and oncogenic activity of YWHAZ/14-3-3zeta in head and neck squamous cell carcinoma. *Int. J. Cancer*, **2009**, *125*, 603–611.
25. Chatterjee, D.; Goldman, M.; Braastad, C. D.; Darnowski, J.; Wyche, J. H.; Pantazis, P.; Goodglick, L.; Reduction of 9-nitrocamptothecin-triggered apoptosis in DU-145 human prostate cancer cells by ectopic expression of 14-3-3zeta. *Int. J. Oncol.*, **2004**, *25*, 503–509.

26. Matta, A.; Bahadur, S.; Duggal, R.; Gupta, S. D.; Ralhan, R.; Over-expression of 14-3-3zeta is an early event in oral cancer. *BMC Cancer*, **2007**, *7*, Article No: 169 (11 pages).
27. Choi, J. E.; Hur, W.; Jung, C. K.; Piao, L. S.; Lyoo, K.; Hong, S. W.; Kim, S. W.; Yoon, H. Y.; Yoon, S. K.; Silencing of 14-3-3ζ over-expression in hepatocellular carcinoma inhibits tumor growth and enhances chemosensitivity to *cis*-diammined dichloridoplatium. *Cancer Lett*., **2011**, *303*, 99–107.
28. Shen, J.; Person, M. D.; Zhu, J.; Abbruzzese, J. L.; Li, D.; Protein expression profiles in pancreatic adenocarcinoma compared with normal pancreatic tissue and tissue affected by pancreatitis as detected by two-dimensional gel electrophoresis and mass spectrometry. *Cancer Res*., **2004**, *64*, 9018–9026.
29. Yang, X.; Cao, W.; Zhang, L.; Zhang, W.; Zhang, X.; Lin, H.; Targeting 14-3-3zeta in cancer therapy. *Cancer Gene Ther*., **2012**, *19*, 153–159.
30. Wang, B.; Yang, H.; Liu, Y. C.; Jelinek, T.; Zhang, L.; Ruoslahti, E.; Fu, H.; Isolation of high-affinity peptide antagonists of 14-3-3 proteins by phage display. *Biochemistry*, **1999**, *38*, 12499–12504.
31. Masters, S. C.; Fu, H.; 14-3-3 proteins mediate an essential anti-apoptotic signal. *J. Biol. Chem*., **2001**, *276*, 45193–45200.
32. Cao, W.; Yang, X.; Zhou, J.; Teng, Z.; Cao, L.; Zhang, X.; Fei, Z.; Targeting 14-3-3 protein, difopein induces apoptosis of human glioma cells and suppresses tumor growth in mice. *Apoptosis*, **2010**, *15*, 230–241.
33. Wu, H.; Ge, J.; Yao, S. Q.; Microarray-assisted high-throughput identification of a cell-permeable small-molecule binder of 14-3-3 proteins. *Angew. Chem. Int. Ed. Engl*., **2010**, *49*, 6528–6532.
34. Arrendale, A.; Kim, K.; Choi, J. Y.; Li, W.; Geahlen, R. L.; Borch, R. F.; Synthesis of a phosphoserine mimetic prodrug with potent 14-3-3 protein inhibitory activity. *Chem. Biol*., **2012**, *19*, 764–771.
35. Corradi, V.; Mancini, M.; Santucci, M. A.; Carlomagno, T.; Sanfelice, D.; Mori, M.; Vignaroli, G.; Falchi, F.; Manetti, F.; Radi, M.; Botta, M.; Computational techniques are valuable tools for the discovery of protein-protein interaction inhibitors: the 14-3-3σ case. *Bioorg. Med. Chem. Lett.*, **2011**, *21*, 6867–6871.
36. Zhao, J.; Du, Y.; Horton, J. R.; Upadhyay, A. K.; Lou, B.; Bai, Y.; Zhang, X.; Du, L.; Li, M.; Wang, B.; Zhang, L.; Barbieri, J. T.; Khuri, F. R.; Cheng, X.; Fu, H.; Discovery and structural characterization of a small molecule 14-3-3 protein-protein interaction inhibitor. *Proc. Natl. Acad. Sci. USA*. **2011**, *108*, 16212–16216.
37. Röglin, L.; Thiel, P.; Kohlbacher, O.; Ottmann, C.; Covalent attachment of

pyridoxal-phosphate derivatives to 14-3-3 proteins. *Proc. Natl. Acad. Sci. USA*, **2012**, *109*, E1051–E1053.

38. Milroy, L. G.; Brunsveld, L.; Ottmann, C.; Stabilization and inhibition of protein-protein interactions: the 14-3-3 case study. *ACS Chem. Biol*., **2013**, *8*, 27–35.
39. Ottmann, C.; Small-molecule modulators of 14-3-3 protein-protein interactions. *Bioorg. Med. Chem*., **2013**, *21*, 4058–4062.
40. Wani, M. C.; Taylor, H. L.; Wall, M. E.; Coggon, P.; McPhail, A. T.; Plant antitumor agents. VI. The isolation and structure of taxol, a novel antileukemic and antitumor agent from *Taxus brevifolia*. *J. Am. Chem. Soc*., **1971**, *93*, 2325–2327.
41. Kino, T.; Hatanaka, H.; Hashimoto, M.; Nishiyama, M.; Goto, T.; Okuhara, M.; Kohsaka, M.; Aoki, H.; Imanaka, H.; FK-506, a novel immunosuppressant isolated from a *Streptomyces*. I. Fermentation, isolation, and physico-chemical and biological characteristics. *J. Antibiot*., **1987**, *40*, 1249–1255.
42. Liu, J.; Farmer, J. D., Jr.; Lane, W. S.; Friedman, J.; Weissman, I.; Schreiber, S. L.; Calcineurin is a common target of cyclophilin-cyclosporin A and FKBP-FK506 complexes. *Cell*, **1991**, *66*, 807–815.
43. Rose, R.; Erdmann, S.; Bovens, S.; Wolf, A.; Rose, M.; Hennig, S.; Waldmann, H.; Ottmann, C.; Identification and structure of small-molecule stabilizers of 14-3-3 protein-protein interactions. *Angew. Chem. Int. Ed. Engl.*, **2010**, *49*, 4129–4132.
44. Richter, A.; Rose, R.; Hedberg, C.; Waldmann, H.; Ottmann, C.; An optimised small-molecule stabiliser of the 14-3-3-PMA2 protein-protein interaction. *Chemistry*, **2012**, *18*, 6520–6527.
45. Ballio, A.; Brufani, M.; Casinovi, C. G.; Cerrini, S.; Fedeli, W.; Pellicciari, R.; Santurbano, B.; Vaciago, A.; The structure of fusicoccin A. *Experientia*, **1968**, *24*, 631–635.
46. Barrow, K. D.; Barton, D. H. R.; Sir Chain, E.; Ohnsorge, U. F. W.; Thomas, R.; Fusicocin. Part II. The constitution of fusicoccin. *J. Chem. Soc. (C)*, **1971**, 1265–1274.
47. Sassa, T.; Togashi, M.; Kitaguchi, T.; The structures of cotylenins A, B, C, D and E. *Agr. Biol. Chem.*, **1975**, *39*, 1735–1744.
48. Ballio, A.; Fusicoccin the vivotoxin of *Fusicoccum amygdali* Del. Chemical properties and biological activity. *Annal. Phytopathol*., **1978**, *10*, 145–156.
49. Marré, E.; Fusicoccin: tool in plant physiology. *Annu. Rev. Plant Physiol. Plant Mol. Biol*., **1979**, *30*, 273–288.
50. Korthout, H. A. A. J.; De Boer, A. H.; A fusicoccin binding protein belongs to the family of 14-3-3 brain protein homologs. *Plant Cell*, **1994**, *6*, 1681–1692.
51. Marra, M.; Fullone, M. R.; Fogliano, V.; Pen, J.; Mattei, M.; Masi, S.; Aducci, P.; The

30-kilodalton protein present in purified fusicoccin receptor preparations is a 14-3-3-like protein. *Plant Physiol*., **1994**, *106*, 1497–1501.

52. Oecking, C.; Eckerskorn, C.; Weiler, E. W.; The fusicoccin receptor of plants is a member of the 14-3-3 superfamily of eukaryotic regulatory proteins. *FEBS Lett*., **1994**, *352*, 163–166.
53. Würtele, M.; Jelich-Ottmann, C.; Wittinghofer, A.; Oecking, C.; Structural view of a fungal toxin acting on a 14-3-3 regulatory complex. *EMBO J*., **2003**, *22*, 987–994.
54. Ottmann, C.; Weyand, M.; Sassa, T.; Inoue, T.; Kato, N.; Wittinghofer, A.; Oecking, C.; A structural rationale for selective stabilization of anti-tumor interactions of 14-3-3 proteins by cotylenin A. *J. Mol. Biol.*, **2009**, *386*, 913–919.
55. Asahi, K.; Honma, Y.; Hazeki, K.; Sassa, T.; Kubohara, Y.; Sakurai, A.; Takahashi, N.; Cotylenin A, a plant-growth regulator, induces the differentiation in murine and human myeloid leukemia cells. *Biochem. Biophys. Res. Commun*., **1997**, *238*, 758–763.
56. Yamamoto-Yamaguchi, Y.; Yamada, K.; Ishii, Y.; Asahi, K.; Tomoyasu, S.; Honma, Y.; Induction of the monocytic differentiation of myeloid leukaemia cells by cotylenin A, a plant growth regulator. *British J. Haematol*., **2001**, *112*, 697–705.
57. Yamada, K.; Honma, Y.; Asahi, K.; Sassa, T.; Hino, K.; Tomoyasu, S.; Differentiation of human acute myeloid leukaemia cells in primary culture in response to cotylenin A, a plant growth regulator. *British J. Haematol*., **2001**, *114*, 814–821.
58. Honma, Y.; Ishii, Y.; Sassa, T.; Asahi, K.; Treatment of human promyelocytic leukemia in the SCID mouse model with cotylenin A, an inducer of myelomonocytic differentiation of leukemia cells. *Leuk. Res*., **2003**, *27*, 1019–1025.
59. Honma, Y.; Ishii, Y.; Yamamoto-Yamaguchi, Y.; Sassa, T.; Asahi, K.; Cotylenin A, a differentiation-inducing agent, and IFN-alpha cooperatively induce apoptosis and have an antitumor effect on human non-small cell lung carcinoma cells in nude mice. *Cancer Res*., **2003**, *63*, 3659–3666.
60. Honma, Y.; Kasukabe, T.; Yamori, T.; Kato, N,; Sassa, T.; Antitumor effect of cotylenin A plus interferon-alpha: possible therapeutic agents against ovary carcinoma. *Gynecol. Oncol*., **2005**, *99*, 680–688.
61. Kasukabe, T.; Okabe-Kado, J.; Kato, N.; Sassa, T.; Honma, Y.; Effects of combined treatment with rapamycin and cotylenin A, a novel differentiation-inducing agent, on human breast carcinoma MCF-7 cells and xenografts. *Breast Cancer Res*., **2005**, *7*, R1097–R1110.
62. Molzan, M.; Kasper, S.; Röglin, L.; Skwarczynska, M.; Sassa, T.; Inoue, T.; Breitenbuecher, F.; Ohkanda, J.; Kato, N.; Schuler, M.; Ottmann, C.; Stabilization of physical RAF/14-3-3 interaction by cotylenin A as treatment strategy for RAS mutant cancers. *ACS Chem. Biol*., **2013**, *8*, 1869–1875.

63. Bunney, T. D.; de Boer, A. H.; Levin, M.; Fusicoccin signaling reveals 14-3-3 protein function as a novel step in left-right patterning during amphibian embryogenesis. *Development*, **2003**, *130*, 4847–4858.
64. de Vries-van Leeuwen, I. J.; Kortekaas-Thijssen, C.; Mandouckou, J. A. N.; Kas, S.; Evidente, A.; de Boer, A. H.; Fusicoccin-A selectively induces apoptosis in tumor cells after interferon-alpha priming. *Cancer Lett*., **2010**, *293*, 198–206.
65. Inoue, T.; Studies on the development of anticancer fusicoccin derivatives which synergize with interferon-α. Doctoral Dissertation, Graduate School of Science, Osaka University, **2010**.
66. Barrow, K. D.; Barton, D. H.; Chain, E.; Ohnsorge, U. F.; Sharma, R. P.; Fusicoccin. Part III. The structure of fusicoccin H. *J. Chem. Soc. Perkin Trans. 1*, **1973**, 1590–1599.
67. Barrow, K. D.; Barton, D. H. R.; Chain, E. B.; Bageenda-Kasujja, D.; Mellows, G.; Fusicoccin. Part IV. The structure of fusicoccin J. *J. Chem. Soc. Perkin Trans. 1*, **1975**, 877–883.
68. Kawakami, K.; Hattori, M.; Inoue, T.; Maruyama, Y.; Ohkanda, J.; Kato, N.; Tongu, M.; Yamada, T.; Akimoto, M.; Takenaga, K.; Sassa, T.; Suzumiya, J.; Honma, Y.; A novel fusicoccin derivative preferentially targets hypoxic tumor cells and inhibits tumor growth in xenografts. *Anticancer Agents Med. Chem*., **2012**, *12*, 791–800.
69. De Vries-van Leeuwen, I. J.; da Costa Pereira, D.; Flach, K. D.; Piersma, S. R.; Haase, C.; Bier, D.; Yalcin, Z.; Michalides, R.; Feenstra, K. A.; Jiménez, C. R.; de Greef, T. F.; Brunsveld, L.; Ottmann, C.; Zwart, W.; de Boer, A. H.; Interaction of 14-3-3 proteins with the estrogen receptor alpha F domain provides a drug target interface. *Proc. Natl. Acad. Sci. USA*, **2013**, *110*, 8894–8899.
70. Tsukiji, S.; Miyagawa, M.; Takaoka, Y.; Tamura, T.; Hamachi, I.; Ligand-directed tosyl chemistry for protein labeling in vivo. *Nat. Chem. Biol*., **2009**, *5*, 341–343.
71. Takahashi, M.; Kawamura, A.; Kato, N.; Nishi, T.; Hamachi, I.; Ohkanda, J.; Phosphopeptide-dependent labeling of 14-3-3ζ proteins by fusicoccin-based fluorescent probes. *Angew. Chem. Int. Ed. Engl*., **2012**, *51*, 509–512.
72. Anders, C.; Higuchi, Y.; Koschinsky, K.; Bartel, M.; Schumacher, B.; Thiel, P.; Nitta, H.; Preisig-Müller, R.; Schlichthörl, G.; Renigunta, V.; Ohkanda, J.; Daut, J.; Kato, N.; Ottmann, C.; A semisynthetic fusicoccane stabilizes a protein-protein interaction and enhances the expression of K^+ channels at the cell surface. *Chem. Biol*., **2013**, *20*, 583–593.
73. Rajan, S.; Wischmeyer, E.; Liu, G. X.; Preisig-Müller, R.; Daut, J.; Karschin, A.; Derst, C.; TASK-3, a novel tandem pore domain acid-sensitive K^+ channel. An extracellular histidine as pH sensor. *J. Biol. Chem*., **2000**, *275*, 16650–16657.
74. Bittner, S.; Budde, T.; Wiendl, H.; Meuth, S. G.; From the background to the spotlight: TASK

channels in pathological conditions. *Brain Pathol*., **2010**, *20*, 999–1009.

75. Rajan, S.; Preisig-Müller, R.; Wischmeyer, E.; Nehring, R.; Hanley, P. J.; Renigunta, V.; Musset, B.; Schlichthörl, G.; Derst, C.; Karschin, A.; Daut, J.; Interaction with 14-3-3 proteins promotes functional expression of the potassium channels TASK-1 and TASK-3. *J. Physiol*., **2002**, *545.1*, 13–26.
76. Zuzarte, M.; Heusser, K.; Renigunta, V.; Schlichthörl, G.; Rinné, S.; Wischmeyer, E.; Daut, J.; Schwappach, B.; Preisig-Müller, R.; Intracellular traffic of the K^+ channels TASK-1 and TASK-3: role of N- and C-terminal sorting signals and interaction with 14-3-3 proteins. *J. Physiol*., **2009**, *587.5*, 929–952.
77. Frisch, S. M.; Francis, H.; Disruption of epithelial cell-matrix interactions induces apoptosis. *J. Cell Biol*., **1994**, *124*, 619–626.
78. Wei, L.; Yang, Y.; Zhang, X.; Yu, Q.; Anchorage-independent phosphorylation of $p130^{Cas}$ protects lung adenocarcinoma cells from anoikis. *J. Cell. Biochem*., **2002**, *87*, 439–449.
79. Kim, J. H.; Lee, S. Y.; Oh, S. Y.; Han, S. I.; Park, H. G.; Yoo, M. A.; Kang, H. S.; Methyl jasmonate induces apoptosis through induction of Bax/Bcl-XS and activation of caspase-3 via ROS production in A549 cells. *Oncol. Rep*., **2004**, *12*, 1233–1238.
80. Martin, D. A.; Siegel, R. M.; Zheng, L.; Lenardo, M. J.; Membrane oligomerization and cleavage activates the caspase-8 (FLICE/MACHα1) death signal. *J. Biol. Chem*., **1998**, *273*, 4345–4349.
81. Rytömaa, M.; Martins, L. M.; Downward, J.; Involvement of FADD and caspase-8 signalling in detachment-induced apoptosis. *Curr. Biol*., **1999**, *9*, 1043–1046.
82. Fukazawa, H.; Mizuno, S.; Uehara, Y.; A microplate assay for quantitation of anchorage-independent growth of transformed cells. *Anal. Biochem*., **1995**, *228*, 83–90.
83. Albelda, S. M.; Buck, C. A.; Integrins and other cell adhesion molecules. *FASEB J*., **1990**, *4*, 2868–2880.
84. Nagafuchi, A.; Takeichi, M.; Transmembrane control of cadherin-mediated cell adhesion: a 94 kDa protein functionally associated with a specific region of the cytoplasmic domain of E-cadherin. *Cell Regul*., **1989**, *1*, 37–44.
85. Suzuki, S. T.; Structural and functional diversity of cadherin superfamily: are new members of cadherin superfamily involved in signal transduction pathway? *J. Cell. Biochem*., **1996**, *61*, 531–542.
86. Hazan, R. B.; Phillips, G. R.; Qiao, R. F.; Norton, L.; Aaronson, S. A.; Exogenous expression of N-cadherin in breast cancer cells induces cell migration, invasion, and metastasis. *J. Cell Biol*., **2000**, *148*, 779–790.
87. Rosso, F.; Giordano, A.; Barbarisi, M.; Barbarisi, A.; From cell-ECM interactions to tissue

engineering. *J. Cell. Physiol*., **2004**, *199*, 174–180.

88. Lock, J. G.; Wehrle-Haller, B.; Strömblad, S.; Cell-matrix adhesion complexes: master control machinery of cell migration. *Semin. Cancer Biol*., **2008**, *18*, 65–76.
89. Fan, T.; Li, R.; Todd, N. W.; Qiu, Q.; Fang, H. B.; Wang, H.; Shen, J.; Zhao, R. Y.; Caraway, N. P.; Katz, R. L.; Stass, S. A.; Jiang, F.; Up-regulation of 14-3-3ζ in lung cancer and its implication as prognostic and therapeutic target. *Cancer Res*., **2007**, *67*, 7901–7906.
90. Kasukabe, T.; Okabe-Kado, J.; Haranosono, Y.; Kato, N.; Honma, Y.; Inhibition of rapamycin-induced Akt phosphorylation by cotylenin A correlates with their synergistic growth inhibition of cancer cells. *Int. J. Oncol*., **2013**, *42*, 767–775.
91. Charras, G. T.; Yarrow, J. C.; Horton, M. A.; Mahadevan, L.; Mitchison, T. J.; Non-equilibration of hydrostatic pressure in blebbing cells. *Nature*, **2005**, *435*, 365–369.
92. Chhabra, E. S.; Higgs, H. N.; The many faces of actin: matching assembly factors with cellular structures. *Nat. Cell Biol*., **2007**, *9*, 1110–1121.
93. Torgerson, R. R.; McNiven, M. A.; The actin-myosin cytoskeleton mediates reversible agonist-induced membrane blebbing. *J. Cell Sci*., **1998**, *111.19*, 2911–2922.
94. Coleman, M. L.; Sahai, E. A.; Yeo, M.; Bosch, M.; Dewar, A.; Olson, M. F.; Membrane blebbing during apoptosis results from caspase-mediated activation of ROCK I. *Nat. Cell Biol*., **2001**, *3*, 339–345.
95. Sebbagh, M.; Renvoizé, C.; Hamelin, J.; Riché, N.; Bertoglio, J.; Bréard, J.; Caspase-3-mediated cleavage of ROCK I induces MLC phosphorylation and apoptotic membrane blebbing. *Nat. Cell Biol*., **2001**, *3*, 346–352.
96. Riou, P.; Villalonga, P.; Ridley, A. J.; Rnd proteins: multifunctional regulators of the cytoskeleton and cell cycle progression. *Bioessays*., **2010**, *32*, 986–992.
97. Tanaka, H.; Katoh, H.; Negishi, M.; Pragmin, a novel effector of Rnd2 GTPase, stimulates RhoA activity. *J. Biol. Chem*., **2006**, *281*, 10355–10364.
98. Chardin, P.; Function and regulation of Rnd proteins. *Nat. Rev. Mol. Cell Biol*., **2006**, *7*, 54–62.
99. Riento, K.; Villalonga, P.; Garg, R.; Ridley, A.; Function and regulation of RhoE. *Biochem. Soc. Trans*., **2005**, *33.4*, 649–651.
100. Oinuma, I.; Kawada, K.; Tsukagoshi, K.; Negishi, M.; Rnd1 and Rnd3 targeting to lipid raft is required for p190 RhoGAP activation. *Mol. Biol. Cell*., **2012**, *23*, 1593–1604.
101. Riou, P.; Kjær, S.; Garg, R.; Purkiss, A.; George, R.; Cain, R. J.; Bineva, G.; Reymond, N.; McColl, B.; Thompson, A. J.; O'Reilly, N.; McDonald, N. Q.; Parker, P. J.; Ridley, A. J.; 14-3-3 proteins interact with a hybrid prenyl-phosphorylation motif to inhibit G proteins. *Cell*, **2013**, *153*, 640–653.

102. Villalonga, P.; Guasch, R. M.; Riento, K.; Ridley, A. J.; RhoE inhibits cell cycle progression and Ras-induced transformation. *Mol. Cell. Biol*., **2004**, *24*, 7829–7840.
103. Gottesbühren, U.; Garg, R.; Riou, P.; McColl, B.; Brayson, D.; Ridley, A. J.; Rnd3 induces stress fibres in endothelial cells through RhoB. *Biol. Open*, **2013**, *2*, 210–216.
104. Madigan, J. P.; Bodemann, B. O.; Brady, D. C.; Dewar, B. J.; Keller, P. J.; Leitges, M.; Philips, M. R.; Ridley, A. J.; Der, C. J.; Cox, A. D.; Regulation of Rnd3 localization and function by protein kinase C alpha-mediated phosphorylation. *Biochem. J*., **2009**, *424*, 153–161.
105. Khongmanee, A.; Lirdprapamongkol, K.; Tit-oon, P.; Chokchaichamnankit, D.; Svasti, J.; Srisomsap, C.; Proteomic analysis reveals important role of 14-3-3σ in anoikis resistance of cholangiocarcinoma cells. *Proteomics*, **2013**, *13*, 3157–3166.
106. Tojkander, S.; Gateva, G.; Lappalainen, P.; Actin stress fibers—assembly, dynamics and biological roles. *J. Cell Sci*., **2012**, *125.8*, 1855–1864.
107. Rubenstein, N. M.; Chan, J. F.; Kim, J. Y.; Hansen, S. H.; Firestone, G. L.; Rnd3/RhoE induces tight junction formation in mammary epithelial tumor cells. *Exp. Cell Res*., **2005**, *305*, 74–82.
108. Miki, H. *ed.*; Regulation of cytoskeleton and the cell movement by signal transduction. *Wakaru Jikken Igaku Shirizu*, **2004**, Yodosha.
109. Xu, W.; Baribault, H.; Adamson, E. D.; Vinculin knockout results in heart and brain defects during embryonic development. *Development*, **1998**, *125*, 327–337.
110. Fanning, A. S.; Ma, T. Y.; Anderson, J. M.; Isolation and functional characterization of the actin binding region in the tight junction protein ZO-1. *FASEB J*., **2002**, *16*, 1835–1847.
111. Fanning, A. S.; Jameson, B. J.; Jesaitis, L. A.; Anderson, J. M.; The tight junction protein ZO-1 establishes a link between the transmembrane protein occludin and the actin cytoskeleton. *J. Biol. Chem*., **1998**, *273*, 29745–29753.
112. Guilluy, C.; Garcia-Mata, R.; Burridge, K.; Rho protein crosstalk: another social network? *Trends Cell Biol*., **2011**, *21*, 718–726.
113. Niessen, C. M.; Gottardi, C. J.; Molecular components of the adherens junction. *Biochim. Biophys. Acta*, **2008**, *1778*, 562–571.
114. Chinnaiyan, A. M.; O'Rourke, K.; Tewari, M.; Dixit, V. M.; FADD, a novel death domain-containing protein, interacts with the death domain of Fas and initiates apoptosis. *Cell*, **1995**, *81*, 505–512.
115. Walczak, H.; Sprick, M. R.; Biochemistry and function of the DISC. *Trends Biochem. Sci*., **2001**, *26*, 452–453.
116. Sprick, M. R.; Weigand, M. A.; Rieser, E.; Rauch, C. T.; Juo, P.; Blenis, J.; Krammer, P. H.;

Walczak, H.; FADD/MORT1 and caspase-8 are recruited to TRAIL receptors 1 and 2 and are essential for apoptosis mediated by TRAIL receptor 2. *Immunity*, **2000**, *12*, 599–609.

117. Bin, L.; Li, X.; Xu, L. G.; Shu, H. B.; The short splice form of Casper/c-FLIP is a major cellular inhibitor of TRAIL-induced apoptosis. *FEBS Lett*., **2002**, *510*, 37–40.
118. Scaffidi, C.; Schmitz, I.; Krammer, P. H.; Peter, M. E.; The role of c-FLIP in modulation of CD95-induced apoptosis. *J. Biol. Chem*., **1999**, *274*, 1541–1548.
119. Rao-Bindal, K.; Rao, C. K.; Yu, L.; Kleinerman, E. S.; Expression of c-FLIP in pulmonary metastases in osteosarcoma patients and human xenografts. *Pediatr. Blood Cancer*, **2013**, *60*, 575–579.
120. Kimchi, A.; DAP genes: novel apoptotic genes isolated by a functional approach to gene cloning. *Biochim. Biophys. Acta*, **1998**, *1377*, F13–F33.
121. Kissil, J. L.; Cohen, O.; Raveh, T.; Kimchi, A.; Structure-function analysis of an evolutionary conserved protein, DAP3, which mediates TNF-α- and Fas-induced cell death. *EMBO J*., **1999**, *18*, 353–362.
122. Miyazaki, T.; Reed, J. C.; A GTP-binding adapter protein couples TRAIL receptors to apoptosis-inducing proteins. *Nat. Immunol*., **2001**, *2*, 493–500.
123. Miyazaki, T.; Shen, M.; Fujikura, D.; Tosa, N.; Kim, H. R.; Kon, S.; Uede, T.; Reed, J. C.; Functional role of death-associated protein 3 (DAP3) in anoikis. *J. Biol. Chem*., **2004**, *279*, 44667–44672.
124. Kawai, T.; Takahashi, K.; Sato, S.; Coban, C.; Kumar, H.; Kato, H.; Ishii, K. J.; Takeuchi, O.; Akira, S.; IPS-1, an adaptor triggering RIG-I- and Mda5-mediated type I interferon induction. *Nat. Immunol*., **2005**, *6*, 981–988.
125. Seth, R. B.; Sun, L.; Ea, C. K.; Chen, Z. J.; Identification and characterization of MAVS, a mitochondrial antiviral signaling protein that activates NF-kappaB and IRF 3. *Cell*, **2005**, *122*, 669–682.
126. Li, H. M.; Fujikura, D.; Harada, T.; Uehara, J.; Kawai, T.; Akira, S.; Reed, J. C.; Iwai, A.; Miyazaki, T.; IPS-1 is crucial for DAP3-mediated anoikis induction by caspase-8 activation. *Cell Death Differ*., **2009**, *16*, 1615–1621.
127. Fukazawa, T.; Fujiwara, T.; Uno, F.; Teraishi, F.; Kadowaki, Y.; Itoshima, T.; Takata, Y.; Kagawa, S.; Roth, J. A.; Tschopp, J.; Tanaka, N.; Accelerated degradation of cellular FLIP protein through the ubiquitin-proteasome pathway in p53-mediated apoptosis of human cancer cells. *Oncogene*, **2001**, *20*, 5225–5231.
128. Abedini, M. R.; Muller, E. J.; Bergeron, R.; Gray, D. A.; Tsang, B. K.; Akt promotes chemoresistance in human ovarian cancer cells by modulating cisplatin-induced, p53-dependent ubiquitination of FLICE-like inhibitory protein. *Oncogene*, **2010**, *29*, 11–25.

129. Midgley, C. A.; Desterro, J. M.; Saville, M. K.; Howard, S.; Sparks, A.; Hay, R. T.; Lane, D. P.; An N-terminal $p14^{ARF}$ peptide blocks Mdm2-dependent ubiquitination *in vitro* and can activate p53 in vivo. *Oncogene*, **2000**, *19*, 2312–2323.
130. Kubbutat, M. H.; Jones, S. N.; Vousden, K. H.; Regulation of p53 stability by Mdm2. *Nature*, **1997**, *387*, 299–303.
131. Knippschild, U.; Oren, M.; Deppert, W.; Abrogation of wild-type p53 mediated growth-inhibition by nuclear exclusion. *Oncogene*, **1996**, *12*, 1755–1765.
132. Ryan, J. J.; Prochownik, E.; Gottlieb, C. A.; Apel, I. J.; Merino, R.; Nuñez, G.; Clarke, M. F.: c-Myc and bcl-2 modulate p53 function by altering p53 subcellular trafficking during the cell cycle. *Proc. Natl. Acad. Sci. USA*, **1994**, *91*, 5878–5882.
133. Gu, W.; Roeder, R.G.; Activation of p53 sequence-specific DNA binding by acetylation of the p53 C-terminal domain. *Cell*, **1997**, *90*, 595–606.
134. Bosari, S.; Viale, G.; Roncalli, M.; Graziani, D.; Borsani, G.; Lee, A. K.; Coggi, G.; p53 gene mutations, p53 protein accumulation and compartmentalization in colorectal adenocarcinoma. *Am. J. Pathol*., **1995**, *147*, 790–798.
135. Wang, K. S.; Chen, G.; Shen, H. L.; Li, T. T.; Chen, F.; Wang, Q. W.; Wang, Z. Q.; Han, Z. G.; Zhang, X.; Insulin receptor tyrosine kinase substrate enhances low levels of MDM2-mediated p53 ubiquitination. *PLoS One*, **2011**, *6*, e23571.
136. Nikolaev, A. Y.; Li, M.; Puskas, N.; Qin, J.; Gu, W.; Parc: a cytoplasmic anchor for p53. *Cell*, **2003**, *112*, 29–40.
137. Liu, G.; Xirodimas, D. P.; NUB1 promotes cytoplasmic localization of p53 through cooperation of the NEDD8 and ubiquitin pathways. *Oncogene*, **2010**, *29*, 2252–2261.
138. Kawai, H.; Wiederschain, D.; Yuan, Z. M; Critical contribution of the MDM2 acidic domain to p53 ubiquitination. *Mol. Cell. Biol*., **2003**, *23*, 4939–4947.
139. Wang, L.; Wu, Q.; Qiu, P.; Mirza, A.; McGuirk, M.; Kirschmeier, P.; Greene, J. R.; Wang, Y.; Pickett, C. B.; Liu, S.; Analyses of p53 target genes in the human genome by bioinformatic and microarray approaches. *J. Biol. Chem*., **2001**, *276*, 43604–43610.
140. Okorokov, A. L.; Rubbi, C. P.; Metcalfe, S.; Milner, J.; The interaction of p53 with the nuclear matrix is mediated by F-actin and modulated by DNA damage. *Oncogene*, **2002**, *21*, 356–367.
141. Danes, C. G.; Wyszomierski, S. L.; Lu, J.; Neal, C. L.; Yang, W.; Yu, D.; 14-3-3zeta down-regulates p53 in mammary epithelial cells and confers luminal filling. *Cancer Res*., **2008**, *68*, 1760–1777.
142. Gu, Y. M.; Jin, Y. H.; Choi, J. K.; Baek, K. H.; Yeo, C. Y.; Lee, K. Y.; Protein kinase A phosphorylates and regulates dimerization of 14-3-3 epsilon. *FEBS Lett*., **2006**, *580*, 305–310.

143. Rajagopalan, S.; Jaulent, A. M.; Wells, M.; Veprintsev, D. B.; Fersht, A. R.; 14-3-3 activation of DNA binding of p53 by enhancing its association into tetramers. *Nucleic Acids Res*., **2008**, *36*, 5983–5991.
144. Schumacher, B.; Mondry, J.; Thiel, P.; Weyand, M.; Ottmann, C.; Structure of the p53 C-terminus bound to 14-3-3: implications for stabilization of the p53 tetramer. *FEBS Lett*., **2010**, *584*, 1443–1448.
145. A private communication from Professor Christian Ottmann, Eindhoven University of Technology, Netherlands.

.

Acknowledgements

This dissertation has been carried out at the Institute for Scientific and Industrial Research, Osaka University, and Department of Chemistry, Graduate School of Science, Osaka University under the guidance of Professor Nobuo Kato.

First of all, I would like to express my most sincere gratitude to my principal supervisor, Professor Nobuo Kato for the continuous support of my doctoral study and research. This thesis would not have been possible without the help, support and patience. I quite simply cannot imagine a better adviser.

I deliver special thanks to Professor Michio Murata and Professor Takashi Kubo as the second readers of this thesis, and I am gratefully indebted to them for their very valuable comments on this thesis.

I am also grateful to Associate Professor Junko Ohkanda for her valuable discussions to solve difficult problems.

I feel grateful to Associate Professor Kunihiro Kaihatsu because he gave me a lot of knowledge on biological experiments.

I have much thanks to Assistant Professor Hajime Nitta for supplying natural fusicoccins and its derivatives.

I express my thanks to Assistant Professor Yusuke Higuchi for his splendid advices and discussions. His knowledge and advices supported my research.

I would like to acknowledge to Assistant Professor Tomikazu Kawano for his advices on stance of researches.

I want to express my gratitude to Professor Takeshi Sassa, Professor emeritus of Yamagata University, for providing natural cotylenins and fusicoccins, besides many helpful suggestions.

My appreciation goes to Professor Yoshio Honma, Professor emeritus of Shimane University, for providing cell lines, besides many helpful suggestions.

I would like to express my gratitude to Dr. Takashi Kasukabe and Dr. Junko Okabe-Kado, Saitama Cancer Center, for a collaborative research.

I also extend my appreciation to all members of Kato Lab for their kind and warm helps during my life as a graduate student; Dr. Masamitsu Hiraoka, Dr. Shuichi Mori, Mr. Nobuyuki Tanaka, Ms. Misuzu Tanno, Dr. Takatsugu Inoue, Dr. Shinnosuke Machida, Mr.

Ichiro Imada, Mr. Taro Enomoto, Mr. Masato Hirano, Mr. Toshio Maki, Mr. Shinya Miyake, Mr. Yuta Fukai, Dr. Shinjiro Sawada, Ms. Yuriko Maruyama, Mr. Kohei Fujii, Mr. Takaaki Monta, Ms. Akie Kawamura, Ms. Chihiro Kondo, Mr. Tomoya Takahashi, Mr. Daisuke Hayashi, Mr. Minoru Yabu, Mr. Takuya Ohzawa, Mr. Yoshinobu Yamaguchi, Mr. Tomohiro Watanabe, Ms. Chiaki Ohura, Mr. Takashi Kanno, Ms. Michiko Takahashi, Mr. Toru Yoneyama, Ms. Mai Tsubamoto, Ms. Tenko Hayashi, Ms. Yiting Zhou, Mr. Ryosuke Ishida, Mr. Yuta Inoue, Mr. Atsushi Kusumoto, Mr. Chenyu Wang, Mr. Kenji Takagi, Ms. Miku Okazaki, Ms. Hiroyo, Matsumura, Ms. Yoriko Kaihatsu, Ms. Junko Hikida, Ms. Azusa Ohta, Mr. Fujio Ito, Mr. Hideaki Furusawa and Ms. Aya Takenaka.

I have appreciate the members of SENJU Pharmaceutical Co., Ltd. for the understanding to my research and help to my works; Dr. Hideyuki Sakai, Dr. Masaaki Kurata, Mr. Shingo Nemoto, Ms. Ikuyo Atsumi, Mr. Yoshinori Yamagiwa and Ms. Kazuyo Sadamoto (Toxicology Research laboratory), Dr. Mitsuyoshi Azuma, Dr. Akira Ohtori and Dr. Hideki Tokushige (R&D Institute), Mr. Tetsuo Kida, Dr. Seiko Kozai and Mr. Keisuke Shinno (the former Toxicological-ADME group), Ms. Fumiko Miyashita-Yano, Ms. Mariko Furukawa and Mr. Masaki Kakehi (the former Toxicology Research Laboratory) and all members.

Finally, I wish to deeply thank to my parents, family and friends for continuous encouragement and support of throughout my research life.

Yu Haranosono

February 2014